I give permission for public access to my thesis and for any copying to be done at the discretion of the archives librarian and/or the College librarian.

_____ _____

Mignon DeVera Johnston Date

ABSTRACT

Seismic anisotropy uses earthquake data to measure the presence of deformation in the Earth's mantle. Upon travel through an anisotropic solid, a shear wave splits into two orthogonal components that have different velocities and vibration directions. A delay time accumulates between the arrival at the Earth's surface of the fast and slow components of the shear wave. Seismometers record both components, the delay time between them (δt) and the orientation of the fast component (φ). Evidence of shear wave splitting (SWS) indicates anisotropy, and thus deformation, somewhere along the raypath. Null measurements ($\delta t = 0$) are evidence for un-split seismic waves, which indicate either a lack of anisotropy beneath that station, anisotropy that is vertically aligned, or shear waves that were already oriented parallel or perpendicular to the fast axis and so were not split upon passing through the mantle.

A small array of seismometers in the southeastern United States recorded an intriguing pattern of splitting and null measurements (Long 2009). Several of the stations closest to the edge of the continent exhibit null measurements in a variety of directions and almost no splitting. These measurements indicate an unusual pattern of mantle deformation in this transition region between thick continental crust and thinner oceanic crust.

In this project, I further investigate the SWS pattern in South Carolina, using a novel data set from the South Carolina Earth Physics Project (SCEPP) seismograph network operated by the University of South Carolina. Between 2001 and 2004, the network of 25 seismometers deployed at high schools across South Carolina collected seismic data. I analyzed these data and found the stations in South Carolina to be dominated by null measurements, with only a few splitting results. At some stations, the null measurements have a clearly defined orientation, while at other stations there are a variety of orientations. The direction of the splitting results match the trends of absolute plate motion and/or fossil anisotropy, and no splitting results were found for the southern-most stations. I conclude that there is a complex pattern of anisotropy occurring beneath South Carolina, and that the two most probable explanations for this pattern are either active mantle flow in a subvertical direction around the edge of the continent or fossil anisotropy.

SHEAR WAVE SPLITTING IN SOUTH CAROLINA, USA

Mignon DeVera Johnston
Mount Holyoke College

Thesis submitted to the Geology Department of Mount Holyoke College

Advisors:

Professor Michelle Markley
Department of Geology, Mount Holyoke College

Professor Maureen Long
Department of Geology and Geophysics, Yale University

May 2010

ACKNOWLEDGEMENTS

This thesis is the result of a year's worth of thought and effort that was made possible by the generous support and encouragement of the following:

- Michelle Markley, my thesis advisor, who always kept me on track, made sure that I kept things in perspective, and treated me to many hot chocolates at Rao's;
- Maureen Long, my advisor at Yale, who first introduced me to shear wave splitting and helped me develop the idea for this project;
- Steve Dunn and Janice Gifford, my thesis committee members, who gave me valuable support and feedback on my work;
- The faculty, staff, and students of the Mount Holyoke College Geology Department who have always inspired me to be the best that I can be;
- Erin Wirth, my go-to person for all things related to seismology, who taught me how to use SplitLab and answered all of my random questions;
- Cecile Vasquez, who knows all there is to know about the Mount Holyoke College Geology Department and who helped me with all the little details of writing and submitting a thesis;

- Sarah Hopson and my friends on the Mount Holyoke College Equestrian and Dressage Teams who were always there to encourage me and keep me rooted in the real world;
- My family, who listened to all of my questions and gave me their best answers, while always being there to help me achieve all that I want to do.

I thank you all for being the best thesis support team imaginable!

TABLE OF CONTENTS

LIST OF FIGURES AND TABLES

1. INTRODUCTION TO SHEAR WAVE SPLITTING

Seismic anisotropy uses earthquake data to measure the presence of deformation in the Earth's mantle (Silver 1996). Three types of waves result from an earthquake: P-waves, S-waves, and surface waves. P-waves, also known as compressional waves, are the fastest-moving waves and are the first to arrive at any given point on the Earth's surface. S-waves, also known as shear waves or secondary waves, move more slowly through the Earth and arrive later. In addition, waves refract, reflect, and change character at significant compositional boundaries within the earth (for example, the core-mantle boundary). Depending on the type of wave and the path it takes through the Earth, it is possible to classify seismic waves into very specific types (Figure 1.1). In this study, I focused on a certain type of shear wave, SKS waves, which travel from the source as S-waves, through the source-side mantle, through the outer core as P-waves, and re-emerge on the receiver-side mantle to travel up to the surface as S-waves (Shearer 1999).

Upon travel through an anisotropic medium, such as certain regions in the mantle or crust, an S-wave splits into two orthogonal components that have different velocities and vibration directions (Silver 1996). A delay time accumulates between the arrival at the Earth's surface of the fast and slow

components of the S-wave. Seismometers record both components, the delay time between them (δt) and the orientation of the fast component (ϕ). Evidence of shear wave splitting (SWS) indicates anisotropy, and thus deformation, somewhere along the raypath, probably in the upper mantle (Silver 1996).

Anisotropy can occur at several locations along a seismic raypath and can result from several different geologic processes (Silver 1996). In this project I focus on deformation in the upper mantle as indicated by lattice preferred orientation (LPO) of olivine. Olivine is the most common mantle mineral, and it develops an LPO during deformation by dislocation creep. This LPO results in anisotropy (Silver 1996). In general, the fast axis of olivine (the [100] axis), and thus the fast splitting direction, aligns with the direction of maximum shear in the upper mantle (Christensen 1984, Nicolas and Christensen 1987, Zhang and Karato 1995). Earthquake wave phases that travel through the mantle and outer core, in particular SKS, are the most useful phases of shear waves for measuring anisotropy in the upper mantle (Silver 1996). The P-to-S conversion at the core-mantle boundary (CMB) ensures that any observed splitting must be the result of receiving-station-side anisotropy between the CMB and the surface (Long and Silver 2009).

Shear wave splitting results have multiple implications for better understanding crust and mantle structure, as well as mantle dynamics. One possible source of shear wave splitting is active flow of the upper mantle flow. In regions where the crustal geology is well understood (e.g. the western United

States), shear wave splitting results appear to correlate well with active mantle flow (Silver and Holt 2002). Another possible source of shear wave splitting is fossil anisotropy. This type of anisotropy results from the LPO of olivine, or other mantle minerals that behave in a similar fashion, becoming "locked-in" when solid state deformation ceases (Silver and Chan 1991). This often occurs during mountain building, and so evidence of fossil anisotropy tells us about mantle flow and Earth processes at the time of the orogenic event (Silver 1996).

More complex situations can arise as a result of multiple layers of anisotropy, mantle flow that is neither vertical nor horizontal (dipping axis of symmetry), or small-scale lateral heterogeneity (Long and Silver 2009). In the case of multiple layers of anisotropy, backazimuthal variation occurs as a periodic variation in both ϕ and δt with a $\pi/2$ periodicity (Silver and Savage 1994). A dipping axis of symmetry also yields a similar periodic variation in splitting results but with a 2π periodicity (Chevrot 2000). Lateral heterogeneity on a small-scale yields varying results within a small region, as the orientation of anisotropy at one spot would vary from that at a nearby spot. In analyzing the results of the present study, I assume that there are not multiple layers of anisotropy or a dipping axis of symmetry. These assumptions are in agreement with the results of previous studies of the eastern United States (Barruol et al. 1997, Fouch et al. 2000).

In addition to splitting results, it is also possible to get null results. A null result is indicated by a clear S-wave arrival that exhibits no splitting (i.e. $\delta t = 0$).

A null result may be produced by one of the following mechanisms: the initial polarization of the S-wave is parallel to either the fast or slow direction, there is no anisotropy beneath the station, or there is vertical mantle flow beneath the station (Long and Silver 2009, Long 2009). If the initial polarization of the S-wave is parallel to either the fast or slow direction, then the wave is already aligned with an allowable direction of motion, and so it is not split. In this case, all of the ϕ-values from the null results at a station will be oriented in one of two perpendicular directions, forming a "cross" shape, since the allowable directions of motion are perpendicular to each other. If there is no anisotropy beneath the station, wave motion is allowed in all directions and so the shear wave experiences no splitting. In this case, the ϕ-values from the null results at a station will be oriented in all directions, forming a "flower" shape, since wave motion is allowed in all orientations. If there is vertical mantle flow beneath the station, the fast axis will be aligned vertically and so the wave motion will be allowed in all directions as well, since S-wave particle motion is perpendicular to the direction of propagation. In this case, the null results will also form a "flower" shape.

Through analysis of shear wave splitting (and null results) and comparison with known information about the geology of a region, it is possible to determine the most likely source of the anisotropy. Depending on the source, it is then possible to determine either the direction of fossil anisotropy or the direction of active asthenospheric flow, which then gives insights to past and present mantle dynamics.

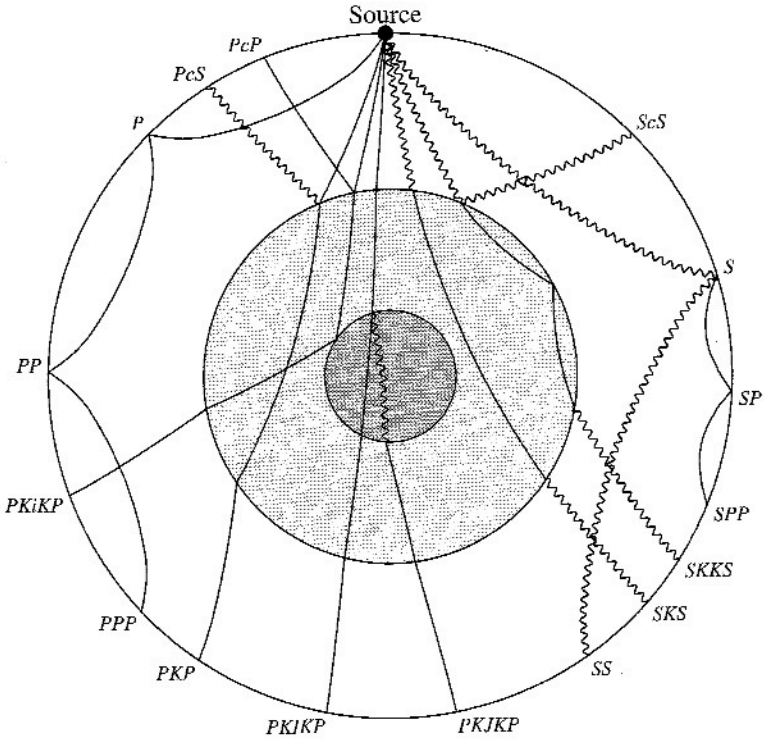

Figure 1.1. Global seismic ray paths and phase names. *P*-waves are shown as solid lines, *S*-waves as wiggly lines. The different shades indicate the inner core (darkest), the outer core (light grey), and the mantle (lightest). The primary focus of this study is the SKS wave. It originates as an *S*-wave at the source, travels through the mantle, is converted to a *P*-wave at the core-mantle boundary (CMB), travels through the outer core, is converted back to an *S*-wave at the CMB, and then travels through the mantle, eventually reaching the Earth's surface. (from Shearer 1999)

2. PREVIOUS STUDIES OF SHEAR WAVE SPLITTING

2.1 Shear Wave Splitting in the Eastern United States

A few studies have investigated shear wave splitting in the eastern United States. The results from these studies generally agree with each other and provide a basic overview of anisotropy beneath the United States. To summarize the two most relevant studies (Barruol et al. 1997, Fouch et al. 2000): splitting results located in the continental interior are roughly parallel with absolute plate motion, but splitting results at the edge of the continent yield a more unusual pattern. To explain this pattern, both studies suggest the possibility that this spatial variation is a result of fossil anisotropy (as discussed in the introduction) and/or sub-vertical asthenospheric flow around a continental keel, discussed below.

2.1.1 The North American Continental Keel

The North American craton, the oldest and thus coldest, part of the continent, is associated with cold, seismically fast material that can extend to a depth of more than 250 kilometers beneath the craton (Grand 1994, Van der Lee and Nolet 1997). Because oceanic crust and lithosphere are so much thinner, the edge of a continent is like a rigid keel at depth. Warmer asthenospheric flow is diverted around the edge of the keel, resulting in upwelling and/or downwelling, both forms of vertical mantle flow. In the case of vertical mantle flow, the fast

and slow axes of olivine are oriented in such a way that SKS waves of all orientations can pass through the mantle without experiencing splitting. Therefore, splitting results from continental keels may be characterized by primarily null results in all orientations.

2.1.2 Results from Previous Studies

Barruol et al. (1997) investigated shear wave splitting in the eastern United States, using an array of portable and permanent seismometers. They found fast directions parallel to absolute plate motion (roughly ENE-WSW) for most regions in the United States (Barruol et al. 1997) (Figure 2.1). However, in the southeastern United States, they found fast directions parallel to the trends of the Grenville orogeny (roughly NE-SW). This deviation from the continental-scale shear wave splitting pattern could be due to fossil anisotropy or to subvertical asthenospheric flow around the edge of the North American craton (Barruol et al. 1997).

A study by Fouch et al. (2000) further explored the general trends of seismic anisotropy in the eastern United States. In addition to seismic data, they developed a numerical model to approximate mantle flow in this region and used it to determine if the shear wave splitting patterns are best explained by fossil anisotropy, active mantle flow, or a combination of both (Fouch et al. 2000). An analysis of their seismic data revealed that for stations above the North American craton, fast directions are primarily parallel to absolute plate motion (Fouch et al. 2000) (Figure 2.2). However, stations near the continent's margins show

variations from this general trend (Fouch et al. 2000). Using the numerical models, they found that seismic anisotropy beneath the continents results from both the lithosphere and the asthenosphere and that the variation in splitting results can be explained by keel morphology, plate motion, lithospheric deformation history, and mantle rheology (Fouch et al. 2000).

2.2 Previous Shear Wave Splitting in South Carolina

A recent study of shear wave splitting in the southeastern United States reveals some intriguing patterns. Stations located towards the interior of the continent yield splitting results that are generally parallel with absolute plate motion and the fabric of the Appalachians (Figure 2.3) (Long 2009, unpublished data). The data set also includes null measurements along the eastern United States (Figure 2.3) (Long 2009, unpublished data). Several of the stations closest to the edge of the continent exhibit null measurements in a variety of directions and almost no splitting (Figure 2.3) (Long 2009, unpublished data). These measurements possibly indicate an unusual pattern of mantle deformation in this transition region between thick continental crust and thinner oceanic crust. South Carolina is a unique location in which to study this transition, as it contains a clear divide between the coastal and mountainous regions (see Appendix I for a detailed overview of South Carolina's geology).

2.3 Locations Analogous to the United States

Australia and South America are two other continents that both possess passive continental margins and a continental keel, and thus are useful for initial comparison with the eastern United States.

Heintz and Kennett (2005) performed an analysis of seismic data from 190 stations across Australia (Figure 2.4). They did not find a relationship between the fast direction of splitting and absolute plate motion (Heintz and Kennett 2005). However, they did find a correlation between splitting results in regions with strong lithospheric fabric and the direction of that fabric, as well as some stations that yielded only null results (Heintz and Kennett 2005). Based on these results that indicate a complex pattern of anisotropy, they conclude that some shear wave splitting is a result of fossil anisotropy, but that other sources, such as flow around a continental keel, could also contribute.

Southeastern Brazil is another location that is similar to the southeastern United States. Heintz et al. (2003) investigated whether shear wave splitting in Brazil is due to active mantle flow, fossil anisotropy, or a combination of the two. Based on an analysis of sixty-nine events, they found that in both the Brasilia belt and the Ribeira belt, fast directions correlate with lithospheric structural trends (Heintz et al. 2003). Additionally, in the Ribeira belt, the fast direction is parallel to absolute plate motion as well (Heinz et al. 2003). When compared to numeric models, the data appear to be best explained by a complex pattern of anisotropy

that is affected by anisotropy in both the lithosphere and the asthenosphere (Heintz et al. 2003).

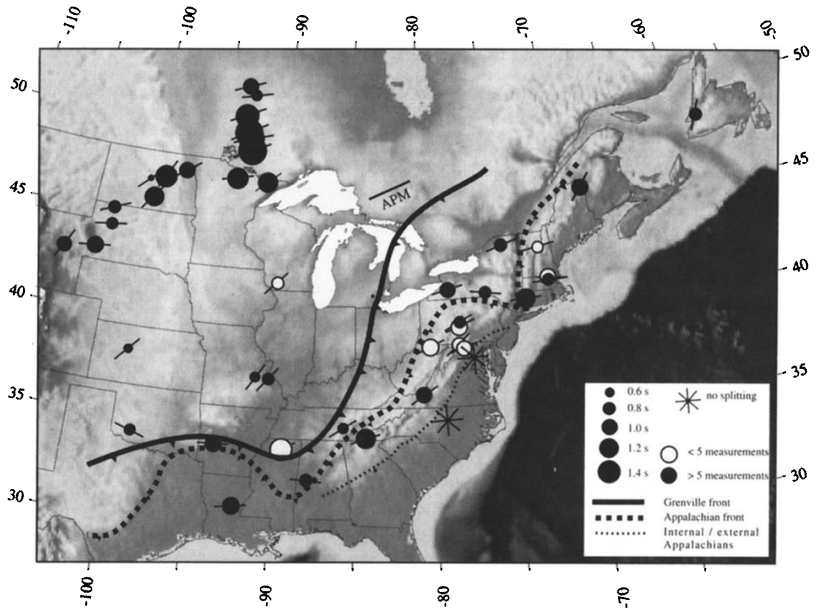

Figure 2.1. Map of the average splitting results from Barruol et al. (1997), and references therein, calculated from individual measurements by weighting each individual measurement by its 95% confidence interval. The size of the circle is proportional to the delay time (in seconds), as indicated in the legend. “No splitting” is a null measurement. The solid dark line indicates the Grenville front, the thick dashed line indicates the Appalachian front, and the thin dotted line indicates the internal/external Appalachians. Most stations show fast directions parallel to absolute plate motion. The North Carolina and Virginia stations located east of the Appalachians yielded no splitting results. (from Barruol et al. 1997)

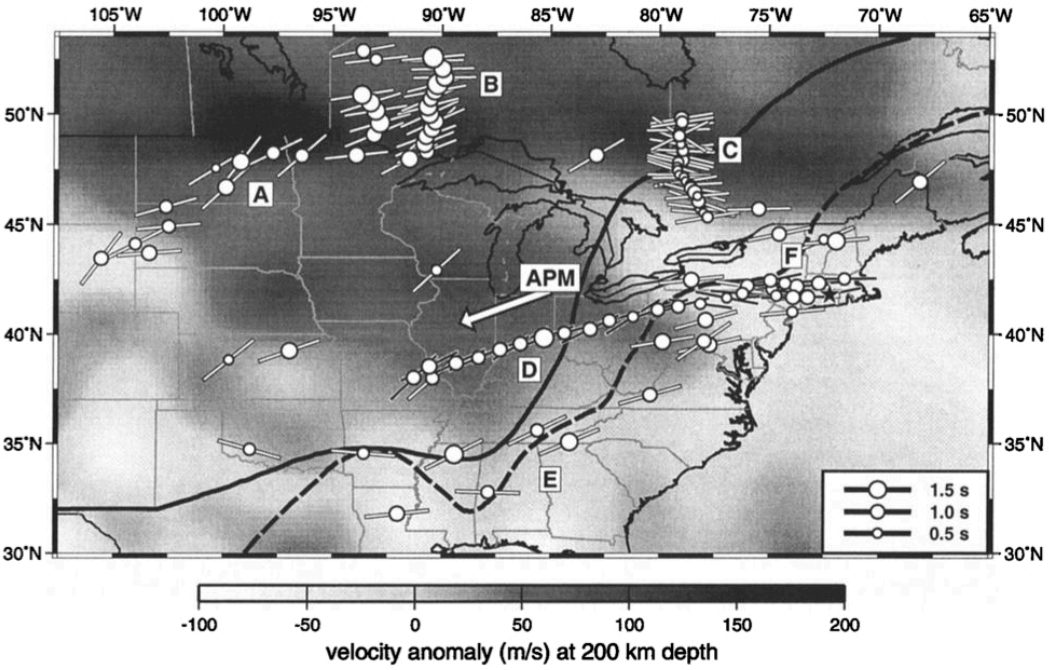

Figure 2.2. Shear wave splitting parameters from several studies in North America (Fouch et al. 2000 and references therein). Fast directions are denoted by azimuth of bar; open circles are scaled to splitting time. Splitting is represented as averaged station parameters. Background is a map view of shear wave velocity anomalies at a depth of 200 km. Fast velocity anomalies are shown by dark shading, and slow velocity anomalies are shown by light shading. The thick solid line indicates the boundary of the Grenville front; the thick dashed line indicates the boundary of the Appalachian front. Almost all stations exhibit fast directions parallel to absolute plate motion. (from Fouch et al. 2000)

a)

b)

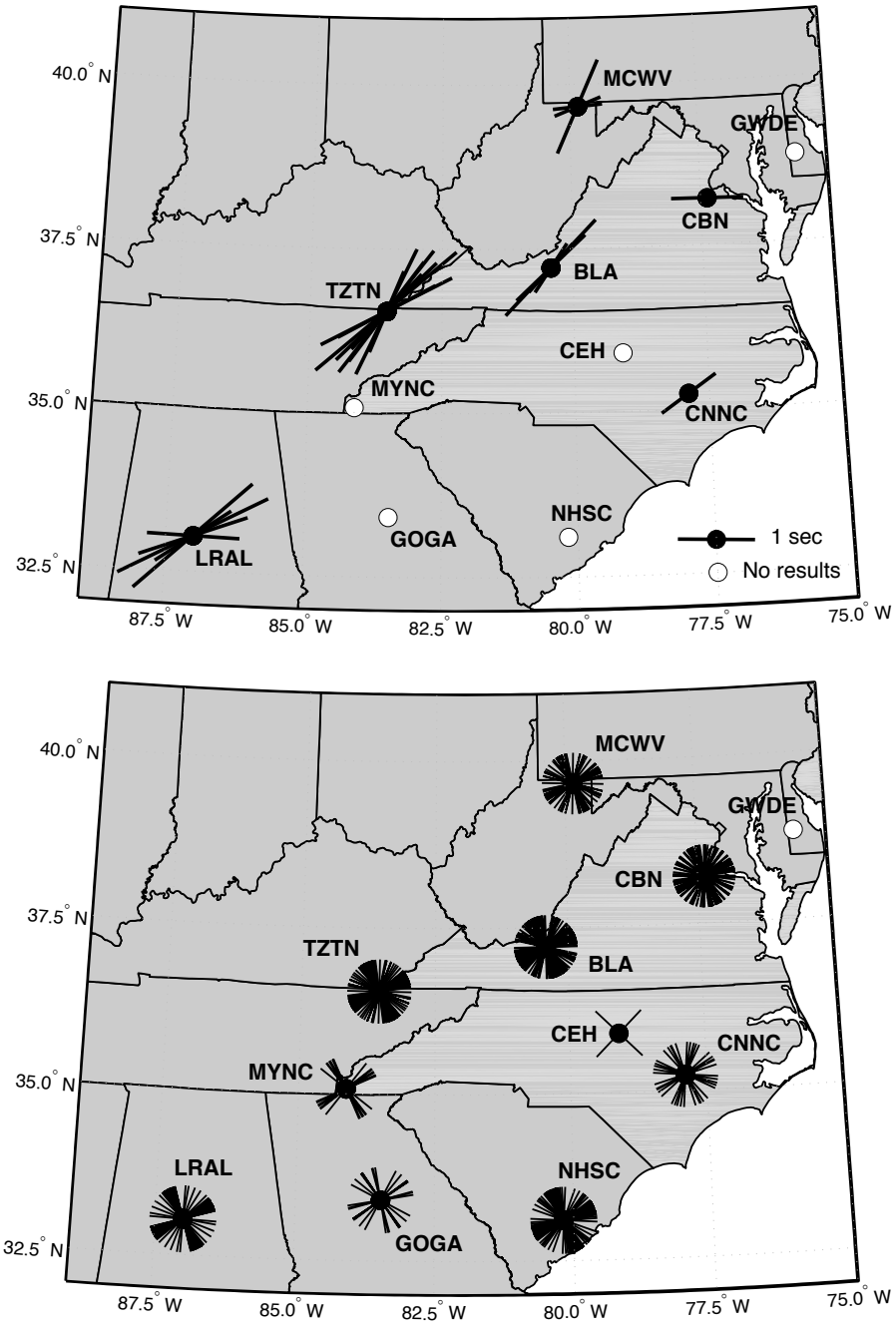

Figure 2.3. (a) Splitting and (b) null results from ten stations in the southeastern United States. All splitting results exhibit fast directions parallel to the grain of the Appalachians and to NE-SW absolute plate motion. Some stations, such as LRAL and MYNC, exhibit clear "cross" null results, while other stations, such as CNNC and CNB, exhibit "flower" null results. (from Long 2009, unpublished data)

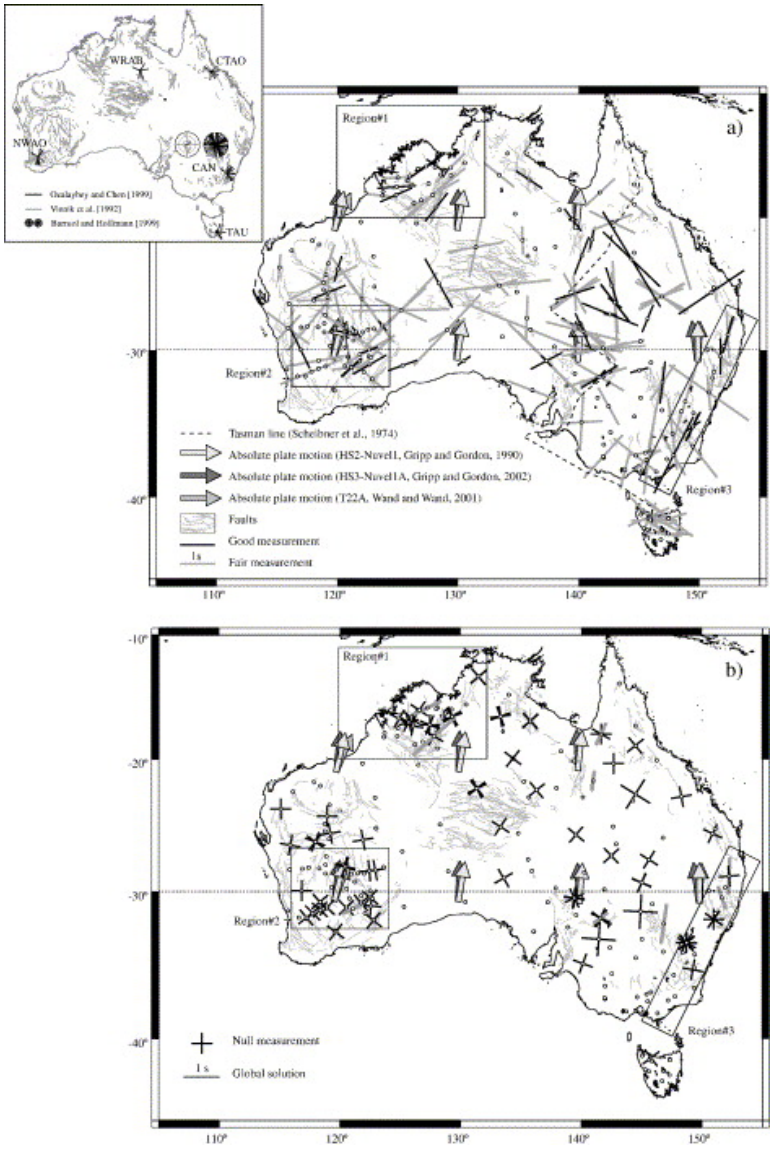

Figure 2.4. Measured directions of the orientation plane of the fast shear wave on the Australian continent from Heintz and Kennent (2005). (a) Good and fair measurements. The length of each line is proportional to the delay time. (b) Null measurements. The length of each line is proportional to the delay time. Crosses denote the absence of splitting: each branch is either parallel or perpendicular to the backazimuth of the incoming waves. Thick arrows represent the absolute plate motion. (from Heintz and Kennent 2005)

3. DATA AND METHODS

3.1 South Carolina Earth Physics Project

This project utilizes data from a temporary seismometer array, the South Carolina Earth Physics Project (SCEPP), which was deployed at high schools across South Carolina from 2001 until 2004. The stations are distributed evenly across the state in the east-west direction, and fairly evenly in the north-south direction (Figure 3.1). A small exception is the most northerly region of the state, along the North Carolina border, in which there are very few stations. However, for the purpose of this study, I am primarily interested in the variation of shear wave splitting from east to west, and so the coverage is excellent.

The array consists of 25 digital seismometers that were operational between 2001 and 2004 (Table 3.1). The length of time each station was in operation varied. Several stations were in operation for approximately 2.75 years, from September 2001 until June 2004, while one station, CREEK was in operation for the shortest amount of time, from 2 February 2004 to 30 June 2004. Each seismometer recorded teleseismic events felt at the station. A few stations recorded greater than 50 events; some recorded none at all. The maximum number of events recorded at a single station was 304 events at station AGBLF.

3.2 Data Acquisition

I obtained this data from the IRIS SeismiQuery database (IRIS 2009). I requested all events of magnitude 5.75 to 9.75, starting from the first of the month after the installation. All events are located within 88° to 130° from the seismometer (Figure 3.2, Appendix II), thus ensuring that the ray path of the wave is near vertical upon arrival (Silver and Chan 1991). The following information is given for each event: date, time, epicenter location, focal depth, magnitude, backazimuth, distance from station, and initial polarization of the wave. I chose to only analyze the SKS phase of the wave, for reasons discussed in the Introduction.

3.3 SplitLab

I use SplitLab, a program developed by Wuestefeld et al. (2008), to identify shear wave splitting from raw seismograph data. SplitLab is a graphical user interface that operates in the MATLAB environment. For each event, I look at the waveform from 60 seconds before the estimated arrival time to 2400 seconds after the estimated arrival time, as the actual SKS wave typically arrives within that window. I then apply a filter of 0.02 to 0.125 Hz to remove unwanted noise without affecting the wave components or splitting parameters. I visually examine each waveform and determine the region in which SWS would be likely, based on timing predictions and waveform shape (Figure 3.3). I then select that region, and ask SplitLab to perform its analysis on it. It uses two different

methods to analyze the waveforms, and I use both together to determine which events yielded useable data.

3.4 Transverse Component Minimization Method

The first method used is the transverse component minimization method, developed by Silver and Chan (1991). For an isotropic medium, a shear wave can be modeled by the following vector function:

$$\mathbf{u}(\omega) = w(\omega)e^{-i\omega T_0}\,\hat{\mathbf{p}} \qquad \text{Eq. 3.1}$$

where $w(\omega)$ is the wavelet function for the waveform, T_0 is the time between the event time and the arrival time, and **p** is a unit vector pointing in the displacement direction and perpendicular to the propagation direction of the wave. To determine the splitting parameters for a wave that has traveled through an anisotropic medium, SplitLab estimates several values for the fast direction (ϕ) and delay time (δt), and by projecting **p** on to the fast and slow directions of the wave, represents analogous information as that determined by Equation 1 as:

$$\Gamma = e^{i\omega\delta T(\phi,\delta t)} \qquad \text{Eq. 3.2.}$$

SplitLab computes the covariance matrix of particle motion and its eigenvalues of all possible pairs of ϕ and δt, to determine which best turns Eq. 3.2 back into the form of Eq. 3.1. Then, it is possible to determine the values of ϕ and δt that best characterize the splitting of the waveform (Silver and Chan 1991). The optimum result for a waveform experiencing shear wave splitting is shown as the radial and transverse components being transformed into simply vertical and linear motion, respectively, that, when recombined, results in an ellipsoid with a

straight line through the long axis (Figure 3.4). If the waveform illustrates a null result, the graph of the initially transformed wave components looks similar to that of a splitting result; however, the particle motion before and after the transformation is linear (Figure 3.5). SplitLab calculates an error space for the ϕ and δt chosen.

Using the quality of the graphs and size of the error space as guides, I then classify the result as good, fair, or poor and determine if it is a null result or not. In a good quality splitting result, the fast and slow corrected waveforms have the same shape, the corrected radial component (Q) remains sinusoidal, the corrected transverse component (T) is linear, the particle motion before correction is clearly elliptical, the particle motion after correction is linear through the long axis of the ellipse, the error space is small, and the best-fitting ϕ and δt determined by the different methods are similar (ϕ-values within 10 degrees of each other and δt-values within 0.2 seconds of each other). In a fair quality splitting result, one or more of the following is true: the fast and slow corrected waveforms will still be fairly similar, although there may be some minor differences; Q remains fairly sinusoidal; T becomes fairly linear, with some small deviations; particle motion before correction is fairly ellipsoidal; particle motion after correction is fairly linear; the error space is still relatively small, but may expand with respect to one of the two parameters; and there will be greater variation within the ϕ- and δt-values. For a null result, the corrected fast and slow waves have a similar shape, particle motion before and after correction is linear, the error space is not well-

constrained, the ϕ-values for the different methods are approximately 45° apart, and the δt-values are bounded by infinity. In the case of a null result, the fast direction is assumed to be the same as or perpendicular to the initial polarization direction of the waveform, since the wave does not diverge from this original direction.

3.5 Rotation-Correlation Method

The second method used is the rotation-correlation method, which uses a grid-search approach to find the coordinate rotation of the shear wave and delay time that best resolves the orthogonal components into linear particle motion (Fukao 1984, Bowman and Ando 1987). Since most of the motion due to the shear wave is in the horizontal plane, only the horizontal components of the waveform are used in this analysis (Bowman and Ando 1987).

To determine the best-fitting angle of rotation and delay time of each event at a station, SplitLab rotates the seismograms at 1° intervals and then calculates the maximum cross-correlation coefficient for delay times of half the sampling rate (Wuestefeld et al. 2008). SplitLab then plots a topographic map of the correlation coefficient on the axes of ϕ versus δt (Figure 3.4, Figure 3.5). To find good or fair splitting results, I look for a small region on this map to enclose the best (ϕ, δt) pair. I also look for elliptical particle motion before the splitting analysis is performed and linear particle motion after the analysis is performed (Figure 3.4). Null results are characterized by linear particle motion both before and after the splitting analysis (Figure 3.5). Using the quality of the graphs and

size of the error space as guides, I then classify the result as good, fair, or poor and determine if it is a null result or not (as discussed in the previous section).

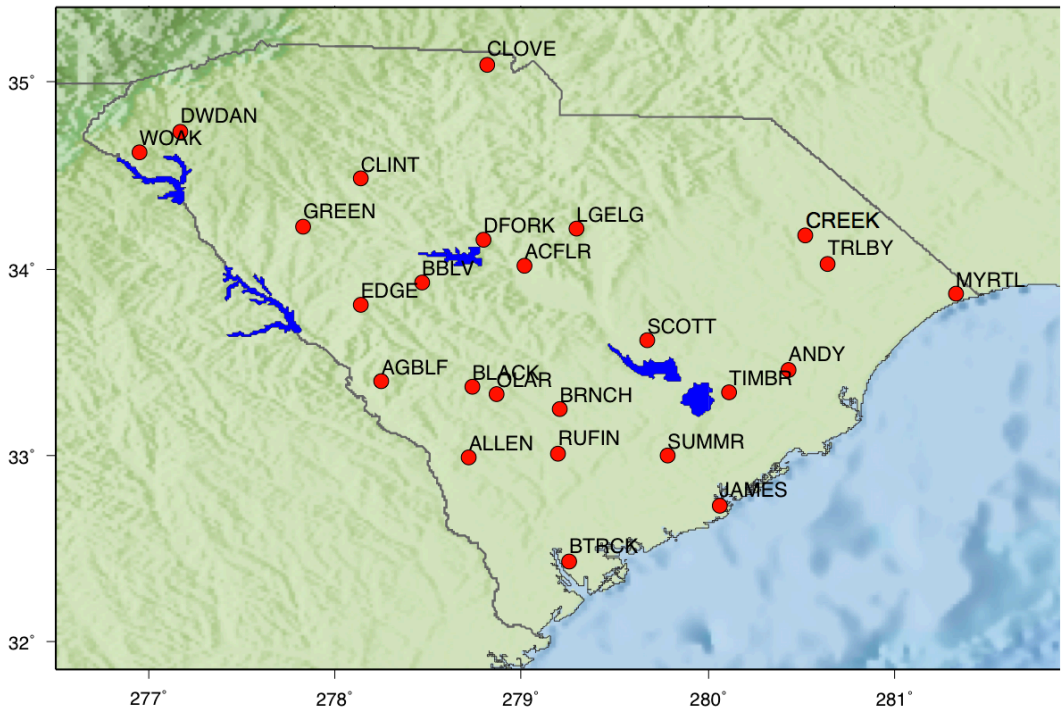

Figure 3.1. Map of all stations in the SCEPP network.

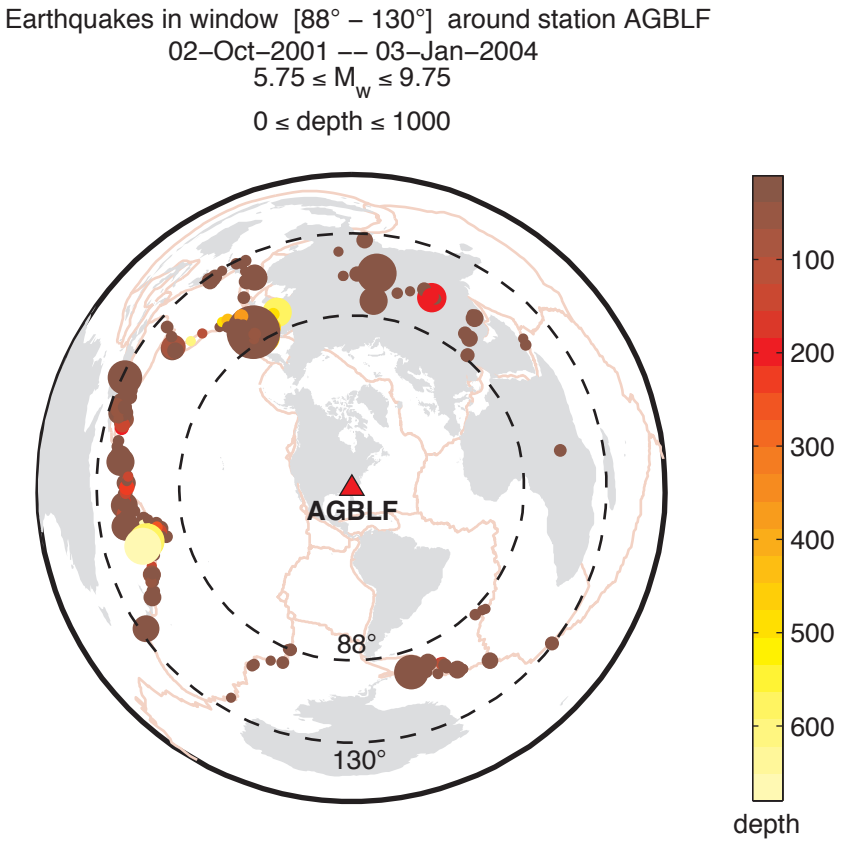

Figure 3.2 Example of a polar projection of all events, represented by colored circles, possibly recorded at a station (AGBLF). These events are of large enough magnitude ($5.75 \leq M_W \leq 9.75$) and at an appropriate distance from the station (88° to 130°) so that it is possible for the station to record the SKS arrival. The depth of the focus of the event is indicated by the color of the circle, and the magnitude of the event is indicated by the size of the circle (larger circles represent larger magnitudes).

Table 3.1. List of all stations used in this study. # Events = the total number of distinguishable events recorded at each station. # Splits = the number of splitting results, both good and fair, at each station. # Nulls = the number of null results, both good and fair, at each station.

Station	Start Date	End Date	Lat (°N)	Lon (°E)	# Events	# Splits	# Nulls
ACFLR	09/17/01	01/24/04	34.02	-80.98	119	0	3
AGBLF	09/11/01	06/30/04	33.40	-81.76	394	0	7
ALLEN	12/06/01	06/27/02	32.99	-81.28	20	0	0
ANDY	03/18/02	06/30/04	33.46	-79.57	0	0	0
BBLV	09/11/01	06/30/04	33.92	-81.53	243	2	2
BLACK	02/15/02	06/30/04	33.37	-81.26	232	0	5
BRNCH	09/11/01	06/30/04	33.25	-80.79	173	0	1
BTRCK	09/11/01	06/30/04	32.43	-80.75	112	0	1
CLINT	11/13/01	06/30/04	34.48	-81.86	144	1	6
CLOVE	01/15/02	06/30/04	35.10	-81.18	71	0	0
CREEK	02/02/04	06/30/04	34.13	-79.33	27	1	0
DFORK	09/17/01	06/30/04	34.15	-81.20	34	0	1
DWDAN	09/11/01	06/30/04	34.74	-82.83	25	0	1
EDGE	10/22/01	06/30/04	33.81	-81.86	0	0	0
GREEN	09/11/01	06/30/04	34.23	-82.17	32	0	1
JAMES	09/11/01	06/30/04	32.73	-79.93	14	0	0
LGELG	09/17/01	06/30/04	34.22	-80.71	22	0	0
MYRTL	09/11/01	06/19/04	33.86	-78.67	0	0	0
OLAR	07/26/02	06/30/04	33.33	-81.13	32	0	0
RUFIN	09/11/01	06/30/04	33.01	-80.81	33	0	1
SCOTT	01/08/03	06/30/04	33.62	-80.32	34	0	0
SUMMR	09/11/01	02/07/03	32.99	-80.22	0	0	0
TIMBR	09/11/01	06/30/04	33.34	-79.89	31	0	3
TRLBY	09/17/01	05/12/03	34.03	-79.36	0	0	0
WOAK	09/17/01	06/30/04	34.62	-83.05	34	0	2

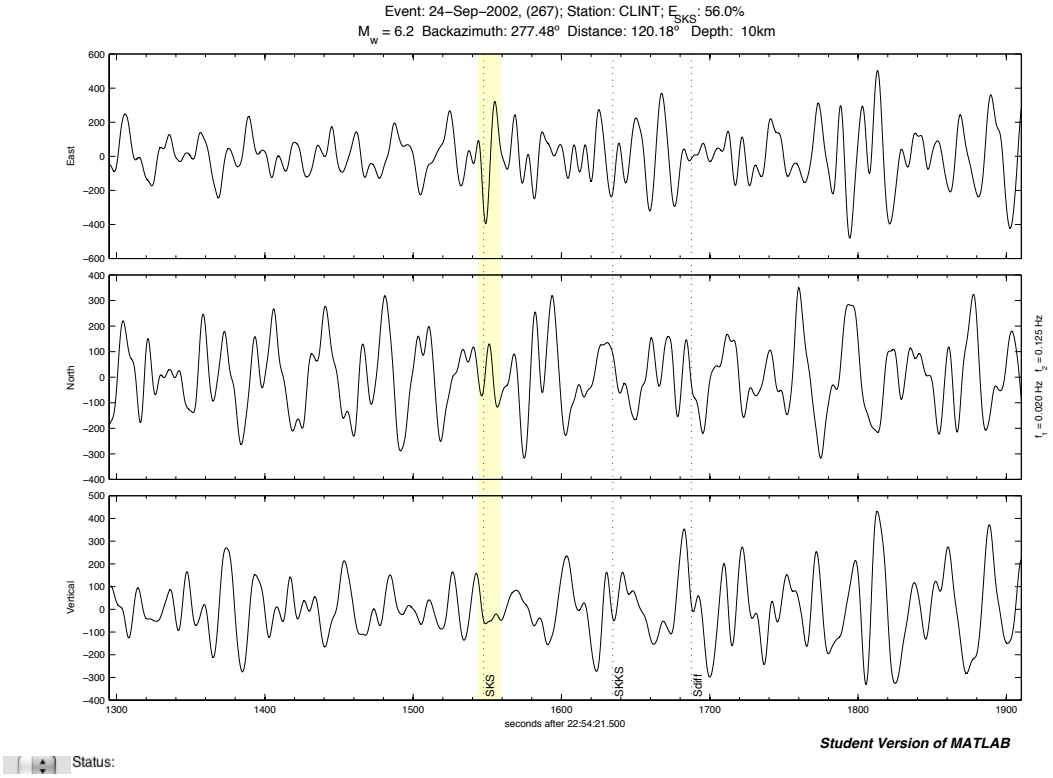

Figure 3.3. Seismograms of the 24 September 2002 event (filter: 0.02 to 0.125 Hz) from the CLINT station. The top seismogram shows the motion in the N direction, the middle seismogram shows the motion in the E direction, and the bottom seismogram shows the motion in the vertical direction. Dashed lines indicate estimated arrival times of the different types of waves. A clear change from random background noise to a sine wave is detectable at the beginning of the highlighted region, marking the arrival of the SKS wave. The highlighted region is the portion of the seismogram used in the analysis.

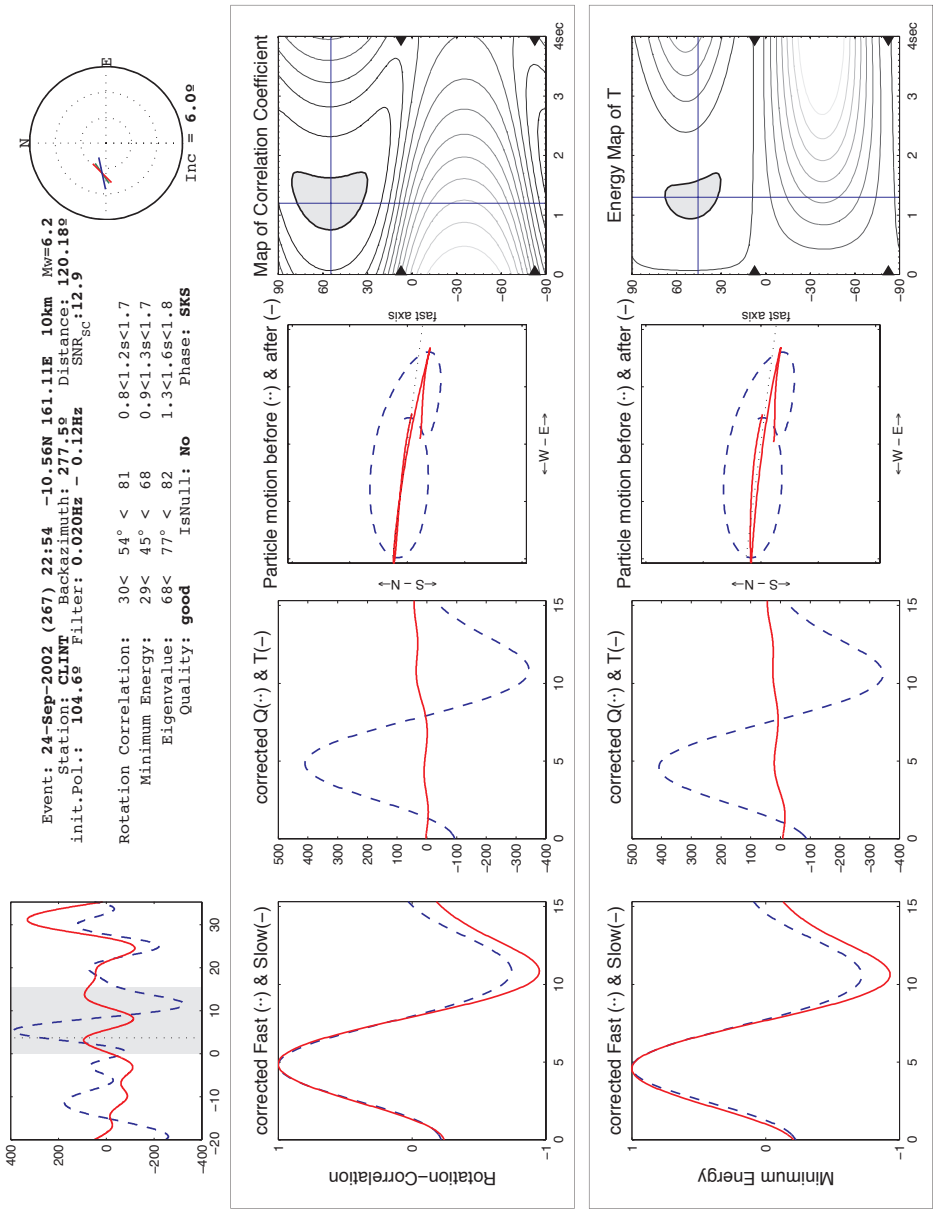

Figure 3.4. Example of a good quality splitting result. This measurement is of an event at the CLINT station that occurred on 24 September 2004. The transverse component minimization method is the lower set of graphs. The rotation-correlation method is the upper set of graphs. For both methods, the corrected fast and slow waves have the same shape, particle motion before correction is elliptical, particle motion after correction is linear through the long axis of the ellipse, the error space is small, and the best-fitting ϕ and δt are similar. The ϕ-values are listed as open intervals in the first column, and the δt-values are listed as open intervals in the second column.

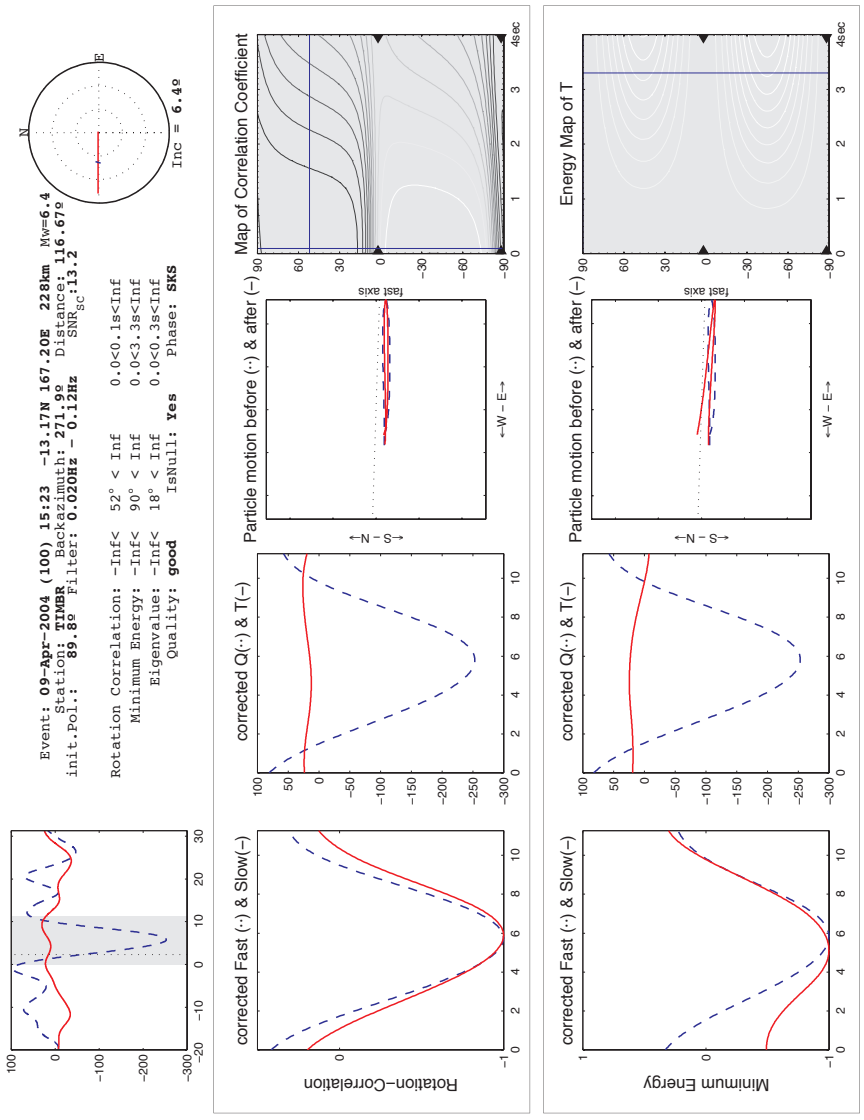

Figure 3.5. Example of a good quality null result. This measurement is of an event at the TIMBR station that occurred on 09 April 2004. The transverse component minimization method is the lower set of graphs. The rotation-correlation method is the upper set of graphs. For both methods, the corrected fast and slow waves have a similar shape, particle motion before and after correction is linear, the error space is not well-constrained, the ϕ-values for the different methods are approximately 45° apart, and the δt-values are bounded by infinity (represented by Inf. or 4.0s, since 4.0s is SplitLab's maximum value for δt). The ϕ-values are listed as open intervals in the first column, and the δt-values are listed as open intervals in the second column.

4. RESULTS

4.1 Usable events

Out of the 1736 total events recorded, there are 70 that were initially suggestive of possible shear wave splitting or a null result. This number of results is typical of temporary station arrays. Out of these 70, there is 1 splitting result classified as ‘good’, 3 splitting results classified as ‘fair’, 10 nulls classified as ‘good’, and 24 nulls classified as ‘fair’, for a total of 38 useable results (Table 4.1, Appendix III). The remaining 32 events are either too noisy or do not yield definitive results to be used in this study. Since the resultant dataset is fairly small, I group both the ‘good’ and ‘fair’ measurements for the splitting results and for the null results together.

4.2 Splitting results

All splitting results are shown in Figure 4.1. The transverse component minimization method and the rotation correlation method yield similar results for all events and so values for the fast direction and the delay time are averaged. Two splitting results occurred at station BBLV. The event on 03 January 2004 had a delay time of 1.6 seconds and a fast polarization direction of 49°, and the event on 25 January 2004 had a delay time of 0.9 seconds and a fast polarization direction of 46.5°. The event at station CLINT occurred on 24 September 2002,

and had a delay time of 1.2 seconds and a fast polarization direction of 49.5°. The event at station CREEK occurred on 07 May 2004 and had a delay time of 1.0 seconds and a fast polarization direction of 24.5°.

All four splitting results have a general NE-SW trend. The event at station CREEK is oriented slightly more north when evaluated with the transverse component minimization method; however, when evaluated with the rotation-correlation method, all of the splitting results have very similar fast directions.

All four of these stations exhibit similar delay times as well. The largest delay time is one of the events at station BBLV, which also exhibits the smallest delay time for the other event that occurred there.

4.3 Null results

Null results occurred at stations throughout the array (Figure 4.2). Both the null result and its orthogonal complement are plotted, since both are allowable directions of wave motion, if the null results from anisotropy. The most null results recorded at a single station is 7, recorded at station AGBLF. Stations with more null results are somewhat clumped in the central western part of the state (Figure 4.2).

At stations that recorded multiple null results, most of the results at each station had similar polarization directions. The polarization direction varied from station to station. Stations with null results that produce a “cross”-shape indicate that shear wave splitting may be occurring at that station, since some shear waves may arrive already oriented in that direction and thus would not be split. Stations

with null results that produce a “flower”-shape can indicate either a complete lack of anisotropy, a vertical fast direction, or complex/multiple layers of anisotropy.

However, twelve of the thirteen stations exhibit a general NE-SW trend in the initial polarization direction of the wave. Two stations, CLINT and ACFLR, have null results with varied polarization directions at the same station. In particular, the directions at station CLINT span practically all 360°. There is no clear east-west trend in the null results moving across the state.

Table 4.1: List of all usable events at all stations. evla = event latitude in °N, evlo = event longitude in °E, rc ϕ and rc δt = fast direction and delay time calculated using the rotation correlation method, sc ϕ and sc δt = fast direction and delay time calculated using the transverse component minimization method, pol_i = initial polarization of the S-wave, 'null?' refers to if the results if a split (no) or null (yes). Bold/non-bold entries differentiate between events.

station	date	evla	evlo	rc ϕ	rc δt	sc ϕ	sc δt	pol_i	null?	quality
CLINT	**09/24/02**	**-10.56**	**161.11**	**54**	**1.2**	**45**	**1.3**	**104.60**	**no**	**good**
BBLV	01/03/04	-22.25	169.68	35	1.2	59	2.1	69.40	no	fair
BBLV	**01/25/04**	**-16.83**	**-174.02**	**41**	**0.8**	**54**	**1**	**87.10**	**no**	**fair**
CREEK	05/07/04	-21.99	170.28	33	0.7	16	1.2	97.80	no	fair
CLINT	**04/26/02**	**13.09**	**144.62**	**89**	**inf**	**42**	**inf**	**135.50**	**yes**	**good**
CLINT	08/02/02	29.28	138.97	81	inf	43	inf	143.80	yes	good
BLACK	08/02/02	29.28	138.97	-70	inf	63	inf	155.60	yes	fair
CLINT	**08/19/02**	**-21.70**	**-179.51**	**31**	**inf**	**-8**	**inf**	**77.70**	**yes**	**good**
AGBLF	**08/19/02**	**-21.70**	**-179.51**	**20**	**inf**	**-21**	**inf**	**64.80**	**yes**	**fair**
AGBLF	12/12/02	-4.79	153.27	42	inf	-81	inf	87.90	yes	fair
BLACK	**12/17/02**	**-56.95**	**-24.83**	**-68**	**inf**	**-23**	**inf**	**327.00**	**yes**	**fair**
CLINT	01/04/03	-20.57	-177.66	34	inf	77	inf	78.80	yes	fair
AGBLF	01/04/03	-20.57	-177.66	17	inf	-22	inf	66.70	yes	fair
CLINT	**01/20/03**	**-10.49**	**160.77**	**59**	**inf**	**12**	**inf**	**106.30**	**yes**	**good**
CLINT	05/13/03	-17.29	167.74	39	inf	-7	inf	83.40	yes	fair
BLACK	**05/26/03**	**38.85**	**141.57**	**-83**	**inf**	**57**	**inf**	**142.60**	**yes**	**fair**
ACFLR	**05/26/03**	**38.85**	**141.57**	**-85**	**inf**	**-40**	**inf**	**133.20**	**yes**	**fair**
AGBLF	07/27/03	-21.08	-176.59	-16	inf	68	inf	68.40	yes	fair
BBLV	07/27/03	-21.08	-176.59	39	inf	-8	inf	83.30	yes	fair
BBLV	**07/27/03**	**47.15**	**139.25**	**-64**	**inf**	**69**	**inf**	**155.50**	**yes**	**good**
BLACK	**07/27/03**	**47.15**	**139.25**	**-64**	**inf**	**-21**	**inf**	**159.10**	**yes**	**good**
ACLFR	09/02/03	-15.23	-173.22	25	inf	72	inf	76.10	yes	fair
BRNCH	**09/27/03**	**50.40**	**87.81**	**57**	**inf**	**16**	**inf**	**198.60**	**yes**	**fair**
ACFLR	09/30/03	-30.44	-177.40	35	inf	-15	inf	82.30	yes	fair
BLACK	**10/08/03**	**42.65**	**144.57**	**-68**	**inf**	**-27**	**inf**	**157.50**	**yes**	**fair**
AGBLF	12/25/03	-22.25	169.49	28	inf	-14	inf	74.10	yes	good
AGBLF	**01/03/04**	**-22.25**	**169.68**	**23**	**inf**	**74**	**inf**	**77.80**	**yes**	**fair**
AGBLF	01/25/04	-16.83	-174.20	22	inf	73	inf	68.00	yes	fair
RUFIN	**03/09/04**	**-32.56**	**-177.97**	**-84**	**inf**	**-36**	**inf**	**54.30**	**yes**	**fair**
WOAK	03/09/04	-32.26	-178.36	16	inf	58	inf	63.50	yes	fair
DFORK	**03/14/04**	**-17.27**	**-172.32**	**28**	**inf**	**75**	**inf**	**76.30**	**yes**	**fair**
GREEN	04/05/04	36.51	71.03	-11	inf	-60	inf	214.20	yes	fair
TIMBR	**04/09/04**	**-13.17**	**167.20**	**52**	**inf**	**90**	**inf**	**89.80**	**yes**	**good**
TIMBR	04/27/04	-17.67	167.76	45	inf	1	inf	87.60	yes	good
DWDAN	**05/29/04**	**34.25**	**141.41**	**-83**	**inf**	**-37**	**inf**	**156.30**	**yes**	**fair**
WOAK	**05/29/04**	**34.25**	**141.41**	**15**	**inf**	**-21**	**inf**	**136.20**	**yes**	**good**
BLACK	**05/29/04**	**34.25**	**141.41**	**-67**	**inf**	**-26**	**inf**	**160.60**	**yes**	**good**
TIMBR	06/22/04	-10.90	166.26	50	inf	15	inf	92.90	yes	fair

a.

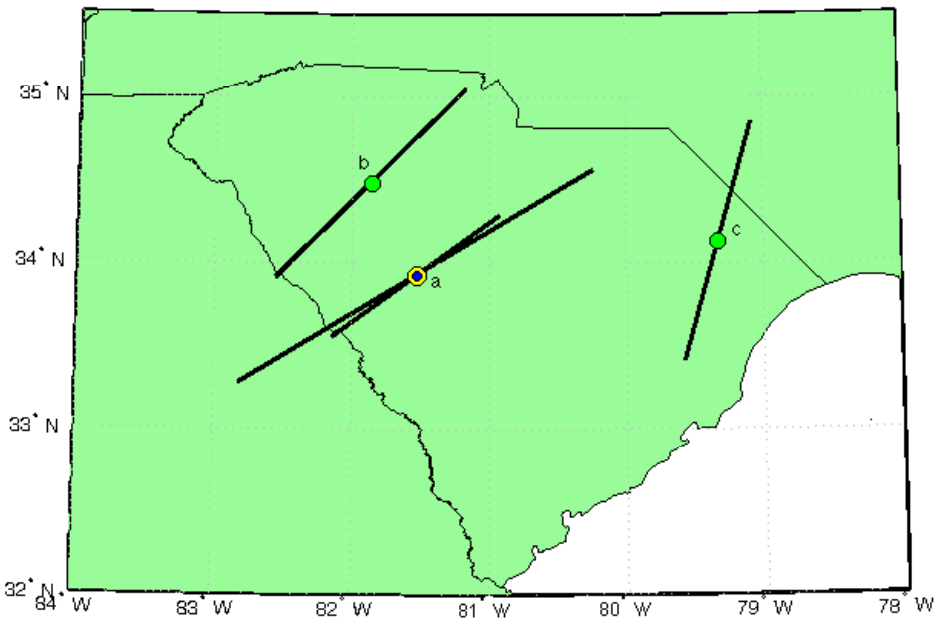

b.

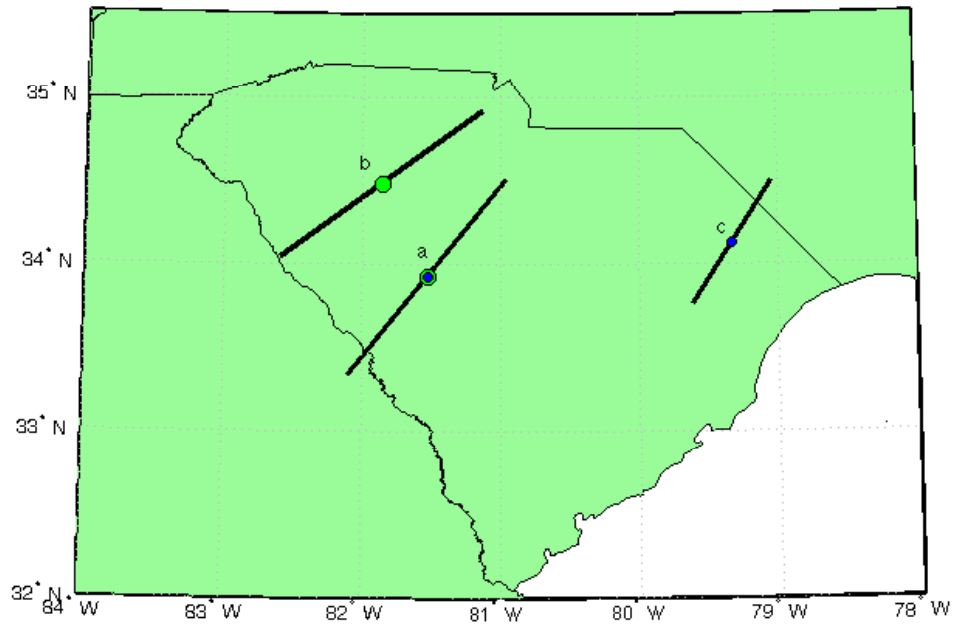

Figure 4.1. All splitting results for both a) transverse component minimization method and b) rotation correlation method. Length of bar is scaled to indicate delay time. The color of circle at station indicates delay time as follows: 2.2s>δt>1.7s is yellow, 1.7s>δt>1.2s is green, 1.2s>δt is blue. Station names are as follows: a) BBLV, b) CLINT, and c) CREEK.

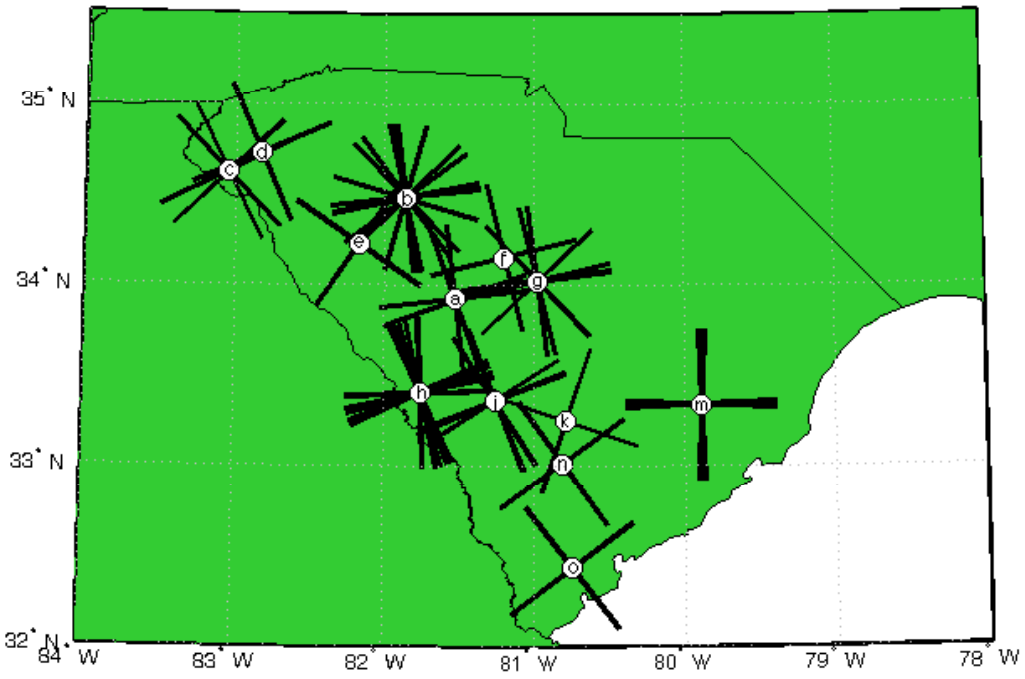

Figure 4.2. Map of all the null results. Both the initial polarization direction and the direction perpendicular to it are plotted for each null result. Station names are as follows: a) BBLV, b) CLINT, c) WOAK, d) DWDAN, e) GREEN, f) DFORK, g) ACFLR, h) AGBLF, i) BLACK, k) BRNCH, m) TIMBR, n) RUFIN, and o) BTRCK.

5. DISCUSSION

The results from this analysis of the SCEEP network indicate an intriguing pattern of anisotropy beneath South Carolina. The high volume of nulls compared with splitting results is in agreement with the previous studies (Barroul et al. 1997, Fouch et al. 2000, Long 2009). Also, the general direction of the few splitting results obtained match the trends of absolute plate motion and/or fossil anisotropy in this region.

There is no definitive spatial pattern between the location of stations with nulls in a variety of polarization directions and stations with splitting results and associated nulls. However, it is worth noting that none of the southern-most stations yielded splitting results. To interpret the results, I evaluate the shear wave splitting patterns in the context of four possible situations.

5.1 Lack of anisotropy

A fourth hypothesis that could explain these SWS splitting is simply that there is no anisotropy beneath South Carolina. In this case, I would expect to have no splitting results, since there is no anisotropy, and that all of the null results would be flower-shaped, since there would be no preferred orientation in which the wave would move through the mantle material.

Since there are relatively few splitting results in this study, these results could be interpreted as aberrations in the data and disregarded. However, the agreement of these results with those of previous studies indicates that the splitting results are plausible, and thus should not be disregarded. Also, not many of the null results exhibit a clear flower shape, and so it is reasonable to conclude that there is anisotropy at some locations in this region. Thus, the observed results are not consistent with this hypothesis, so a lack of anisotropy beneath South Carolina is not a possible explanation for the SWS patterns.

5.2 Fossil anisotropy

The first possible interpretation is that these results reflect splitting parallel to the grain of the lithosphere, i.e. fossil anisotropy. As discussed earlier, fossil anisotropy would result in shear wave splitting with fast directions parallel to the known maximum shear direction. Therefore, I would expect the presence of fossil anisotropy in the study region to be indicated by clear splitting results, in a roughly NE-SW orientation, parallel with the maximum direction of shear of the Appalachian belt. All splitting results, using both methods, exhibit very close to NE-SW orientations (Figure 4.1). Therefore, it is possible that the observed SWS is due to fossil anisotropy located in the Appalachian belt. The spatial locations of the stations where the splitting results occurred also support this interpretation, as splitting results occurred primarily in the parts of the state underlain by the Appalachian belt. Under this interpretation, I would regard the splitting result at

the CREEK station to be a possible erroneous measure, and would wait for more data at this location to determine if it is an actual split or not.

The null results also somewhat support this hypothesis, with the exception of the results from station CLINT, and possibly ACFLR (Figure 4.2). In the case of fossil anisotropy, I would expect null results to exhibit two clear orthogonal components, forming a "cross", since null results would only occur in the event that the initial polarization of the SKS wave was parallel or orthogonal to the orientation of the fast direction. At all stations where the null results form crosses, with the exception of TIMBR, the fast direction is oriented NE-SW, parallel to the direction of maximum shear of the Grenville belt. This observation is consistent with the fossil anisotropy interpretation, because for a wave to remain unsplit, it must already be oriented in the direction of the maximum shear in the rocks. It is worth noting that at stations with only one or two measurements, such as GREEN or BRNCH, it is difficult to definitively determine if the observed pattern is, in fact, a cross, or if there is simply not enough data.

5.3 Absolute plate motion

A second possible interpretation is that the observed SWS patterns are due to asthenospheric flow associated with absolute plate motion (APM). In this case, I would expect the splitting results to be oriented parallel to absolute plate motion, in this case, ENE-WSW, for similar reasons as in the fossil anisotropy, except that in this case, there is active deformation. The observed splitting results are somewhat consistent with this APM hypothesis, as they are oriented in a general

NE-SW direction. With so few results, it is difficult to determine if they are actually oriented ENE-WSW and thus parallel with absolute plate motion. As there are no results that suggest a drastically different orientation from NE-SW, it is possible that APM is a source of anisotropy in this region.

Since the APM is so similar to the orientation of the fossil anisotropy, an analysis of the null results in the context of APM is essentially the same as for the situation of fossil anisotropy. Vertical asthenospheric flow, which is not associated with APM, is discussed in the next section. Therefore, from a joint analysis of the splitting and null results, it appears that anisotropy due to APM is a viable interpretation.

5.4 Flow around a continental keel

In the situation of flow around a continental keel causing the observed patterns, I would expect inland stations to exhibit splitting results consistent with the rest of the continental interior and "cross" null results with an arm parallel to the general direction of the splitting. In this case, the direction of shear wave splitting in the continental interior is generally NE-SW (Barruol et al. 1997, Fouch et al. 2000, Long unpub.). For stations located closer to the edge of the continent, I would expect primarily "flower" null results, due to the vertical flow around the edge of the continental keel, as discussed earlier.

The results from my work reflect this situation fairly well. All of the splitting results are located in the part of the state closed to the continental interior and match previously determined continental trends well (Figure 2.2, Figure 2.3,

Appendix I). The null results are not as clear; however, the fact that the majority of the results are null results and not splits indicates that there is a prevalence of nulls, which could be expected in a situation of vertical asthenospheric flow. Also, the null results extend to the coastline, indicating the possibility of vertical mantle flow in that region. As many stations have relatively few results, it is difficult to tell if the observed null results are cross- or flower-shaped. Thus, it is possible that mantle flow around a continental keel is the cause of the observed SWS patterns.

5.5 Transition zone at the continental keel

A careful analysis of the three remaining interpretations suggests that a combination of the three, where stations to the interior of the continent exhibit splitting parallel with fossil anisotropy and/or APM and stations at the edge of the keel exhibit “flower” null results, is the best explanation for the observed results of this study. As stated earlier, in the interior of a continental keel, I would expect SWS results to be in agreement with the rest of the continent, and to the outside of the continental keel, I would expect results typical of vertical mantle flow. In this study, the splitting results are located towards the interior of the continent and match results from previous studies. Additionally, the splitting results are oriented in such a way that can be explained by either fossil anisotropy or APM, since the orientation of the fast directions in both these situations is similar. Further studies of this area will help to better constrain the orientation of the splitting results, thus indicating which interpretation is more plausible.

The null results also support this combination interpretation, as null results are prevalent throughout the state, and there is some indication of "flower" shapes at a few stations, such as CLINT and ACFLR. Also, many of the stations at the coast yielded only one or two null results, and so it is difficult to determine if the observed result is a cross or a flower. I would expect future studies to find that the pattern of nulls at these stations is flower-shaped, since that would be consistent with my hypothesis.

Therefore, these observations support the interpretations that the observed SWS patterns are due to fossil anisotropy or mantle flow around a continental keel. They also indicate that it is possible to identify a transition zone by a change in the pattern of seismic anisotropy. In South Carolina, this transition zone must occur over a short distance, as stations in the northwestern part of the state are similar to those farther inland, while stations in the southeastern part of the state indicate much more varied results. Therefore, I can tentatively conclude that the transition zone occurs along the NE-SW trending line dividing off the coastal third of the state.

5.6 Comparison with studies at analogous locations

These results are similar to the SWS results from Australia and Brazil. At all three locations, the fast directions are found to be parallel to lithospheric structures that could contribute to fossil anisotropy. Additionally, in both Brazil and South Carolina, APM is parallel with these structural trends, making it difficult to determine if APM or fossil anisotropy is the single source for the

splitting. In Australia, APM is not parallel to fossil anisotropy, and the available results indicate splitting tentatively consistent with fossil anisotropy, rather than APM. Also, the presence of "flower"-shaped null results near the coast at all three locations could be either the result of active mantle flow around a continental keel or simply the lack of anisotropic material closer to the coast. Therefore, the results from South Carolina are consistent with results from similar locations elsewhere in the world, and additional information is needed to determine the source of anisotropy at these three locations.

5.7 Evaluation of stations

While this study contributes further understanding to the dynamics of this region, the results are not definitive, and further work is needed. The stations used in this study are fairly noisy. Located at high schools, they experience a fair amount of human traffic and associated seismic noise. Therefore, results from many events recorded at these stations had to be discarded because of the high level of background noise.

Additionally, these stations were only in operation for a short time period. Although a few stations were in operations for almost two years, many were in operation for less than a year. This lack of temporal resolution further hindered the analysis by limiting the number of events to analyze and making it difficult to determine if an observation at a station was an anomaly or part of a trend.

Fortunately, there are plans to improve this data set. The USArray network of seismometers is sweeping across the nation, and is expected to arrive on the

East Coast within the next few years. This array of permanent and portable seismometers will be carefully located and installed to minimize background noise. They will be in operation for several years, thus allowing for a more complete picture of the lithospheric and asthenospheric structure beneath South Carolina.

6. CONCLUSIONS

Through the analysis of seismic events across South Carolina, I concluded that the intriguing patterns found by previous studies are robust, not artifacts. Since the stations in South Carolina are dominated by null measurements, with only a few splitting results, I conclude that there is a complex pattern of anisotropy occurring beneath South Carolina. Two equally plausible explanations of this pattern are fossil anisotropy and active mantle flow around a continental keel. Both of these explanations are in agreement with my data as stations further inland exhibit fast directions in agreement with absolute plate motion and/or fossil anisotropy, as is found elsewhere in the continental interior. Stations in the southeast part of the state exhibit no splitting results, which is in agreement with a simple lack of anisotropy or models of mantle flow around a continental keel. Further research may confirm these interpretations, and is expected to commence in a few years.

7. APPENDIX I: SOUTH CAROLINA GEOLOGY

South Carolina is located on the east coast of the United States and is bordered by North Carolina to the north, Georgia to the southwest, and the Atlantic Ocean to the southeast. It contains a large coastal plain, extending from the coast to a little more than halfway up the state (Figure 7.1) (Willoughby et al. 2005). The coastal plain consists of Jurassic-age to present-day sediments and sedimentary rocks, with the youngest deposits located closest to the ocean (Willoughby et al. 2005). In the northwestern part of the state, the main geologic provinces are the Carolina slate belt, the Charlotte belt, the Inner Piedmont, and the Kings Mountain belt, all which trend NE- SW (Figure 7.2) (Taylor 1989). These geologic provinces are defined and cut by faults, shear zones, and thrust sheets (Willoughby et al. 2005). Underlying the surface rocks is assumed to be the Grenville belt, a suite of metasediments intruded by granites and anorthosites (Taylor 1989).

The Carolina slate belt and the Charlotte belts are composed of a thick sequence of metamorphosed mafic volcanic and sedimentary rocks (Taylor 1989). The metamorphism in the slate belt is greenschist grade, while the metamorphism in the Charlotte belt is upper amphibolite grade (Taylor 1989). This metamorphism mostly likely occurred during the Taconic orogeny in the early to

middle Paleozoic, as a Cambrian island arc sequence was accreted onto the continent (Taylor 1989).

The metamorphic rocks of the Inner Piedmont are also of amphibolite facies (Horton 2006). The three main rock types of this area are a muscovite-biotite gneiss, a muscovite schist, and an amphibolite (Horton 2006). They are deformed continental slope and rise sediments that were possibly caught between the continent and Charlotte/Carolina belts and metamorphosed during the Taconic orogeny (Taylor 1989).

The Kings Mountain belt is a small region, situated almost exclusively in South Carolina (Figure 7.2). It consists primarily of metavolcanic and metasedimentary rocks such as hornblende gneiss and amphibolite, felsic schist and gneiss, and metatuff, as well as biotite-muscovite schist, quartz-sericite phyllite and schist, phyllitic metasiltstone and quartzite (Horton 2006). Most of the metamorphism of these rocks occurred during the Alleghanian orogeny (Horton 2006).

Igneous intrusions are found throughout the metamorphic rocks in the northwestern part of the state (Willoughby et al. 2005). The primary rock types are granite and gabbro, with some diorite and tonalite (Horton 2006). These igneous rocks occur primarily as dikes and other small bodies within the larger metamorphic complex (Horton 2006). Radiometric dating indicates a mid- to late-Paleozoic age for these rocks (Horton 2006).

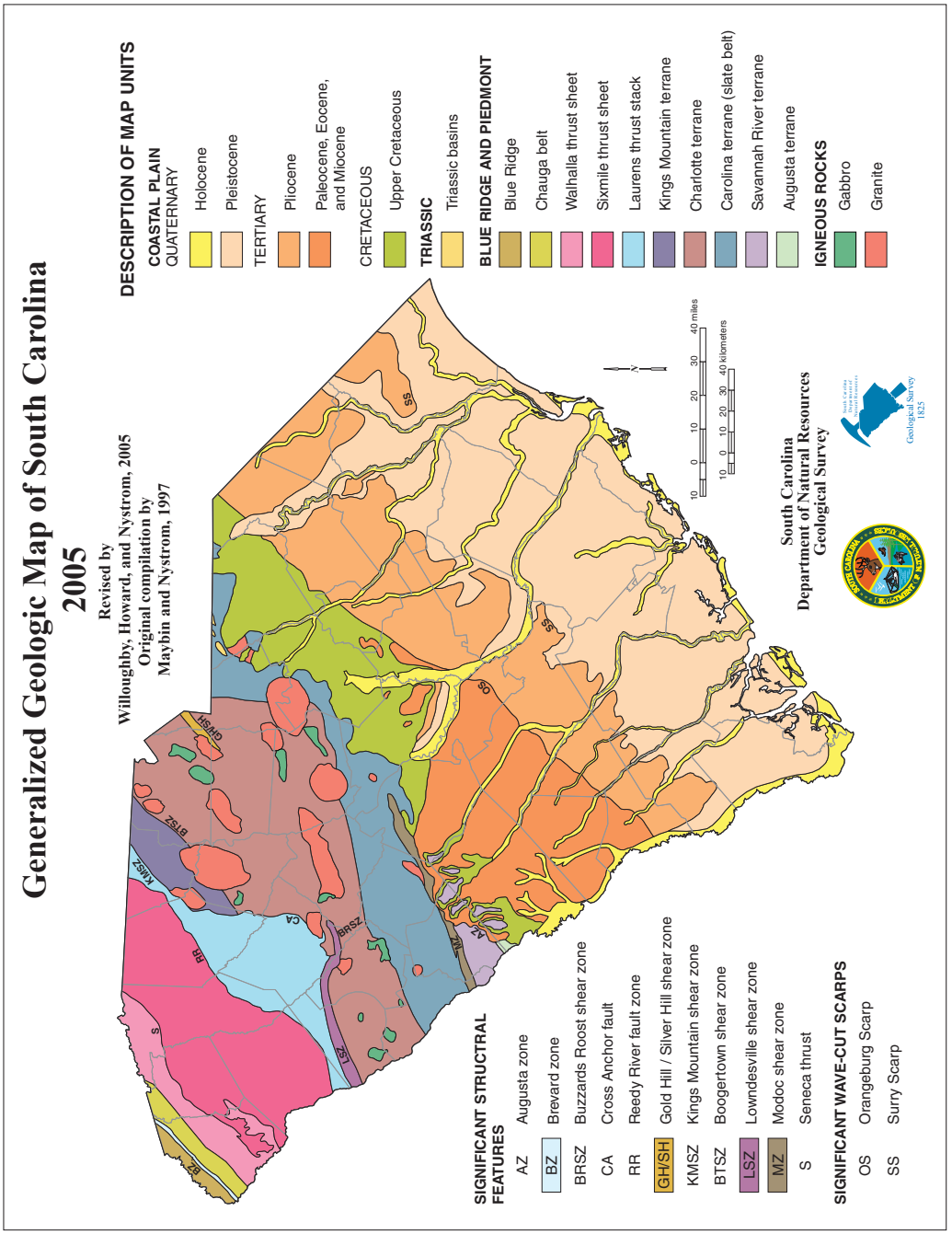

Figure 7.1 Generalized geologic map of South Carolina by Willoughby, Howard, and Nystrom (2005). Sedimentary rocks cover the southern and eastern portions of the state, while metamorphic rocks dominate in the northwestern portion of the state. Small igneous bodies are also found in the northwestern part of the state, along with several faults and shear zones.

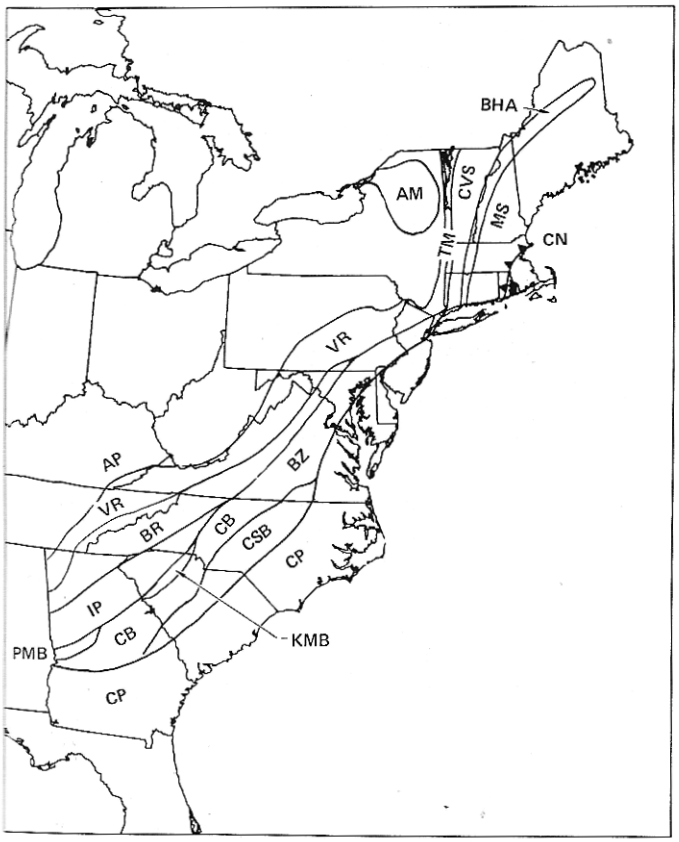

Figure 7.2. Major geologic provinces in the Appalachian mountain belt, from Taylor 1989. CP = Coastal Plain, CSB = Carolina slate belt, KMB = Kings Mountain belt, IP = Inner Piedmont.

8. APPENDIX II: DISTRIBUTION OF EARTHQUAKES

Event distributions for the twenty stations at which earthquakes were recorded. Each event is represented by a colored circle. These events are of large enough magnitude ($5.75 \leq M_W \leq 9.75$) and at an appropriate distance from the station (88° to 130°) so that it is possible for the station to record the SKS arrival. The depth of the focus of the event is indicated by the color of the circle, and the magnitude of the event is indicated by the size of the circle (larger circles represent larger magnitudes).

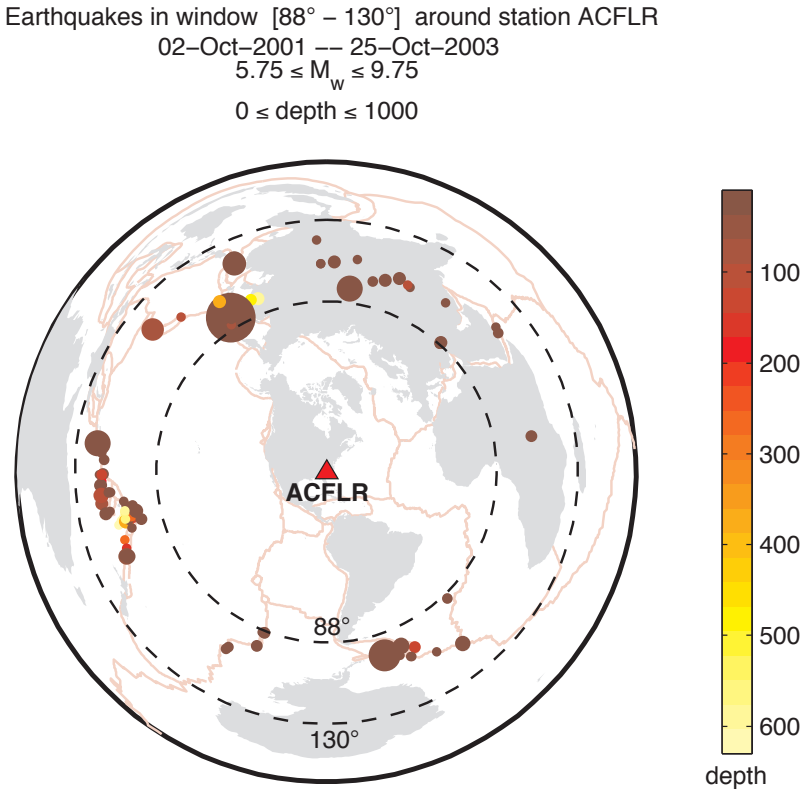

Earthquakes in window [88° – 130°] around station AGBLF
02–Oct–2001 –– 03–Jan–2004
$5.75 \leq M_w \leq 9.75$
$0 \leq \text{depth} \leq 1000$

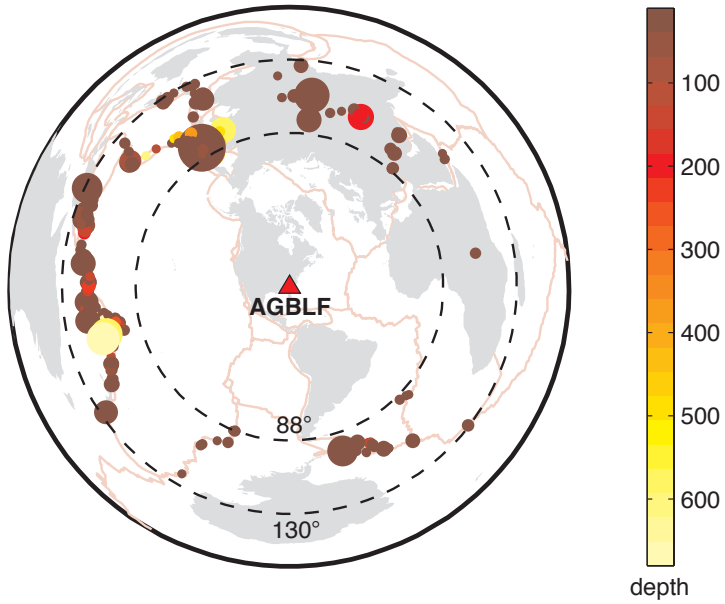

Earthquakes in window [88° – 130°] around station ALLEN
02–Apr–2002 –– 22–Jun–2002
$5.75 \leq M_w \leq 9.75$
$0 \leq \text{depth} \leq 1000$

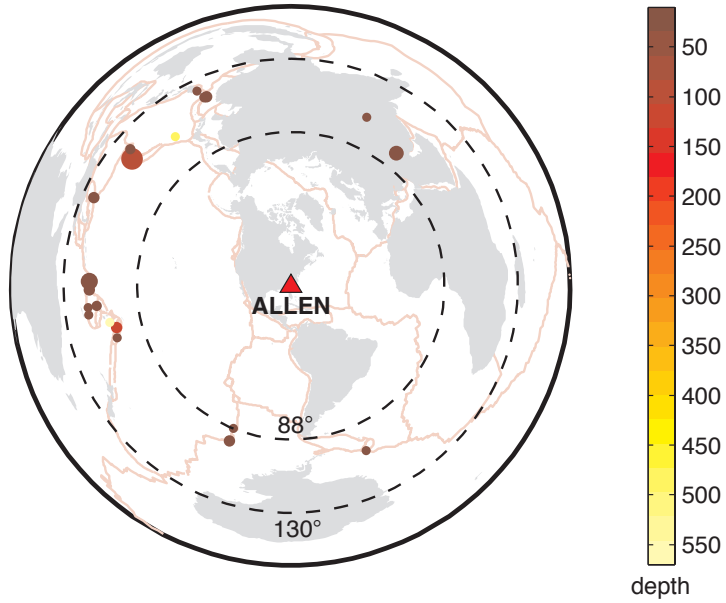

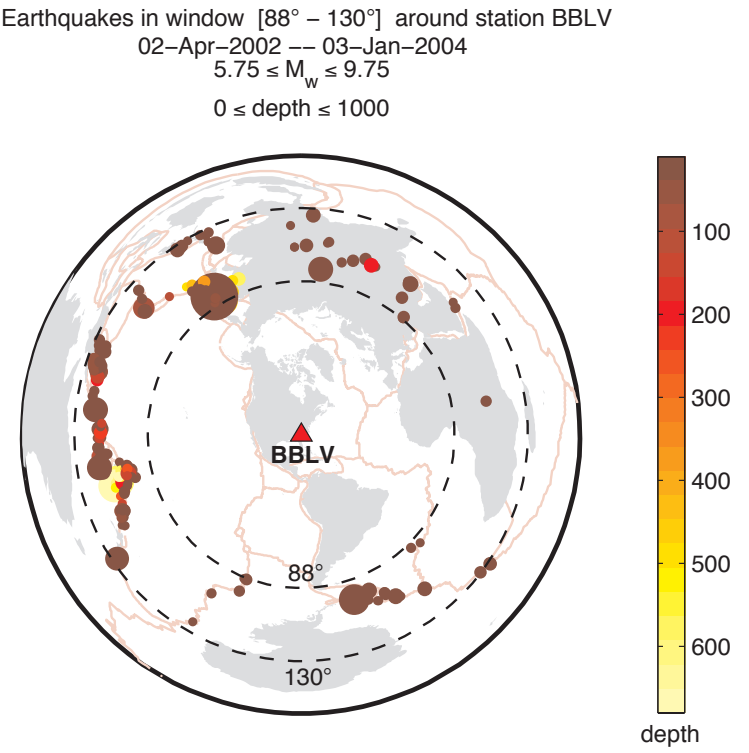
Earthquakes in window [88° – 130°] around station BBLV
02–Apr–2002 –– 03–Jan–2004
5.75 ≤ M_w ≤ 9.75
0 ≤ depth ≤ 1000
BBLV
88°
130°
100
200
300
400
500
600
depth

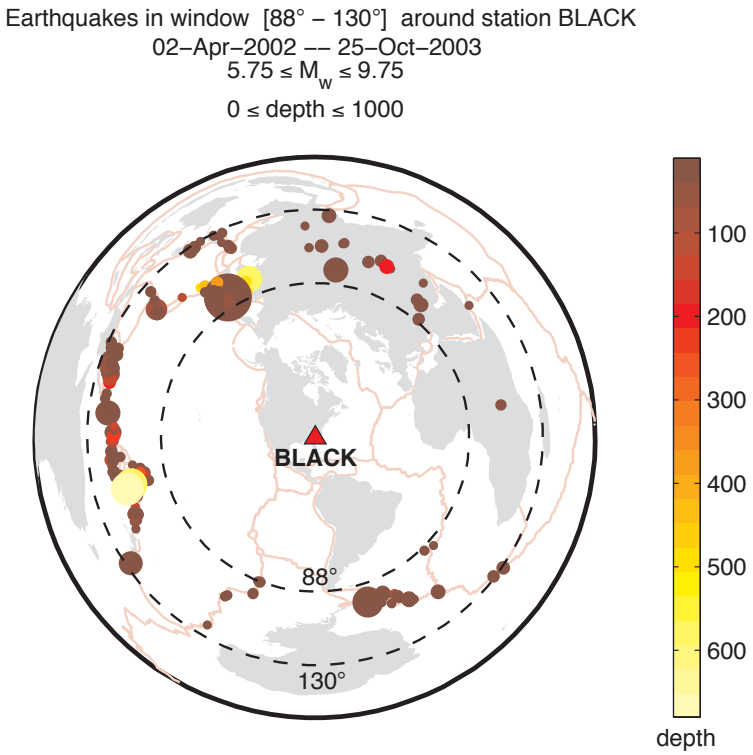
Earthquakes in window [88° – 130°] around station BLACK
02–Apr–2002 –– 25–Oct–2003
5.75 ≤ M_w ≤ 9.75
0 ≤ depth ≤ 1000
BLACK
88°
130°
100
200
300
400
500
600
depth

Earthquakes in window [88° – 130°] around station BRNCH
02–Apr–2002 –– 25–Oct–2003
$5.75 \leq M_w \leq 9.75$
$0 \leq \text{depth} \leq 1000$

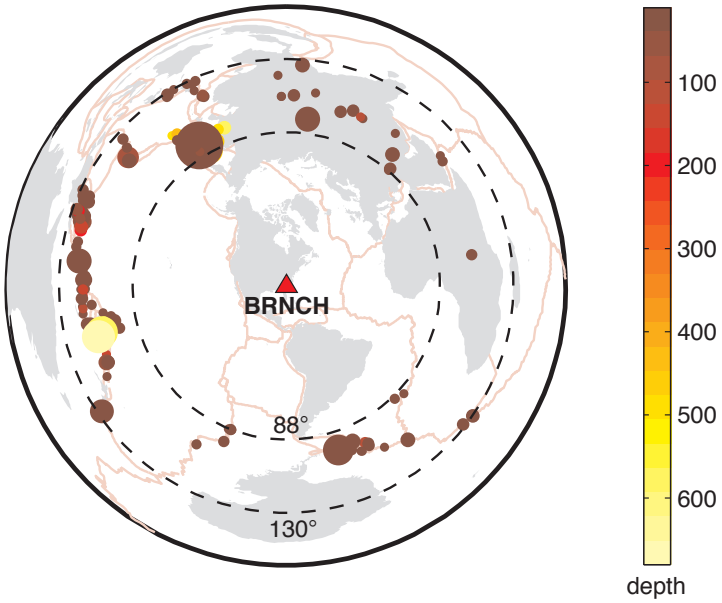

Earthquakes in window [88° – 130°] around station BTRCK
02–Apr–2002 –– 24–Sep–2002
$5.75 \leq M_w \leq 9.75$
$0 \leq \text{depth} \leq 1000$

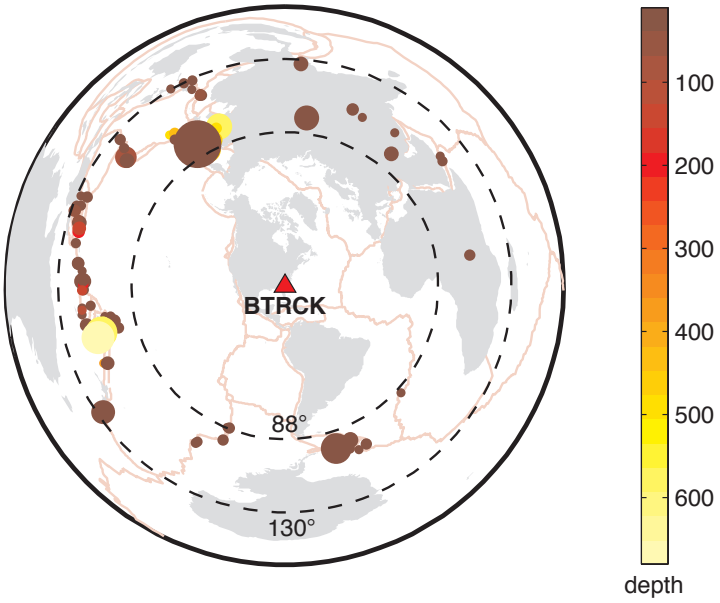

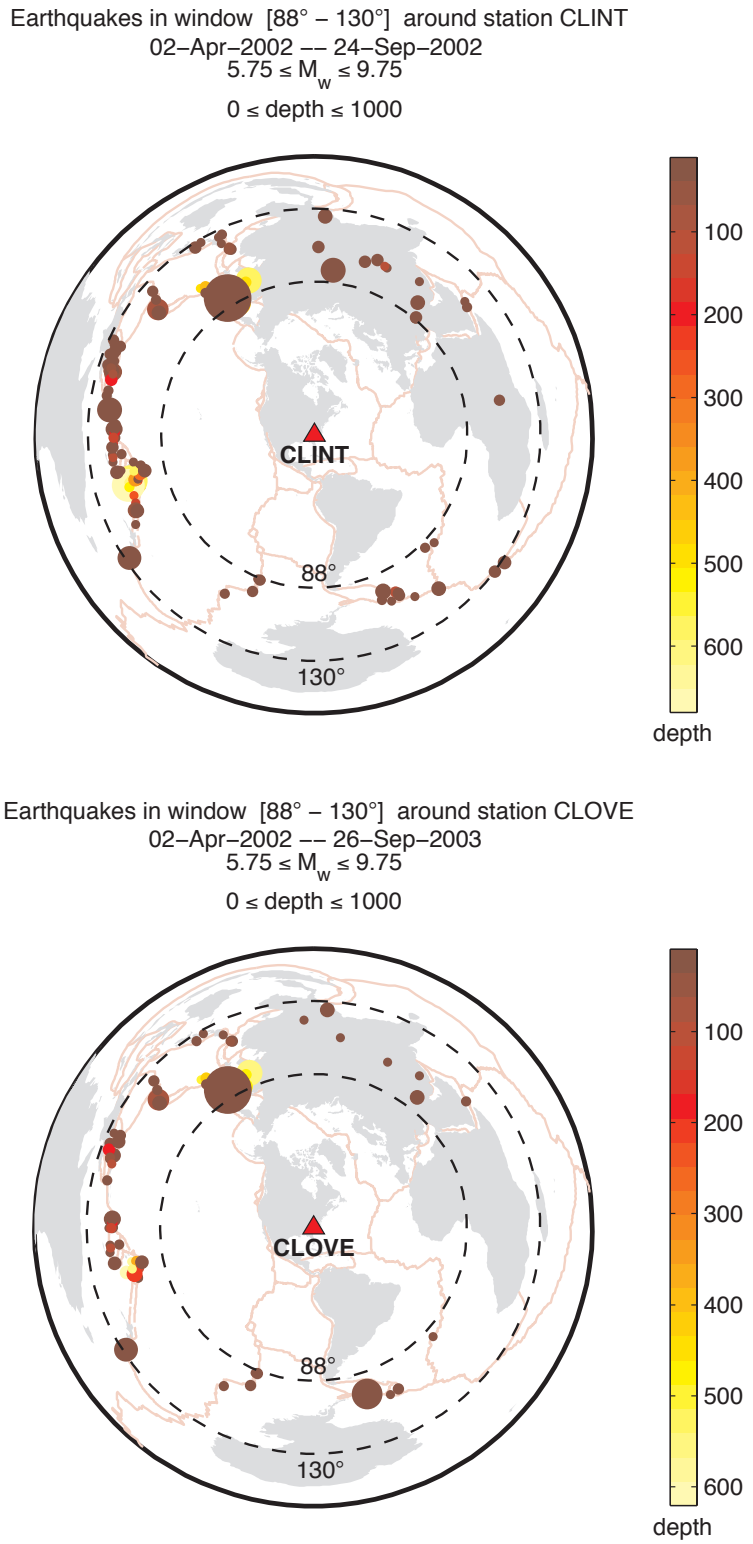
Earthquakes in window [88° – 130°] around station CLINT
02–Apr–2002 –– 24–Sep–2002
5.75 ≤ M_w ≤ 9.75
0 ≤ depth ≤ 1000
CLINT
88°
130°
100
200
300
400
500
600
depth
Earthquakes in window [88° – 130°] around station CLOVE
02–Apr–2002 –– 26–Sep–2003
5.75 ≤ M_w ≤ 9.75
0 ≤ depth ≤ 1000
CLOVE
88°
130°
100
200
300
400
500
600
depth

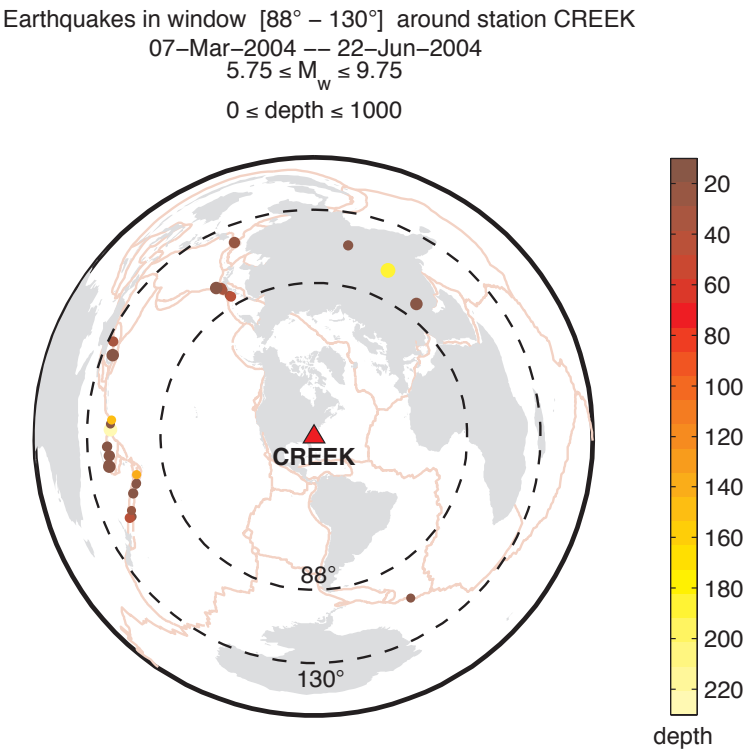
Earthquakes in window [88° – 130°] around station CREEK
07–Mar–2004 –– 22–Jun–2004
5.75 ≤ M_w ≤ 9.75
0 ≤ depth ≤ 1000
CREEK
88°
130°
20
40
60
80
100
120
140
160
180
200
220
depth

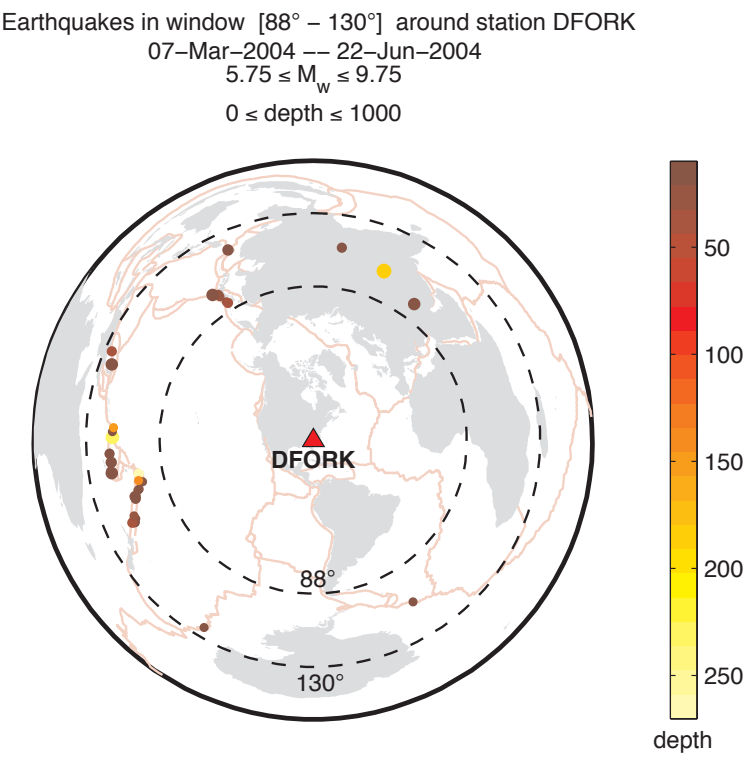
Earthquakes in window [88° – 130°] around station DFORK
07–Mar–2004 –– 22–Jun–2004
5.75 ≤ M_w ≤ 9.75
0 ≤ depth ≤ 1000
DFORK
88°
130°
50
100
150
200
250
depth

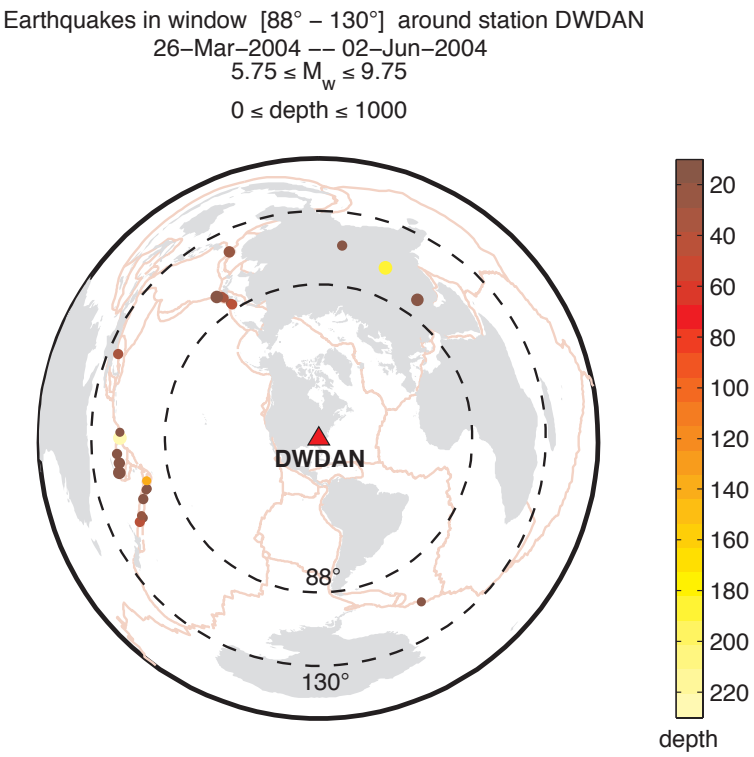
Earthquakes in window [88° – 130°] around station DWDAN
26–Mar–2004 –– 02–Jun–2004
5.75 ≤ M_w ≤ 9.75
0 ≤ depth ≤ 1000
DWDAN
88°
130°
20
40
60
80
100
120
140
160
180
200
220
depth

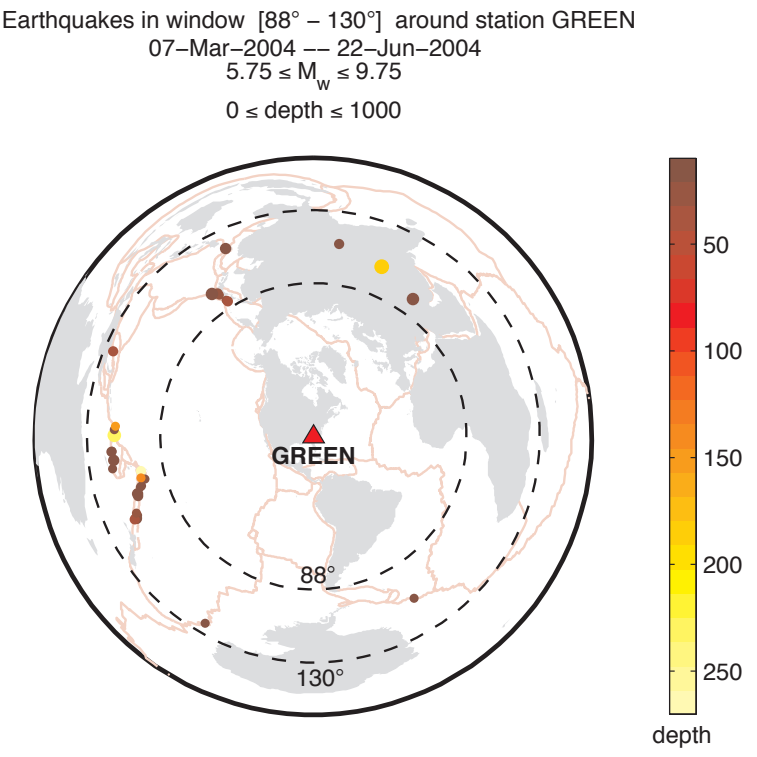
Earthquakes in window [88° – 130°] around station GREEN
07–Mar–2004 –– 22–Jun–2004
5.75 ≤ M_w ≤ 9.75
0 ≤ depth ≤ 1000
GREEN
88°
130°
50
100
150
200
250
depth

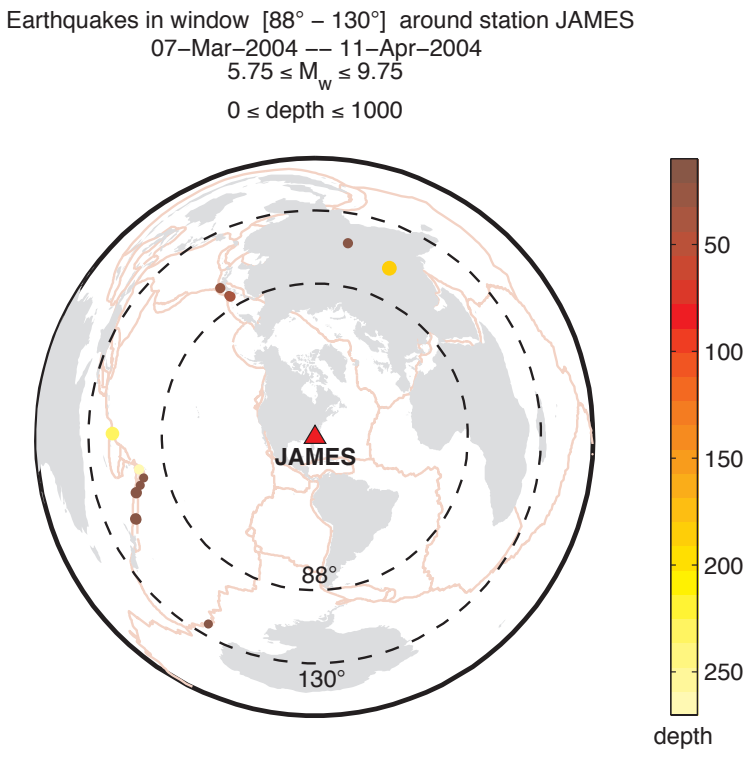
Earthquakes in window [88° – 130°] around station JAMES
07–Mar–2004 –– 11–Apr–2004
5.75 ≤ M_w ≤ 9.75
0 ≤ depth ≤ 1000
JAMES
88°
130°
50
100
150
200
250
depth

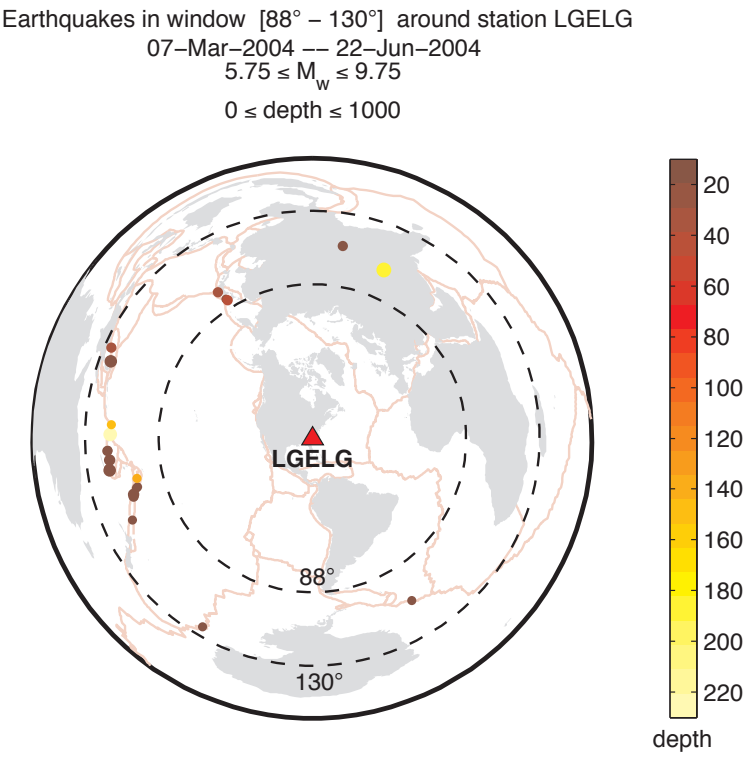
Earthquakes in window [88° – 130°] around station LGELG
07–Mar–2004 –– 22–Jun–2004
5.75 ≤ M_w ≤ 9.75
0 ≤ depth ≤ 1000
LGELG
88°
130°
20
40
60
80
100
120
140
160
180
200
220
depth

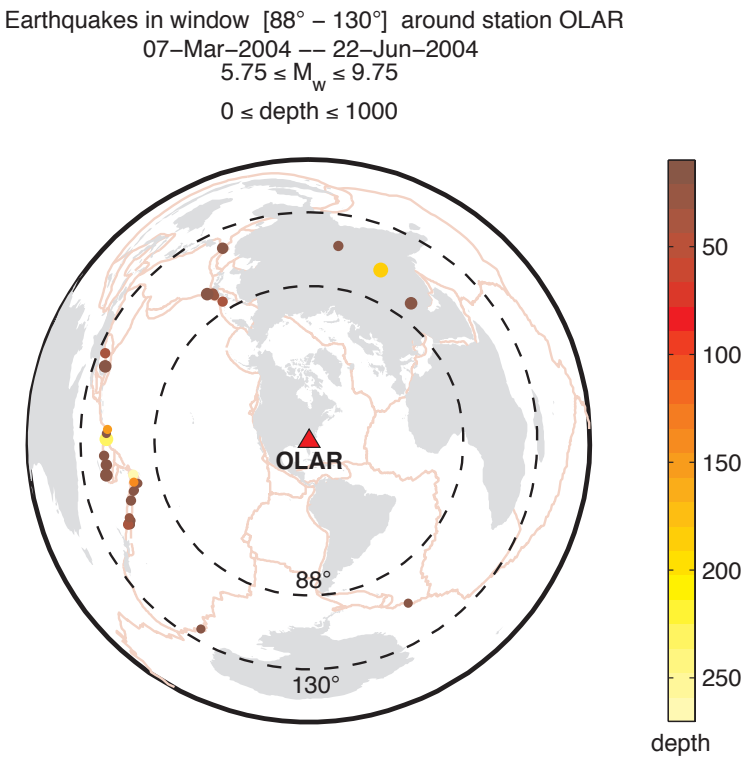
Earthquakes in window [88° – 130°] around station OLAR
07–Mar–2004 –– 22–Jun–2004
5.75 ≤ M_w ≤ 9.75
0 ≤ depth ≤ 1000
OLAR
88°
130°
50
100
150
200
250
depth

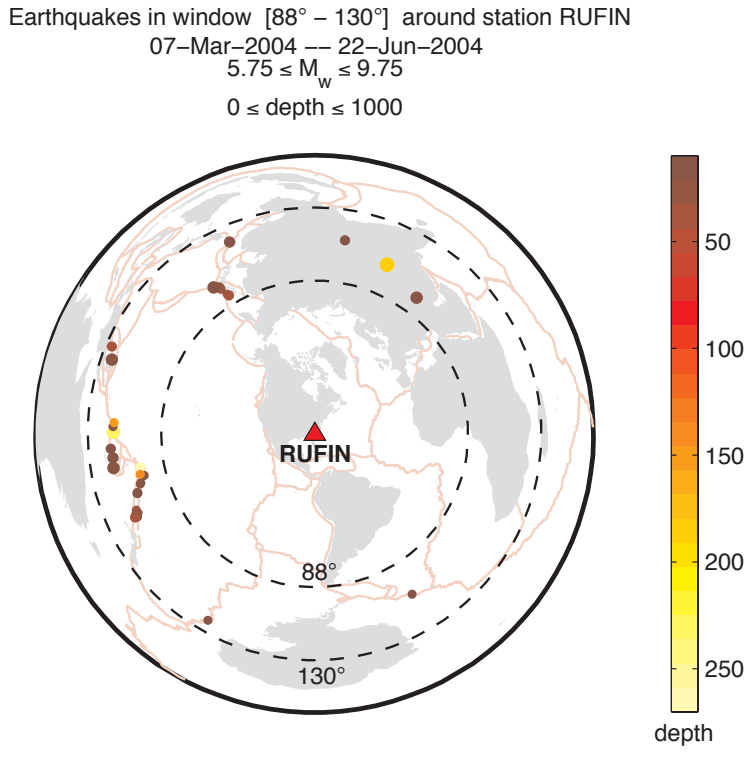
Earthquakes in window [88° – 130°] around station RUFIN
07–Mar–2004 –– 22–Jun–2004
5.75 ≤ M_w ≤ 9.75
0 ≤ depth ≤ 1000
RUFIN
88°
130°
50
100
150
200
250
depth

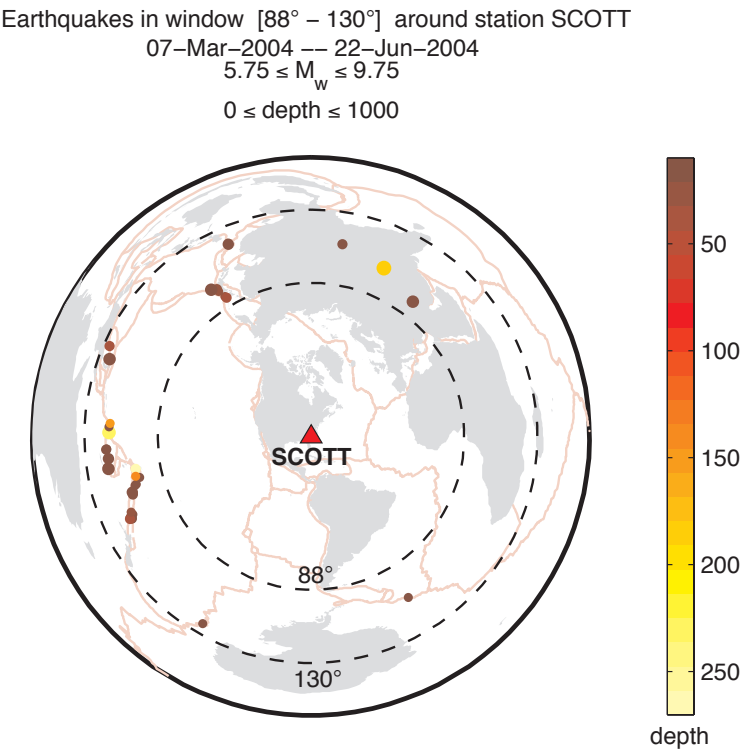
Earthquakes in window [88° – 130°] around station SCOTT
07–Mar–2004 –– 22–Jun–2004
5.75 ≤ M_w ≤ 9.75
0 ≤ depth ≤ 1000
SCOTT
88°
130°
50
100
150
200
250
depth

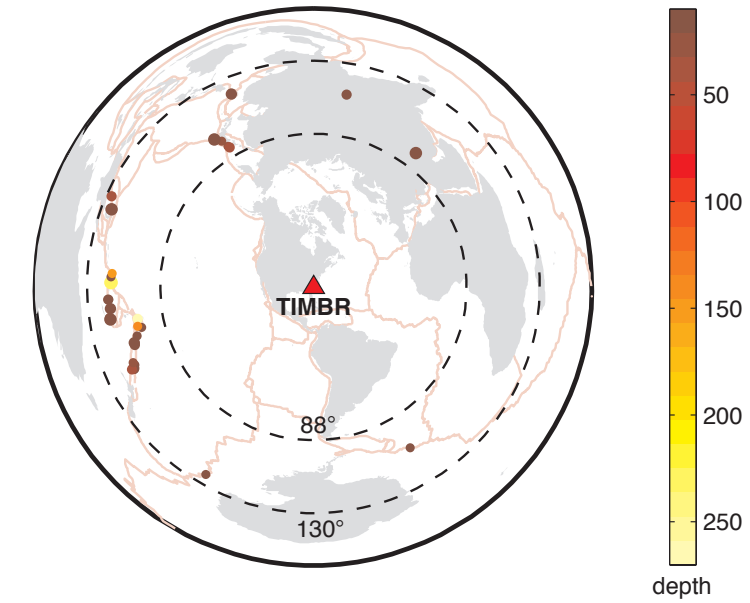
Earthquakes in window [88° – 130°] around station TIMBR
07–Mar–2004 –– 22–Jun–2004
5.75 ≤ M_w ≤ 9.75
0 ≤ depth ≤ 1000
TIMBR
88°
130°
50
100
150
200
250
depth

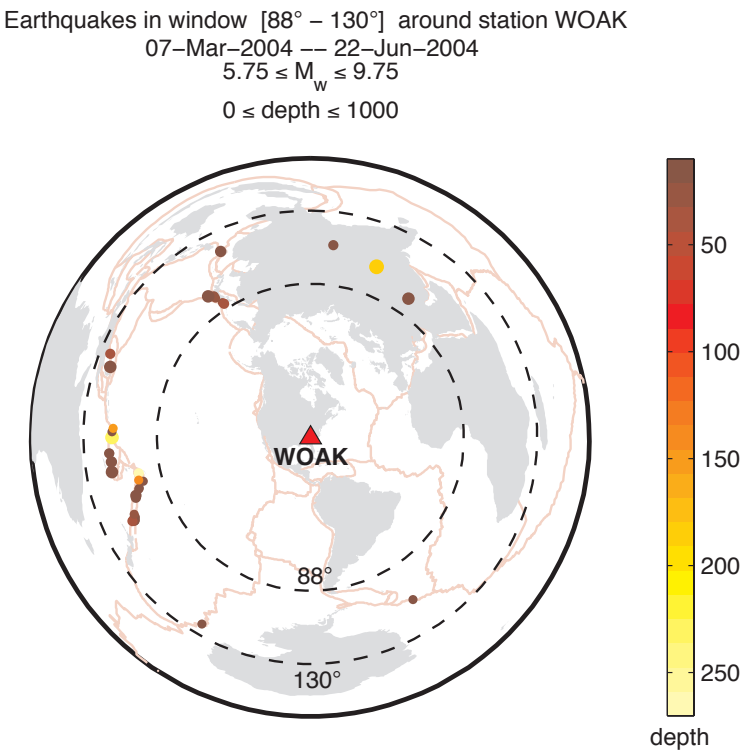
Earthquakes in window [88° – 130°] around station WOAK
07–Mar–2004 –– 22–Jun–2004
5.75 ≤ M_w ≤ 9.75
0 ≤ depth ≤ 1000
WOAK
88°
130°
50
100
150
200
250
depth

9. APPENDIX III: SPLITLAB PRINTOUTS

SplitLab printouts of all 38 usable events, sorted by type of result (split or null) and then by date. In each printout, the transverse component minimization method is the lower set of graphs, and the rotation-correlation method is the upper set of graphs.

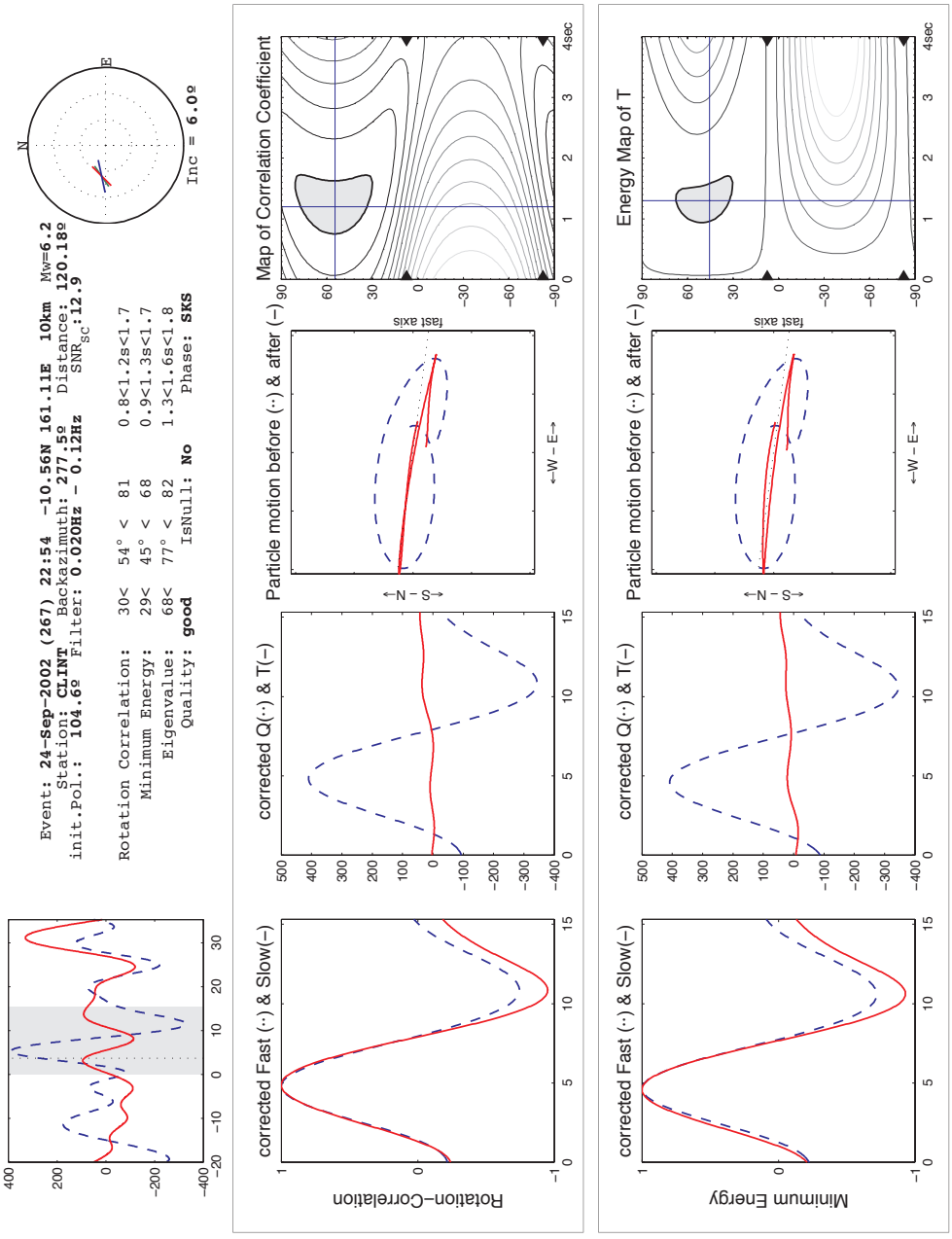

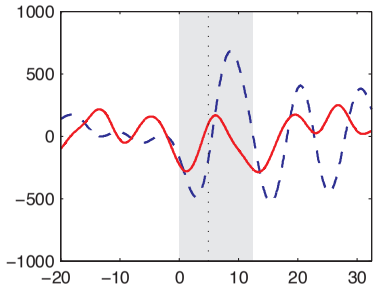

Event: **03-Jan-2004 (003) 16:23 -22.25N 169.68E 22km** Mw=7.1
Station: **BBLV** Backazimuth: **261.1º** Distance: **118.84º**
init.Pol.: **69.4º** Filter: **0.020Hz - 0.12Hz** SNR_{SC}:**13.8**

Rotation Correlation:	11<	35° <	59	0.5<1.2s<2.1
Minimum Energy:	27<	59° <	72	1.0<2.1s<3.7
Eigenvalue:	3<	15° <	31	1.3<1.4s<1.7

Quality: **fair** IsNull: **No** Phase: **SKS**

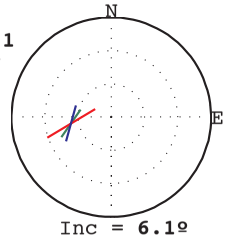

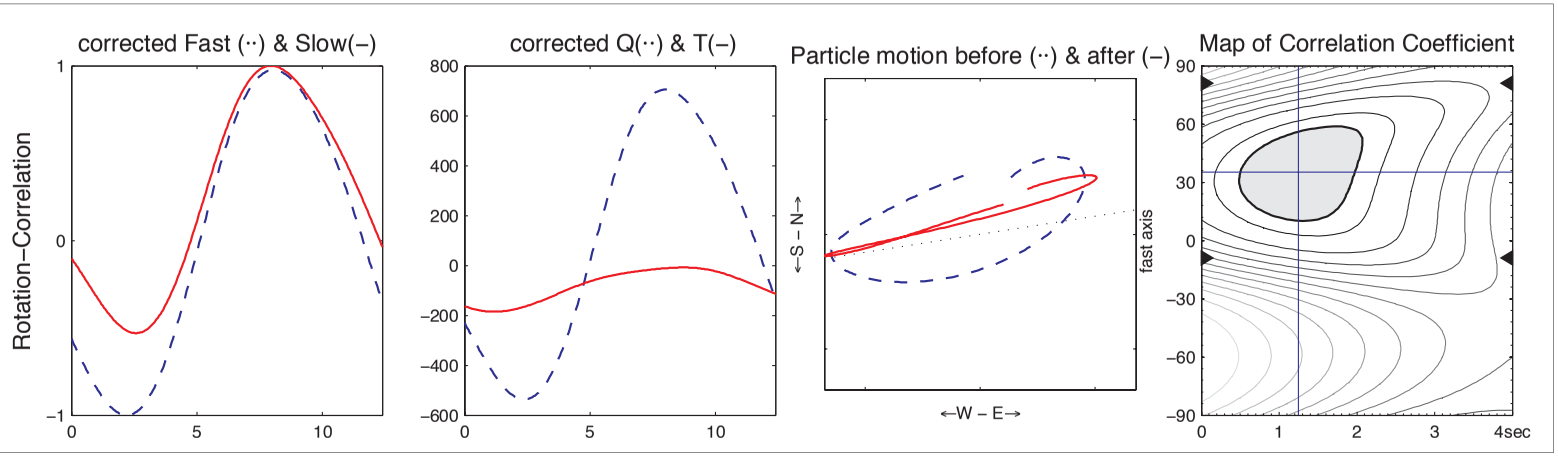

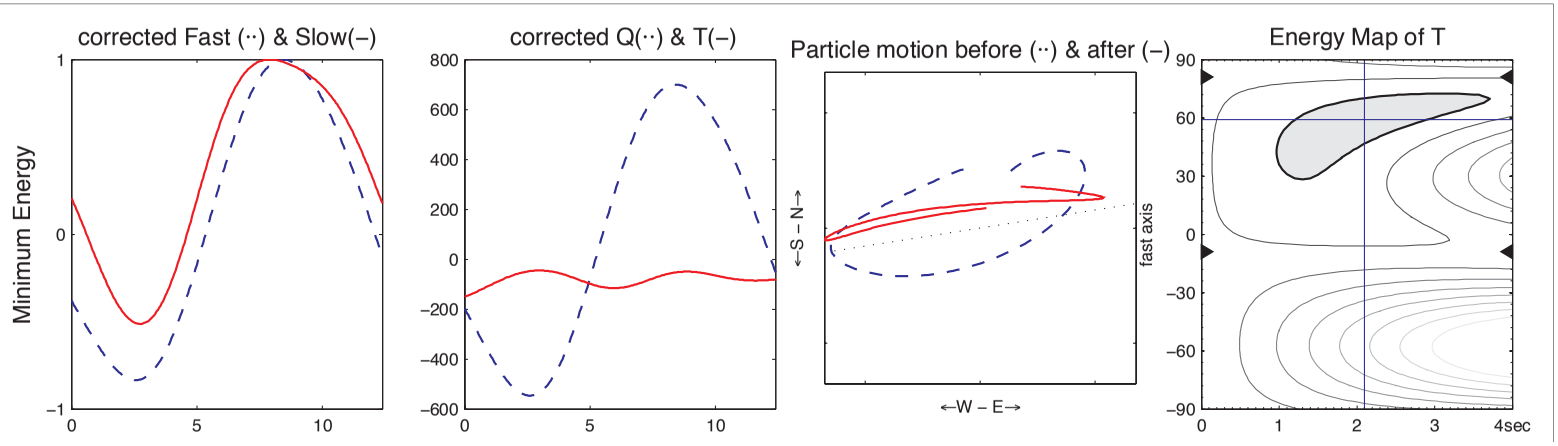

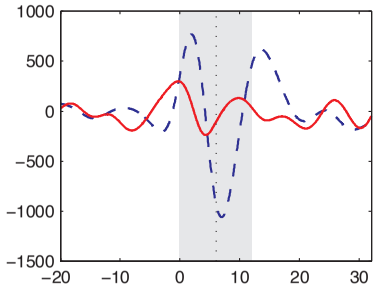

Event: **25-Jan-2004 (025) 11:43 -16.83N -174.20E 130km Mw=6.6**
Station: **BBLV** Backazimuth: **258.2º** Distance: **102.95º**
init.Pol.: **87.1º** Filter: **0.020Hz - 0.12Hz** SNR_{SC}:**12.8**

Rotation Correlation:	2<	41° <	67	0.1<0.8s<1.7
Minimum Energy:	27<	54° <	68	0.6<1.0s<1.6
Eigenvalue:	74<	76° <	82	1.8<2.4s<3.1

Quality: **fair** IsNull: **No** Phase: **SKS**

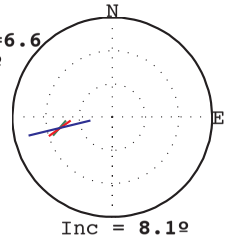

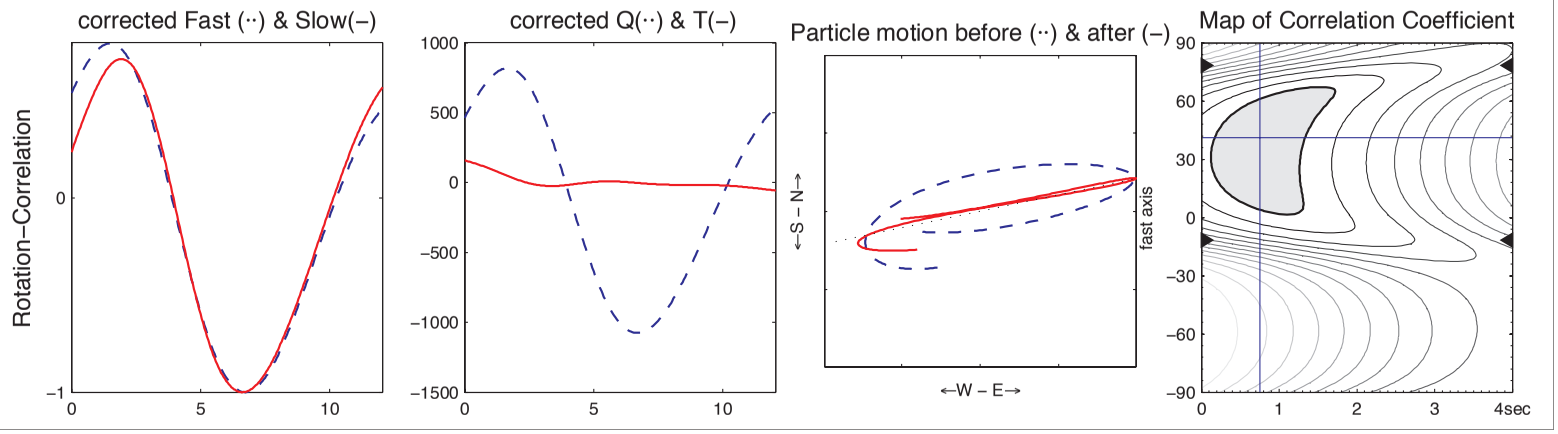

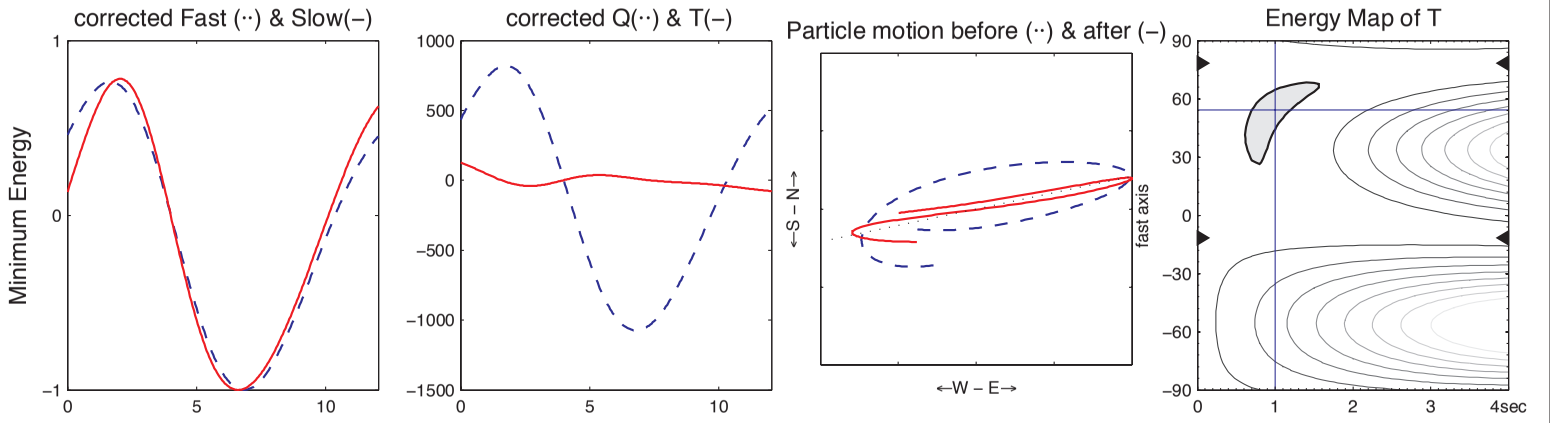

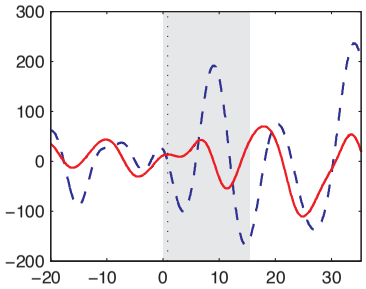

Event: **07-May-2004 (128) 01:26 -21.99N 170.28E 14km Mw=6.3**
Station: **CREEK** Backazimuth: **261.6º** Distance: **118.52º**
init.Pol.: **97.8º** Filter: **0.020Hz - 0.12Hz** SNR_{SC}: **8.1**

Rotation Correlation:	9<	33° <	61	0.2<0.7s<1.4
Minimum Energy:	1<	16° <	52	0.6<1.2s<2.4
Eigenvalue:	74<	80° <	86	1.8<2.4s<3.1

Quality: **fair** IsNull: **No** Phase: **SKS**

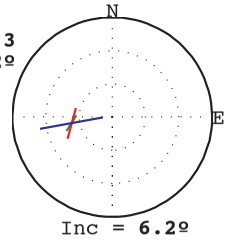

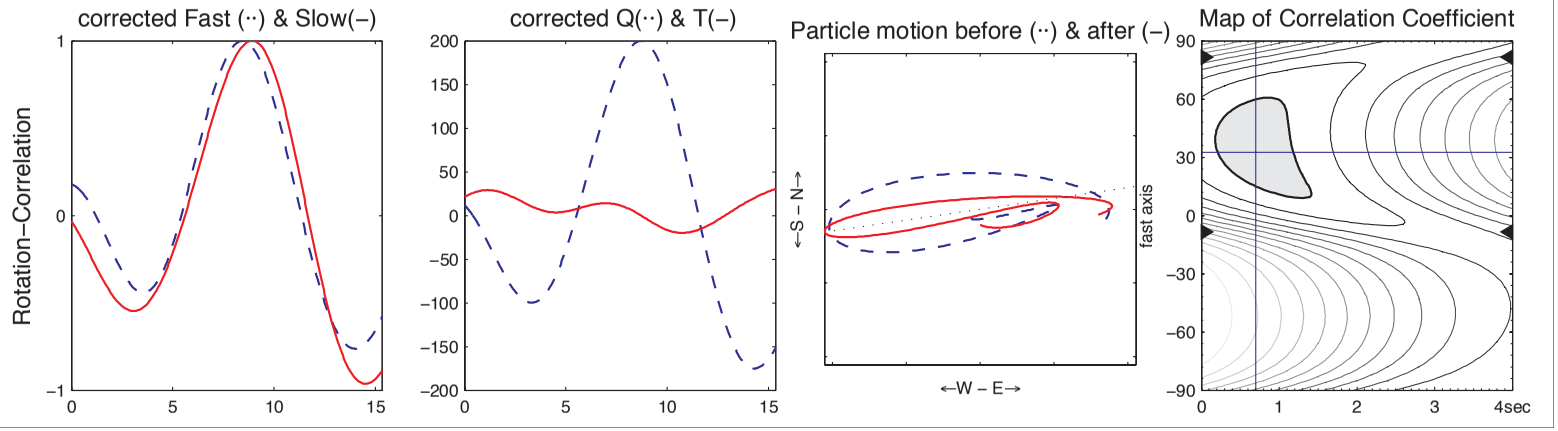

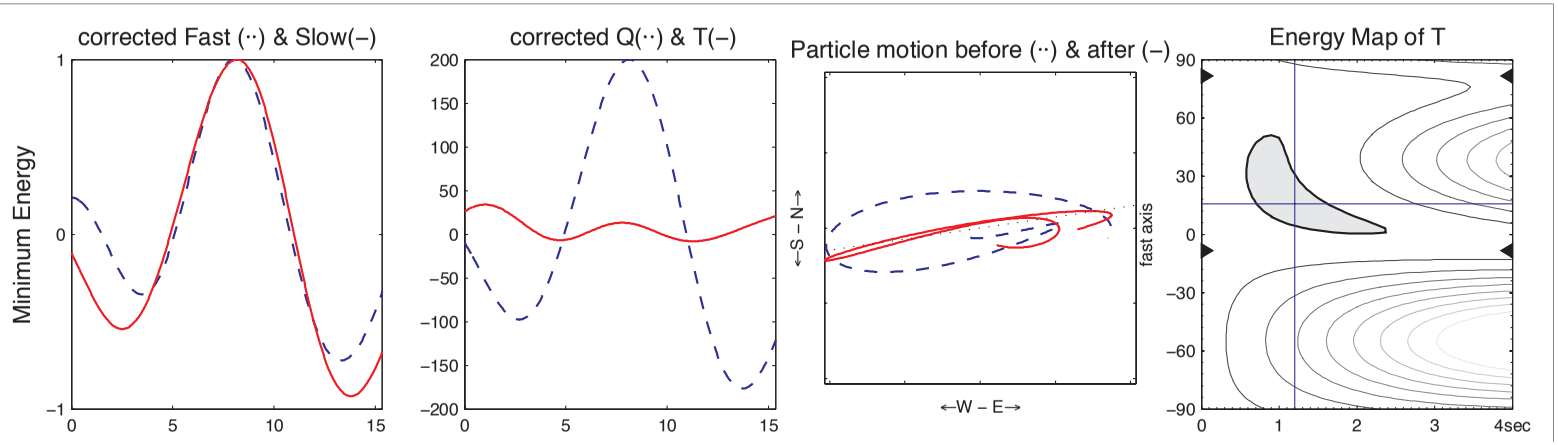

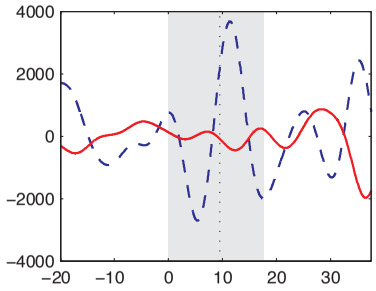

Event: **26-Apr-2002 (116) 16:06 13.09N 144.62E 86km Mw=7.0**
Station: **CLINT** Backazimuth: **310.2º** Distance: **117.24º**
init.Pol.: **135.5º** Filter: **0.020Hz – 0.12Hz** SNR_{SC}:**13.0**

Rotation Correlation:	63<	89° < −64	0.0<0.1s<0.4
Minimum Energy:	41<	42° < 56	0.4<4.0s<4.0
Eigenvalue:	46<	−48° < −46	0.0<1.2s<3.4

Quality: **good** IsNull: **Yes** Phase: **SKS**

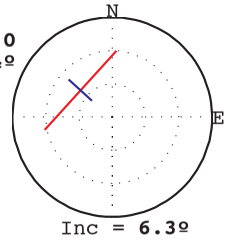

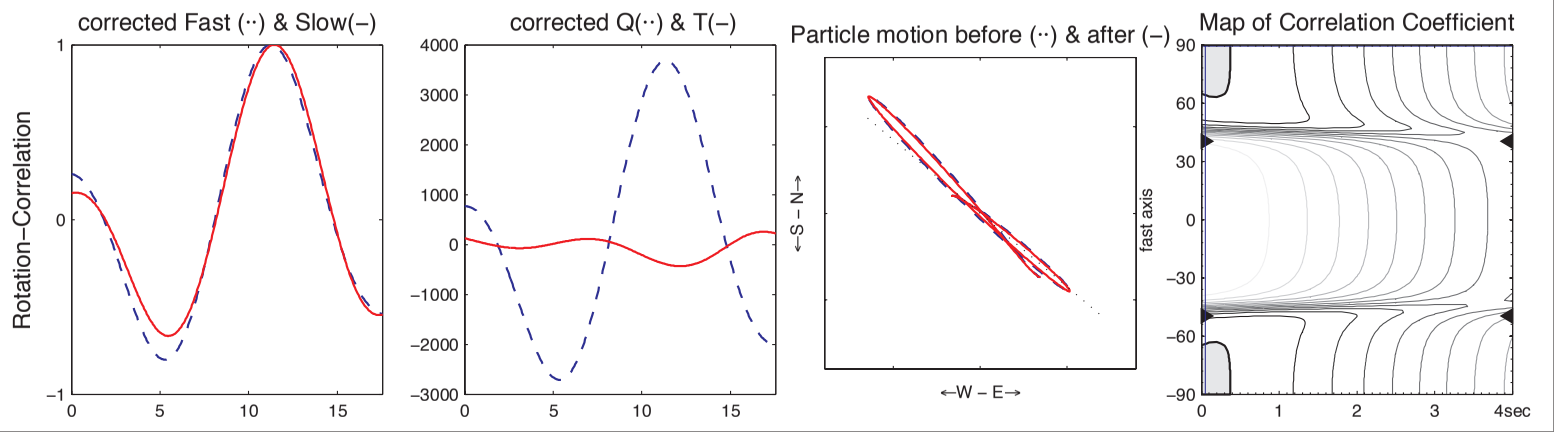

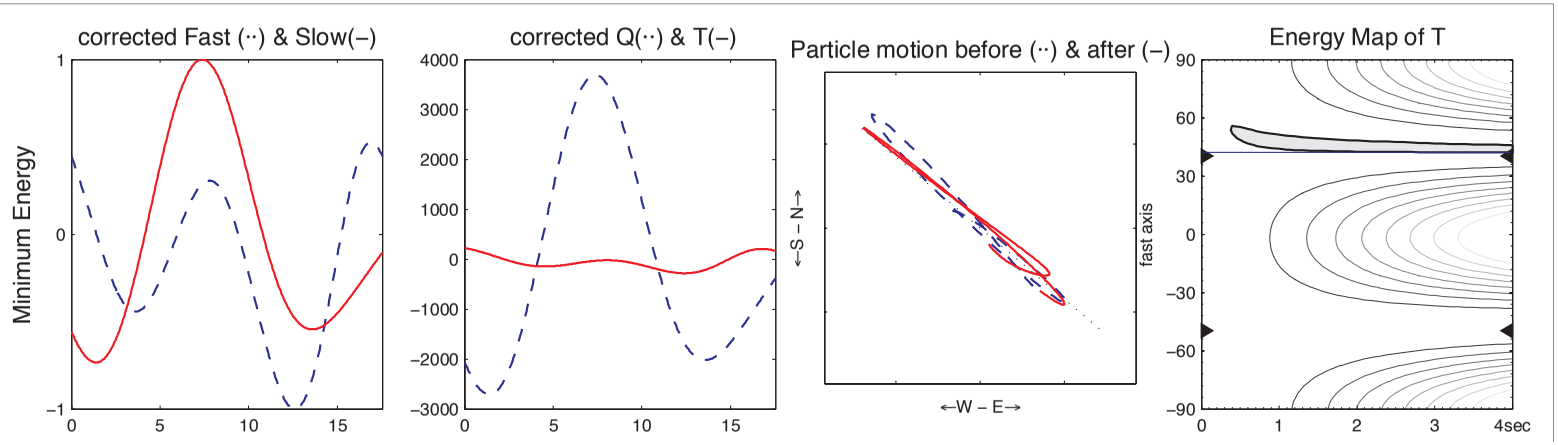

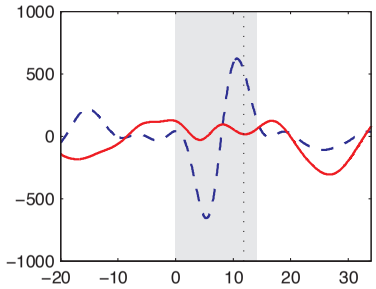

Event: **02-Aug-2002 (214) 23:11 29.28N 138.97E 426km Mw=6.2**
Station: **CLINT** Backazimuth: **325.3º** Distance: **107.43º**
init.Pol.: **143.8º** Filter: **0.020Hz - 0.12Hz** SNR_{SC}:**12.8**

Rotation Correlation:	72< −81° < −55	0.0<0.2s<0.9
Minimum Energy:	−Inf< −43° < Inf	0.0<1.0s<Inf
Eigenvalue:	58< −45° < −39	0.1<0.8s<2.0

Quality: **good** IsNull: **Yes** Phase: **SKS**

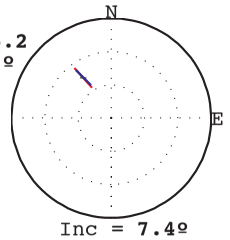

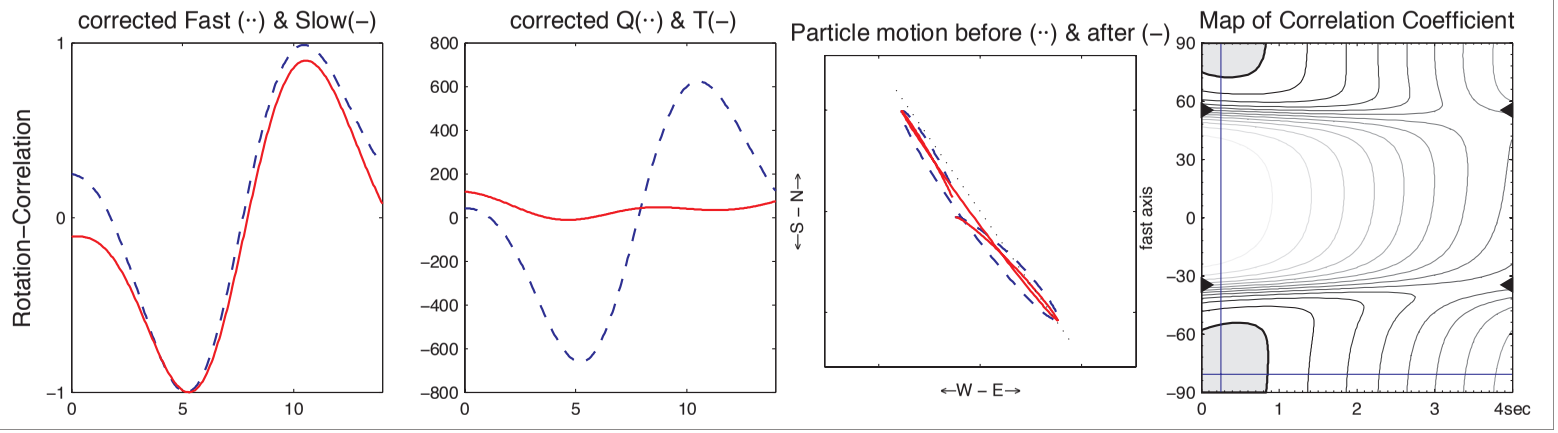

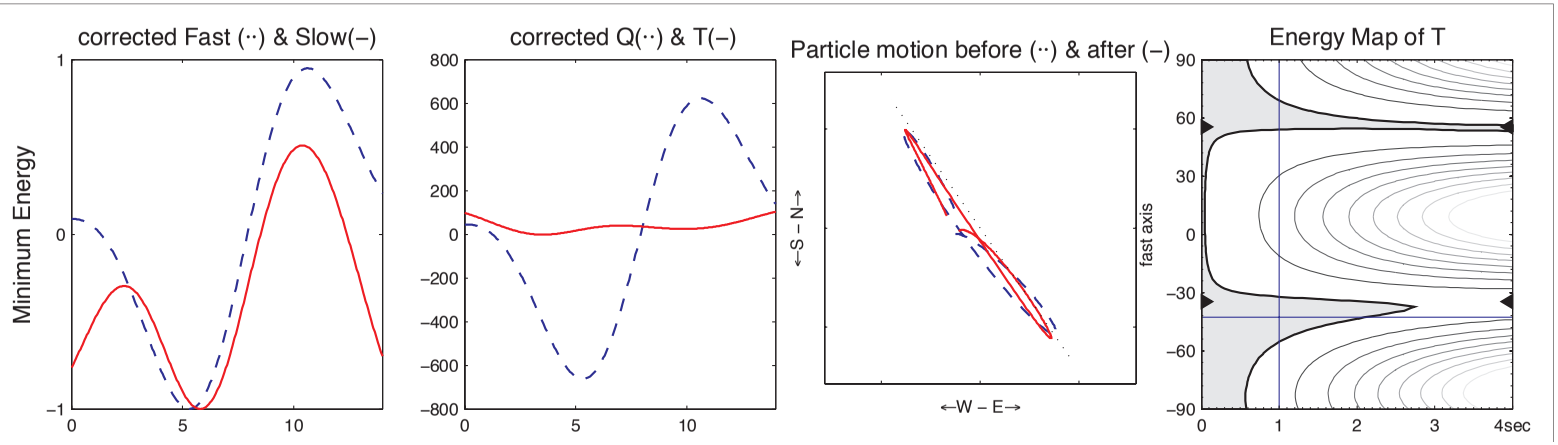

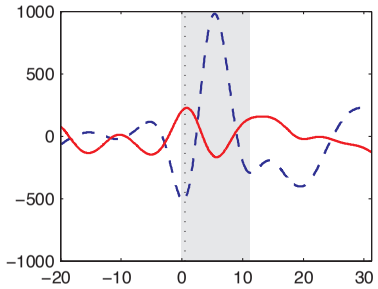

Event: **02-Aug-2002 (214) 23:11 29.28N 138.97E 426km Mw=6.2**
Station: **BLACK** Backazimuth: **325.3º** Distance: **107.43º**
init.Pol.: **155.6º** Filter: **0.020Hz - 0.12Hz** SNR_{SC}:**11.7**

Rotation Correlation: -Inf< -70° < Inf 0.0<0.1s<Inf
Minimum Energy: 60< 63° < 70 2.0<4.0s<4.0
Eigenvalue: 70< 69° < 70 2.7<3.0s<3.3
Quality: **fair** IsNull: **Yes** Phase: **SKS**

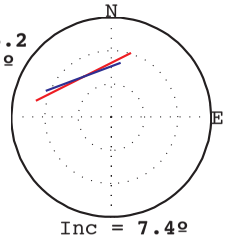

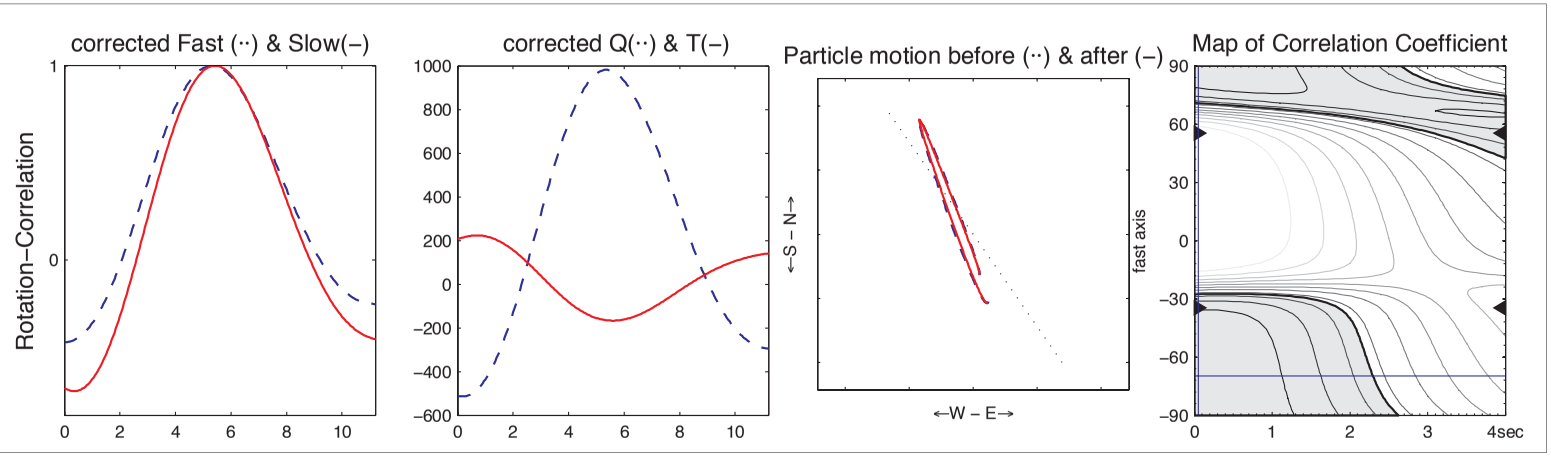

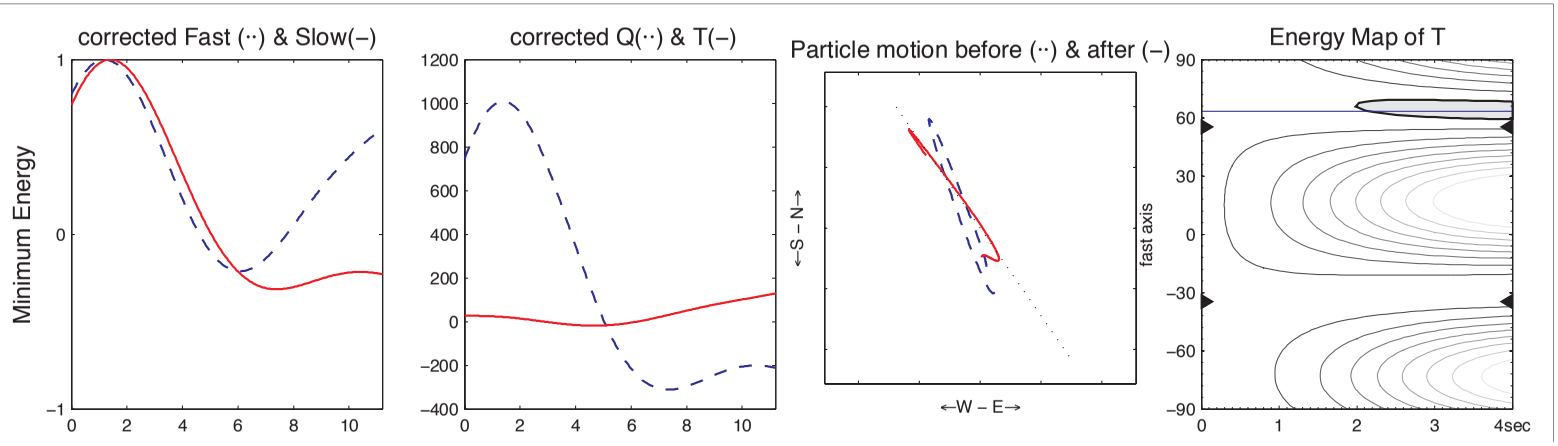

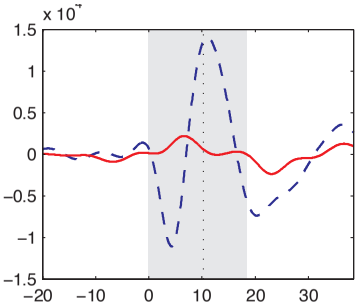

Event: **19-Aug-2002 (231) 11:01 -21.70N -179.51E 580km Mw=7.6**
Station: **CLINT** Backazimuth: **256.5º** Distance: **109.73º**
init.Pol.: **77.7º** Filter: **0.020Hz - 0.12Hz** SNR_{SC}:**34.9**

Rotation Correlation: -Inf< 31° < Inf 0.0<0.3s<Inf
Minimum Energy: -Inf< -8° < Inf 0.0<2.0s<Inf
Eigenvalue: -9< 6° < 64 0.3<0.7s<3.0
Quality: **good** IsNull: **Yes** Phase: **SKS**

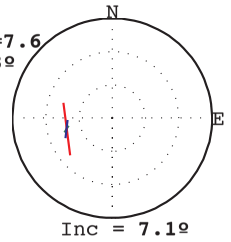

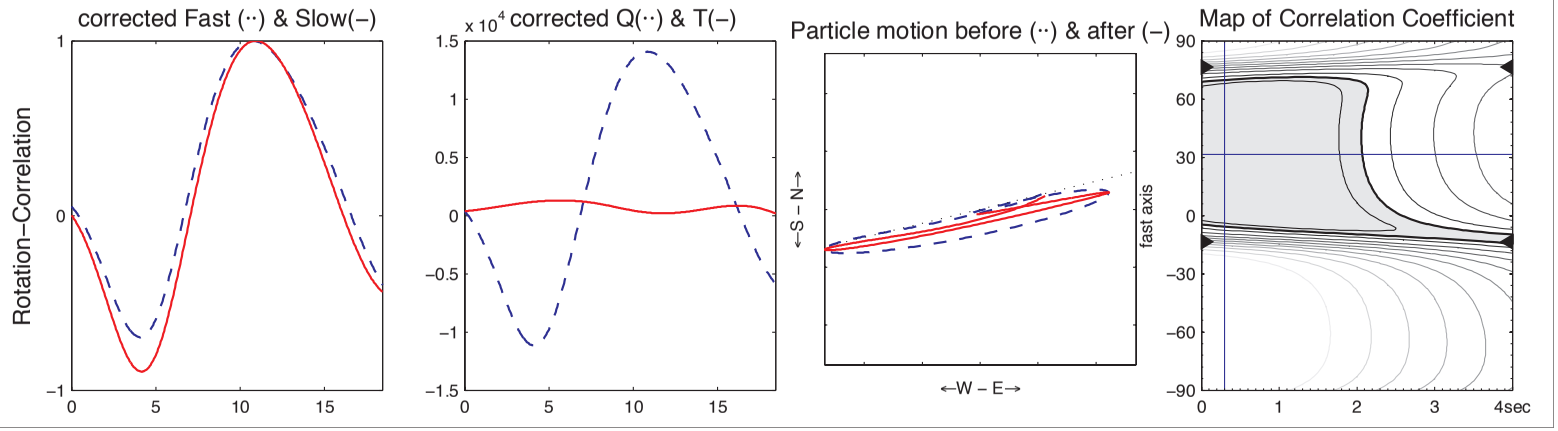

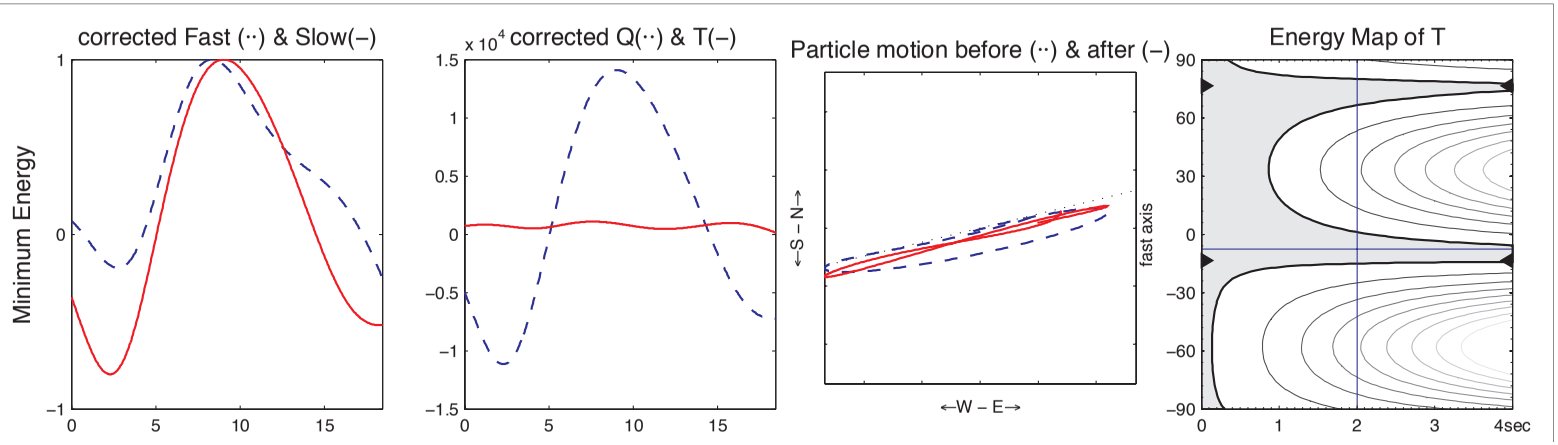

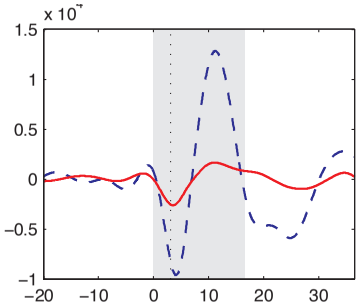

Event: **19-Aug-2002 (231) 11:01 -21.70N -179.51E 580km** Mw=**7.6**
Station: **AGBLF** Backazimuth: **255.4º** Distance: **107.95º**
init.Pol.: **64.8º** Filter: **0.020Hz - 0.12Hz** SNR_{SC}: **6.3**

Rotation Correlation: -22< 20° < 63 0.0<0.0s<2.6
Minimum Energy: -Inf< -21° < Inf 0.0<4.0s<Inf
Eigenvalue: -Inf< -29° < Inf 0.0<0.1s<Inf
Quality: **fair** IsNull: **Yes** Phase: **SKS**

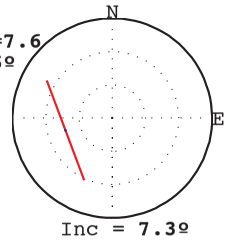

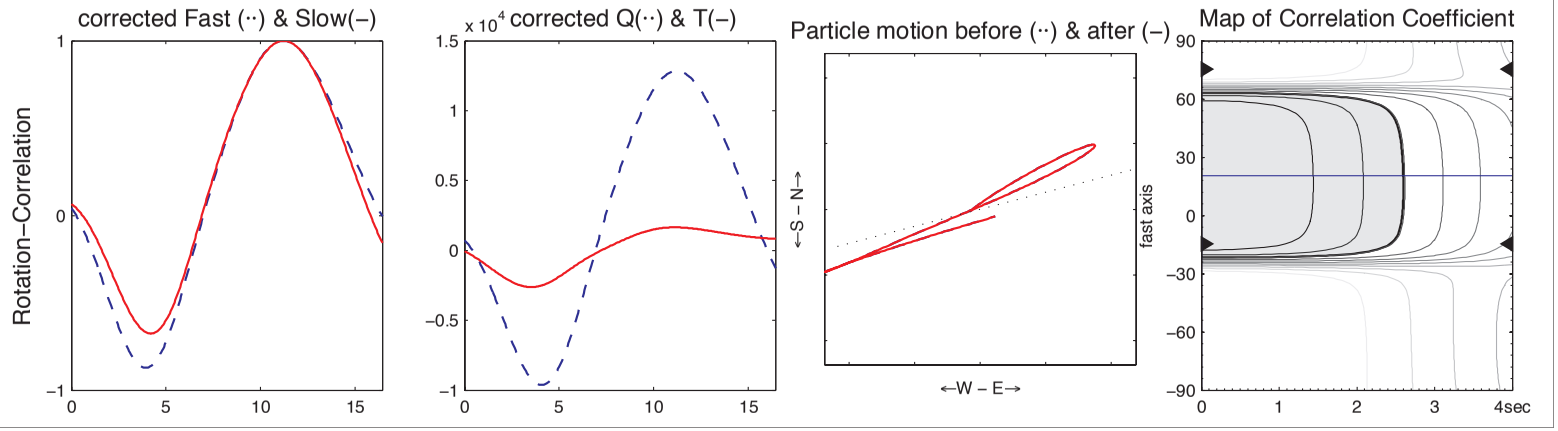

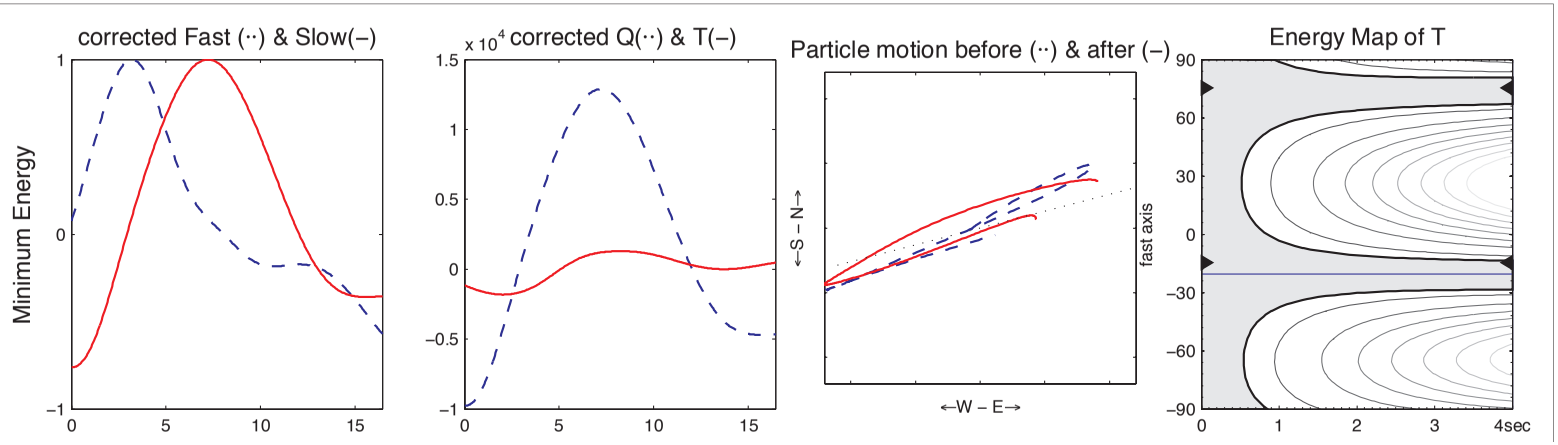

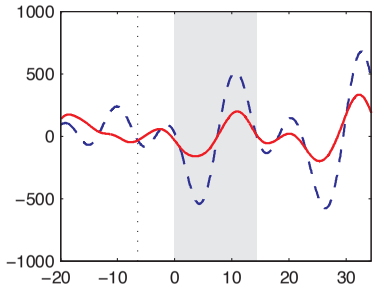

Event: **12-Dec-2002 (346) 08:30 -4.79N 153.27E 34km Mw=6.6**
Station: **AGBLF** Backazimuth: **286.7º** Distance: **121.52º**
init.Pol.: **87.9º** Filter: **0.020Hz - 0.12Hz** SNR_{SC}: **3.6**

Rotation Correlation: -Inf< 42° < Inf 0.0<0.1s<Inf
Minimum Energy: -Inf< -81° < Inf 0.0<4.0s<Inf
Eigenvalue: -Inf< 89° < Inf 0.0<2.7s<Inf
Quality: **fair** IsNull: **Yes** Phase: **SKS**

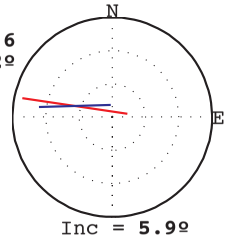

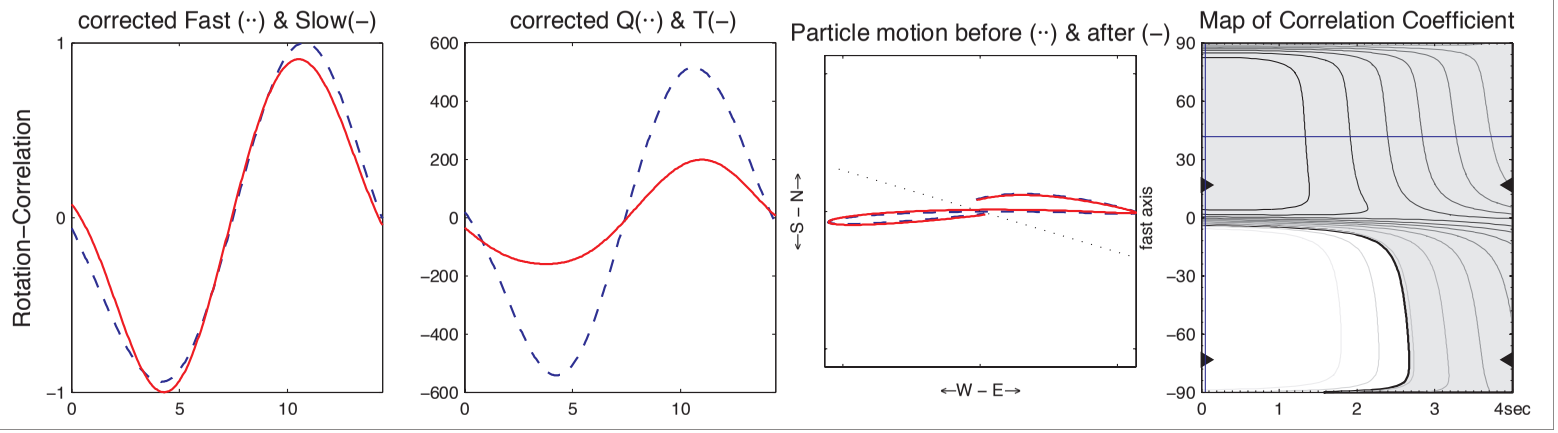

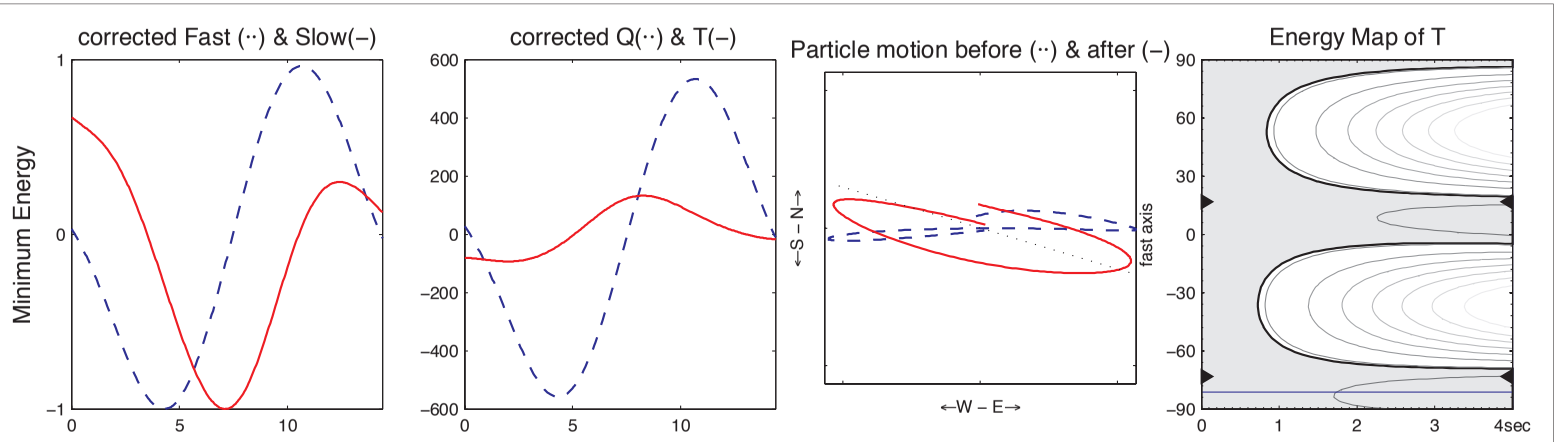

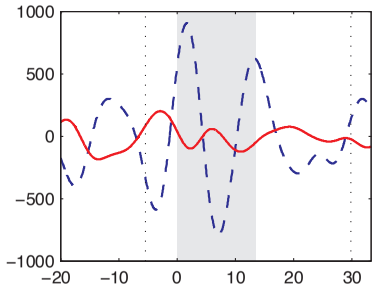

Event: **17-Dec-2002 (351) 04:32 -56.95N -24.83E 10km** Mw=6.2
Station: **BLACK** Backazimuth: **153.0º** Distance: **101.51º**
init.Pol.: **327.0º** Filter: **0.020Hz - 0.12Hz** SNR_{SC}:**17.6**

Rotation Correlation: −86< **−68°** < −51 0.0<**0.0s**<0.1
Minimum Energy: −27< **−23°** < −23 2.2<**3.3s**<4.0
Eigenvalue: −31< **−27°** < −29 3.8<**4.0s**<4.0
Quality: **fair** IsNull: **Yes** Phase: **SKS**

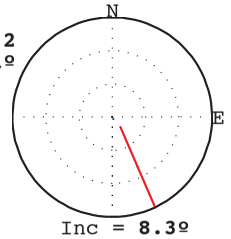

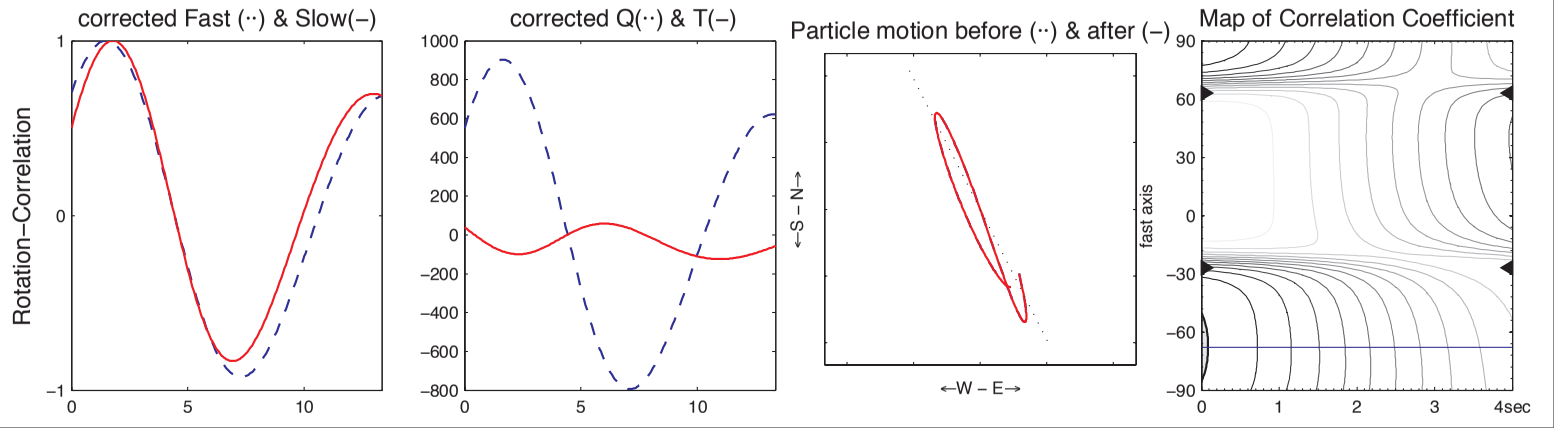

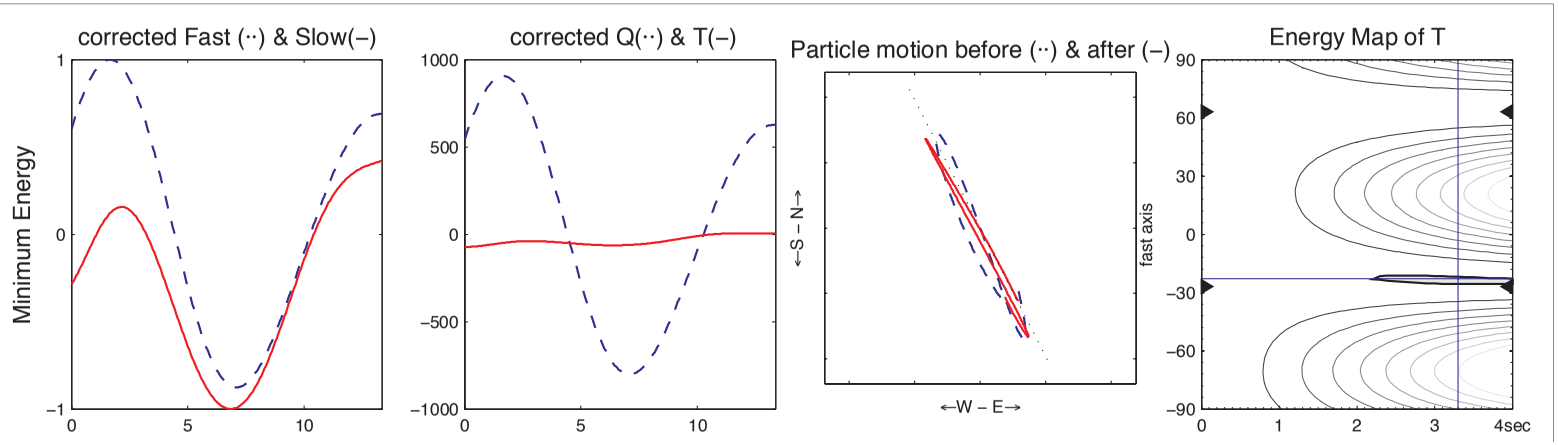

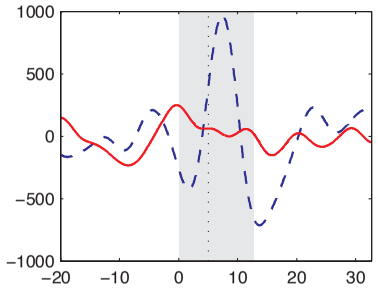

Event: **04-Jan-2003 (004) 05:15 -20.57N -177.66E 378km Mw=6.5**
Station: **CLINT** Backazimuth: **256.6º** Distance: **107.68º**
init.Pol.: **78.8º** Filter: **0.020Hz - 0.12Hz** SNR_{SC}: **9.9**

Rotation Correlation: -Inf< 34° < Inf 0.0<0.0s<Inf
Minimum Energy: -Inf< 77° < Inf 0.0<2.1s<Inf
Eigenvalue: -Inf< 77° < Inf 0.0<1.1s<Inf
Quality: **fair** IsNull: **Yes** Phase: **SKS**

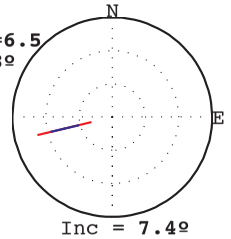

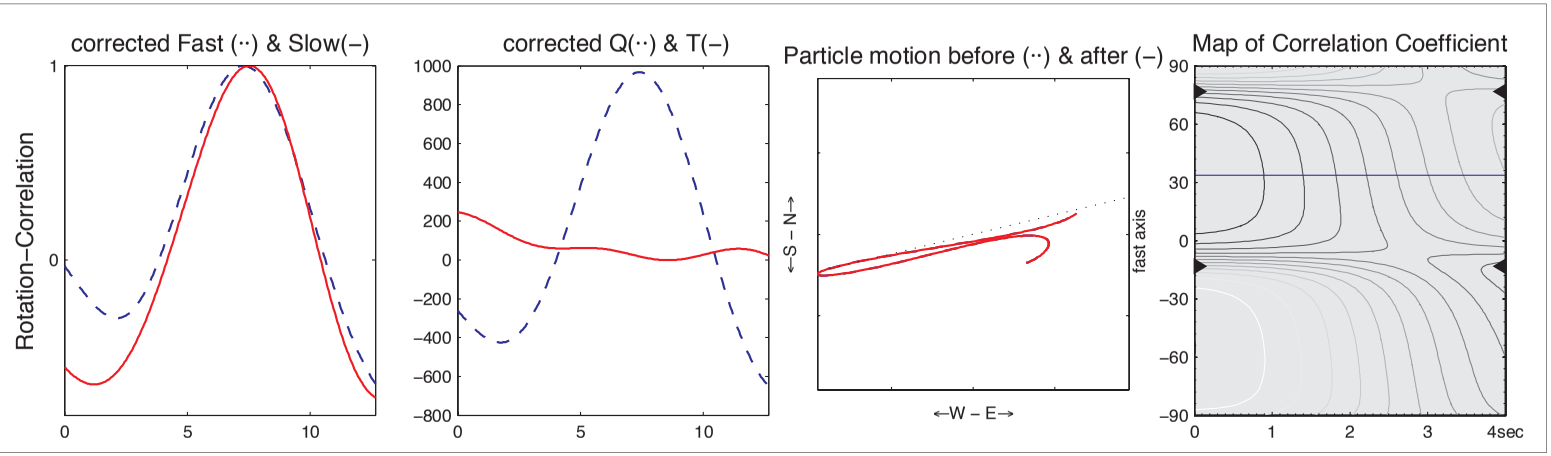

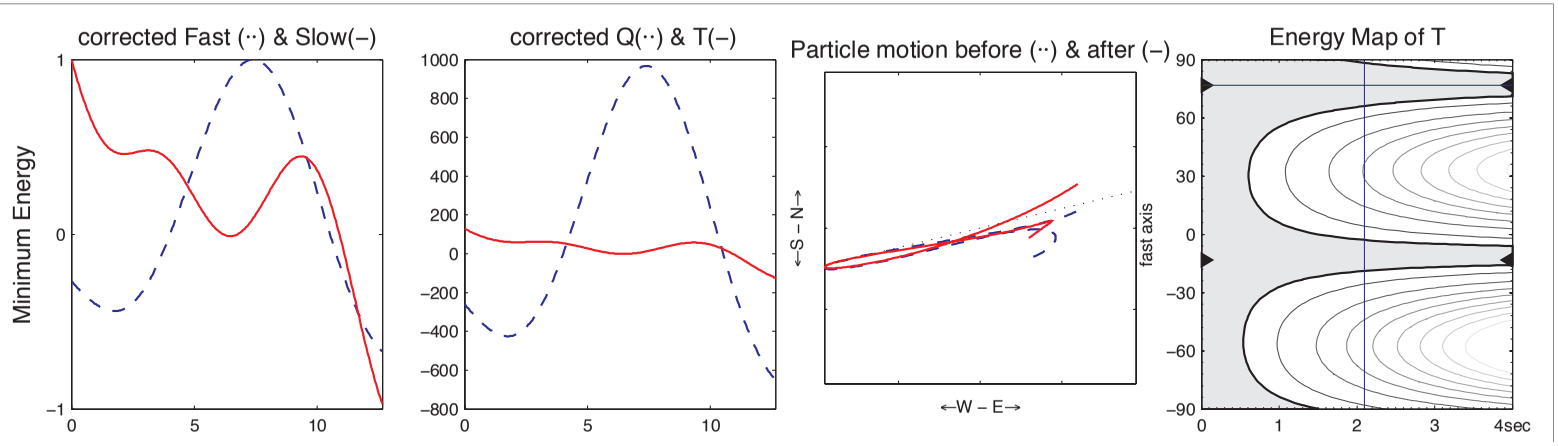

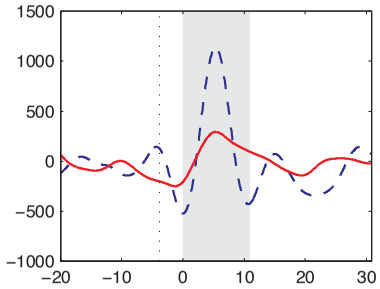

Event: **04-Jan-2003 (004) 05:15 -20.57N -177.66E 378km Mw=6.5**
Station: **AGBLF** Backazimuth: **255.5º** Distance: **105.89º**
init.Pol.: **66.7º** Filter: **0.020Hz - 0.12Hz** SNR_{SC}:**12.7**

Rotation Correlation: -Inf< 17° < Inf 0.0<0.0s<Inf
Minimum Energy: -Inf< -22° < Inf 0.0<4.0s<Inf
Eigenvalue: 58< 70° < -86 0.3<2.2s<4.0
Quality: **fair** IsNull: **Yes** Phase: **SKS**

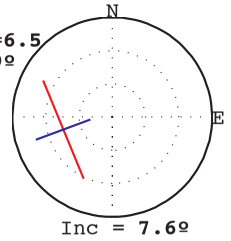

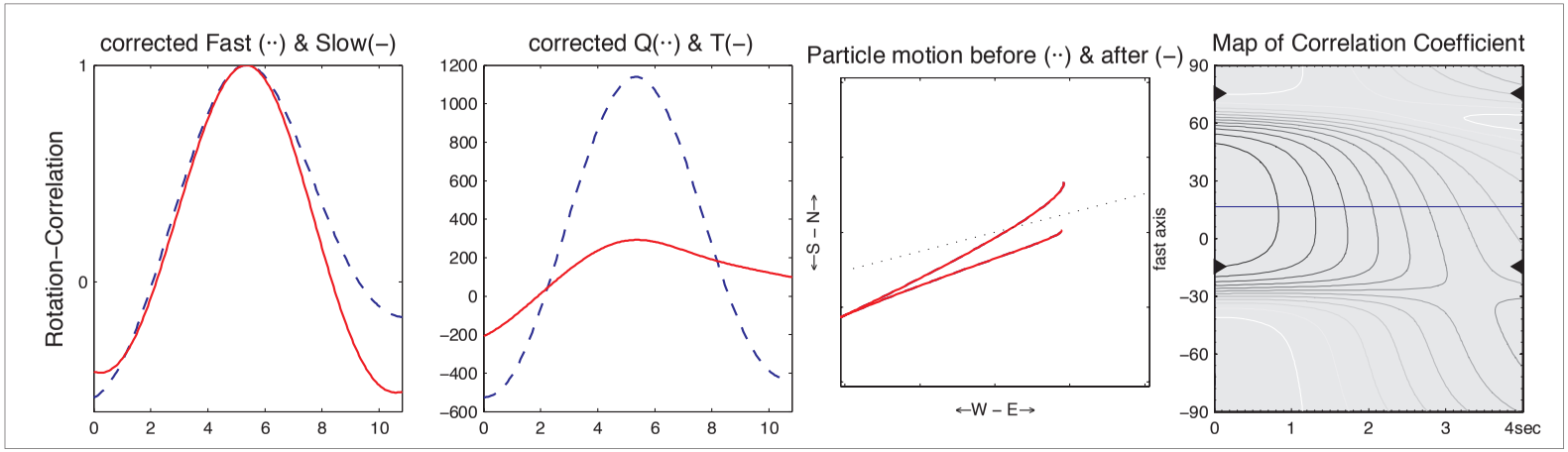

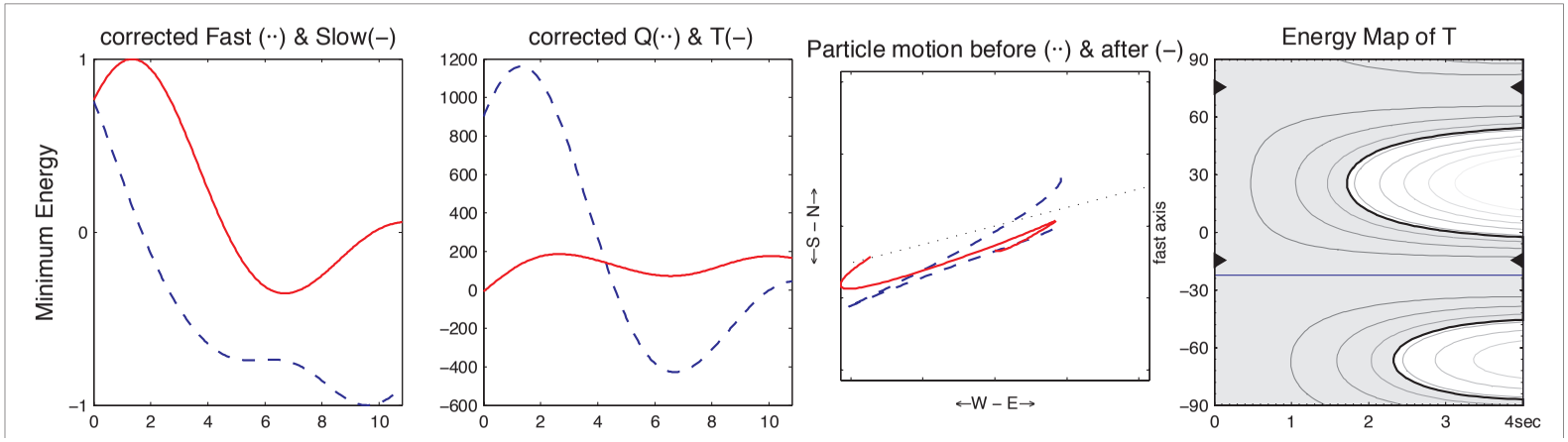

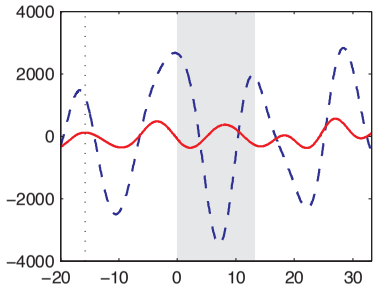

Event: **20-Jan-2003 (020) 08:43 -10.49N 160.77E 33km Mw=7.3**
Station: **CLINT** Backazimuth: **277.8º** Distance: **120.42º**
init.Pol.: **106.3º** Filter: **0.020Hz - 0.12Hz** SNR_{SC}:**40.6**

Rotation Correlation:	-Inf<	59° < Inf	0.0<0.0s<Inf
Minimum Energy:	11<	12° < 13	2.6<4.0s<4.0
Eigenvalue:	-82<	-78° < -82	1.9<2.1s<2.3

Quality: **good** IsNull: **Yes** Phase: **SKS**

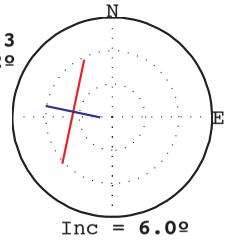

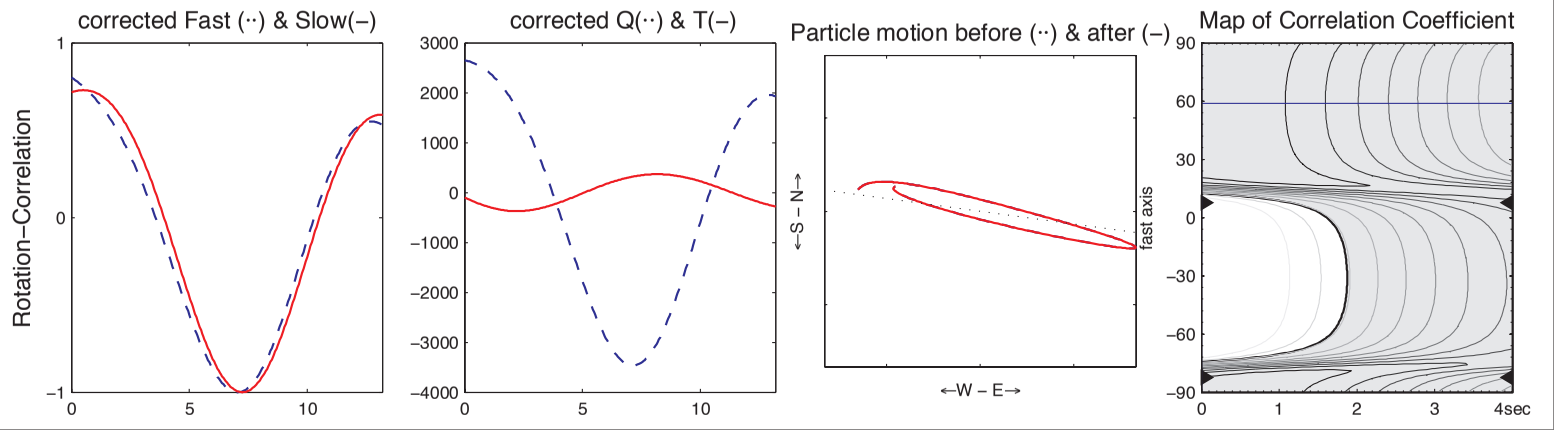

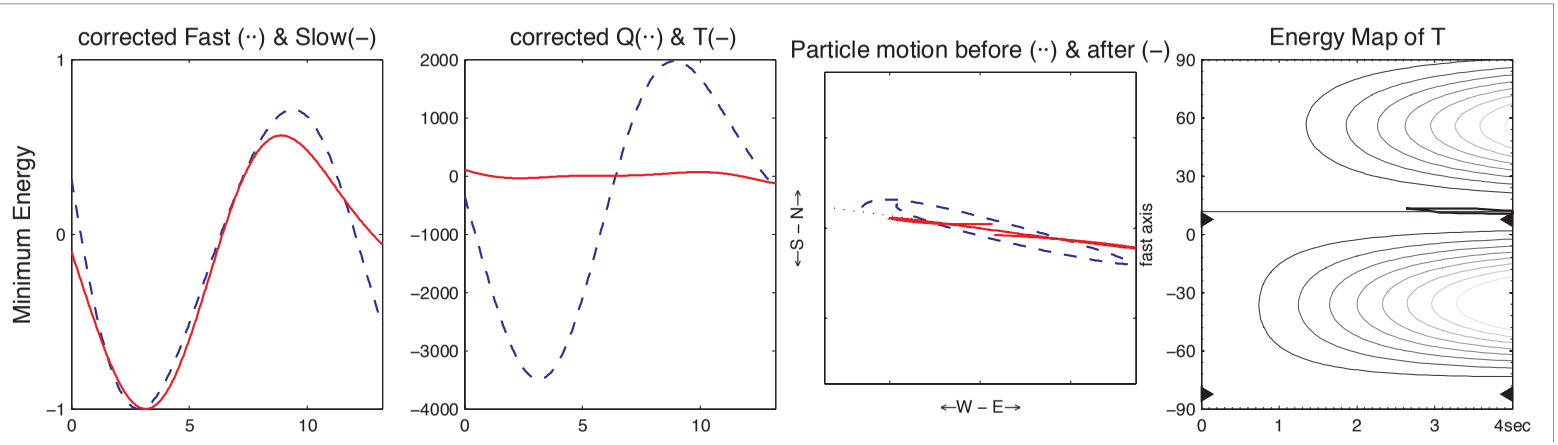

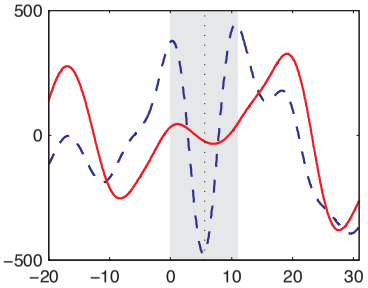

Event: **13-May-2003 (133) 21:21 −17.29N 167.74E 33km** Mw=6.3
Station: **CLINT** Backazimuth: **267.1º** Distance: **118.11º**
init.Pol.: **83.4º** Filter: **0.020Hz - 0.12Hz** SNR_{SC}:**29.7**

Rotation Correlation:	−8<	39° <	86	0.0<0.0s<3.0
Minimum Energy:	−13<	−7° <	−7	0.9<2.4s<4.0
Eigenvalue:	86<	−73° <	−5	0.1<0.3s<4.0

Quality: **fair** IsNull: **Yes** Phase: **SKS**

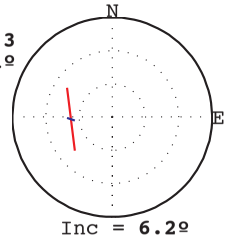

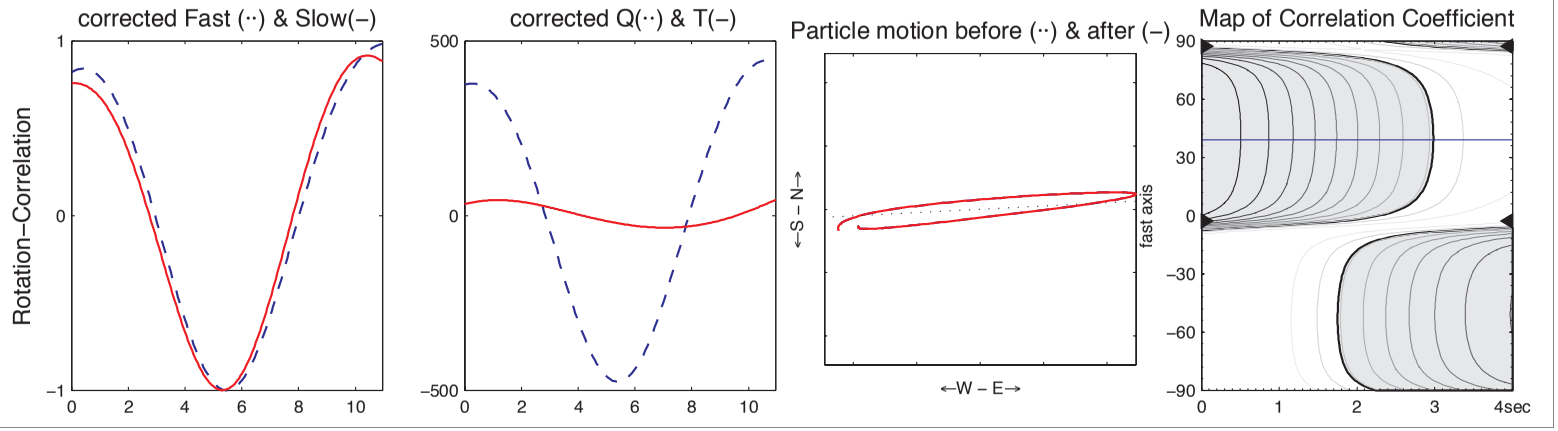

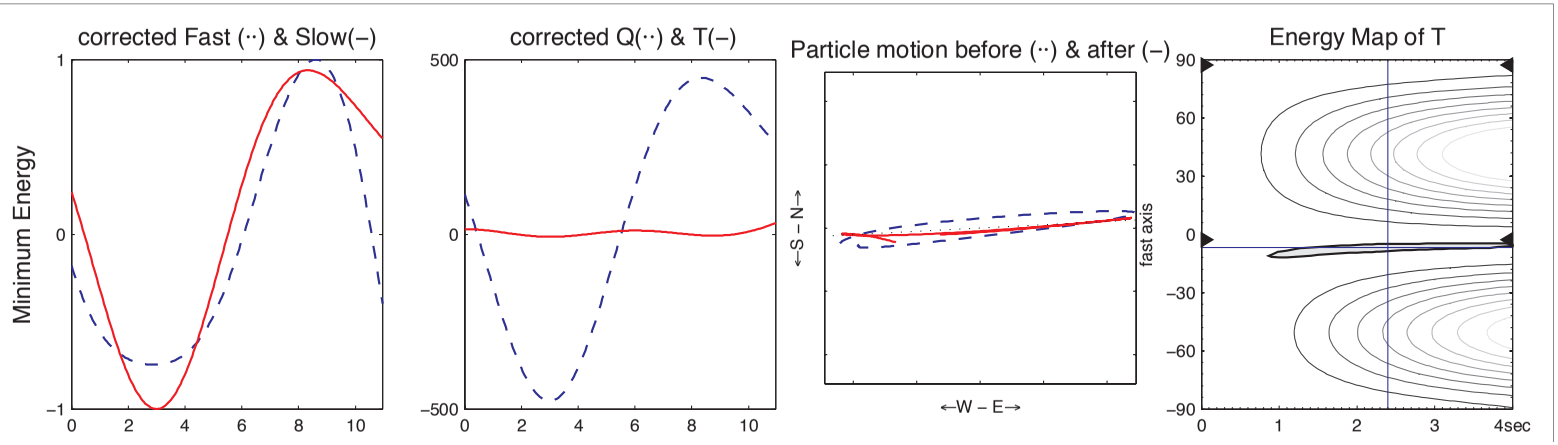

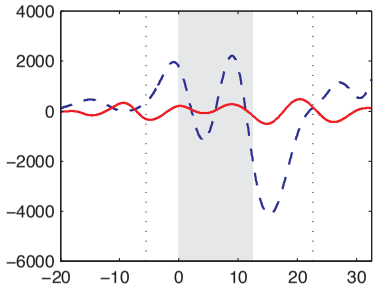

Event: **26-May-2003 (146) 09:24 38.85N 141.57E 68km Mw=7.0**
Station: **BTRCK** Backazimuth: **328.8º** Distance: **98.25º**
init.Pol.: **142.6º** Filter: **0.020Hz - 0.12Hz** SNR_{SC}:**24.4**

Rotation Correlation:	75< −83° < −61	0.0<0.0s<0.0
Minimum Energy:	58< 57° < 58	3.0<4.0s<4.0
Eigenvalue:	−37< −31° < −31	0.1<0.1s<0.3

Quality: **fair** IsNull: **Yes** Phase: **SKS**

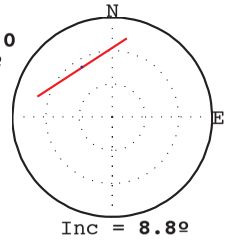

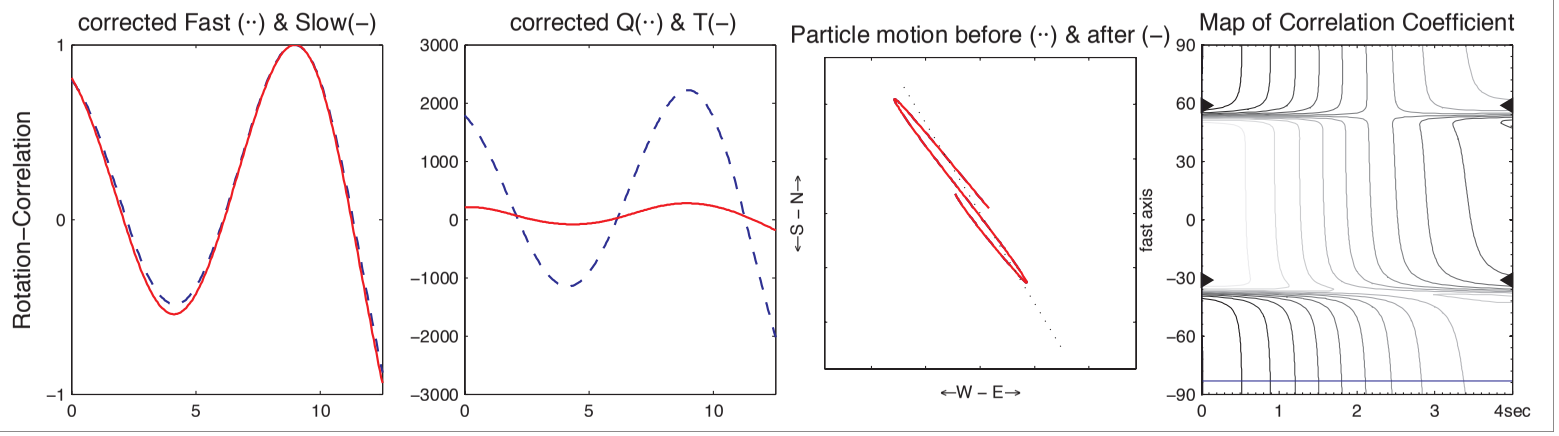

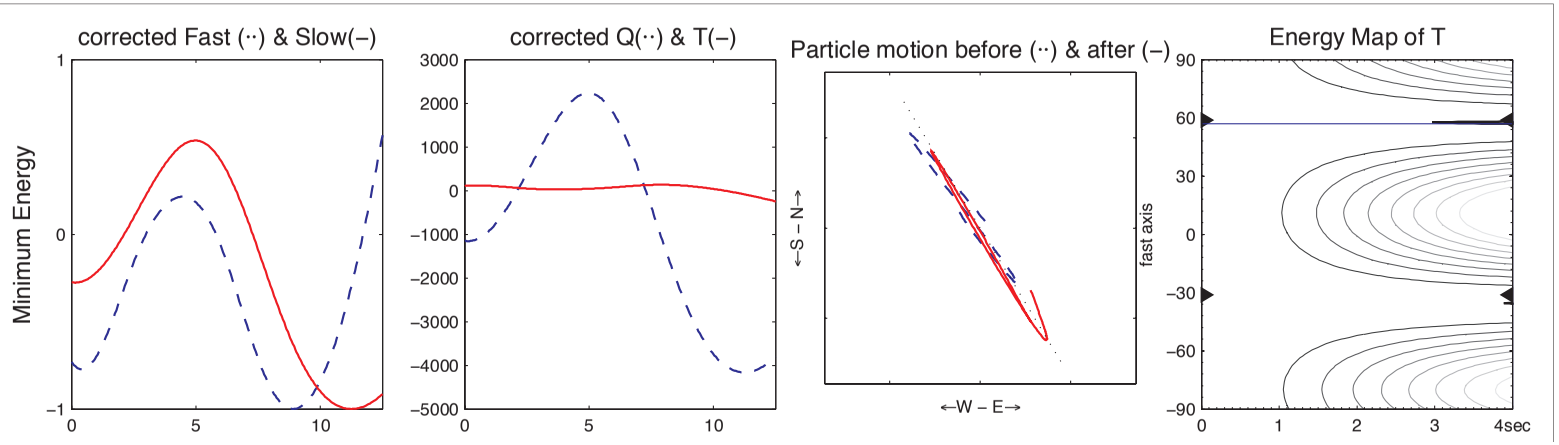

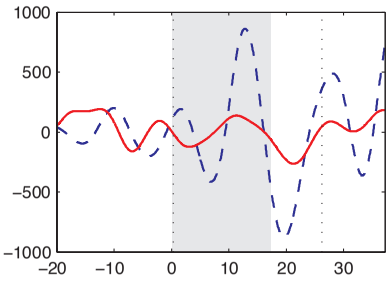

Event: **26-May-2003 (146) 09:24 38.85N 141.57E 68km Mw=7.0**
Station: **ACFLR** Backazimuth: **327.9º** Distance: **97.16º**
init.Pol.: **133.2º** Filter: **0.020Hz - 0.12Hz** SNR_{sc}: **6.5**

Rotation Correlation: -Inf< -85° < Inf 0.0<0.2s<Inf
Minimum Energy: -Inf< -40° < Inf 0.0<2.7s<Inf
Eigenvalue: -Inf< 48° < Inf 0.0<3.9s<Inf
Quality: **fair** IsNull: **Yes** Phase: **SKS**

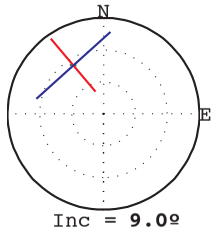

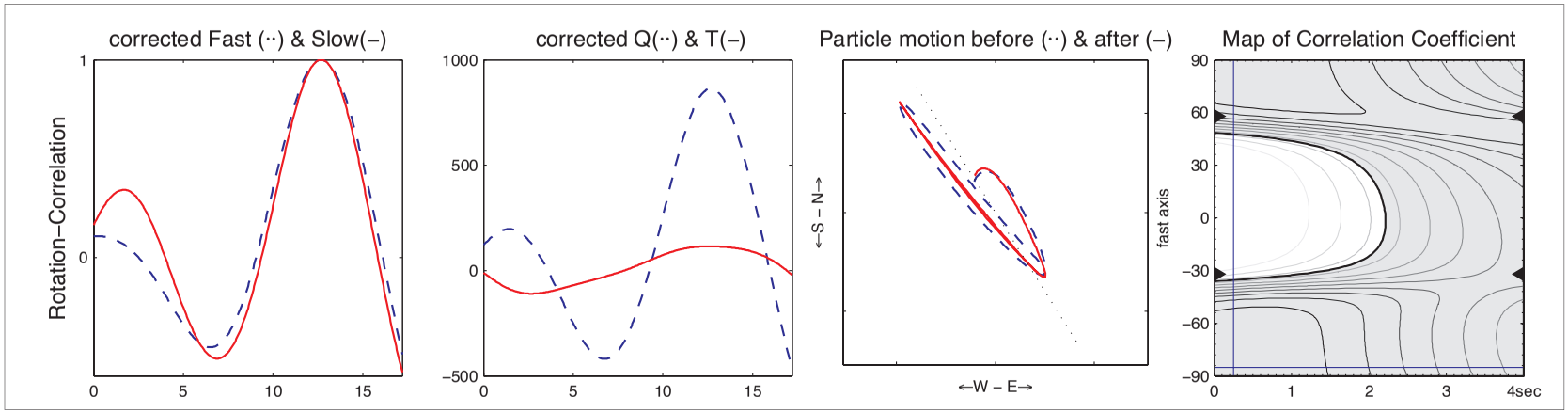

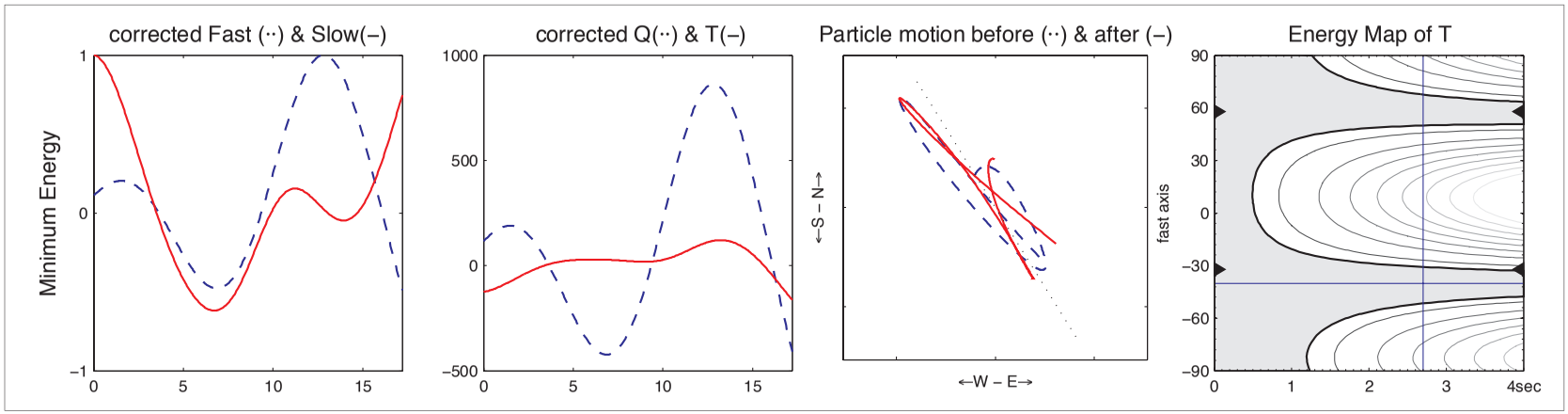

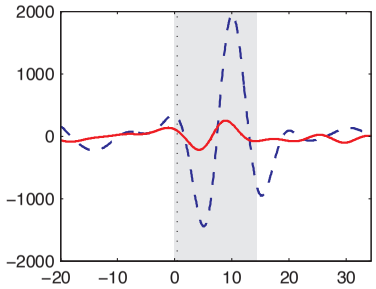

Event: **27-Jul-2003 (208) 02:04 -21.08N -176.59E 213km Mw=6.6**
Station: **AGBLF** Backazimuth: **254.5º** Distance: **105.28º**
init.Pol.: **68.4º** Filter: **0.020Hz - 0.12Hz** SNR_{SC}:**15.9**

Rotation Correlation:	−16<	24° <	64	0.0<0.2s<1.1
Minimum Energy:	68<	71° <	74	1.6<3.5s<4.0
Eigenvalue:	−19<	45° <	68	0.2<0.3s<2.0

Quality: **fair** IsNull: **Yes** Phase: **SKS**

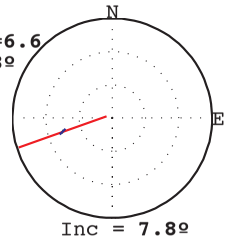

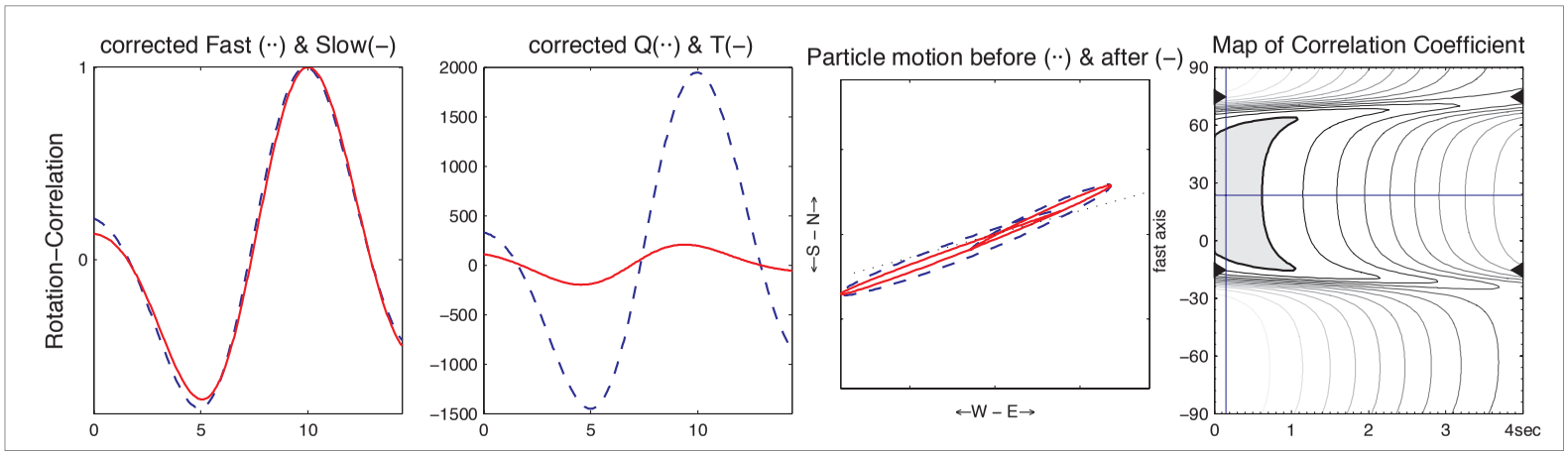

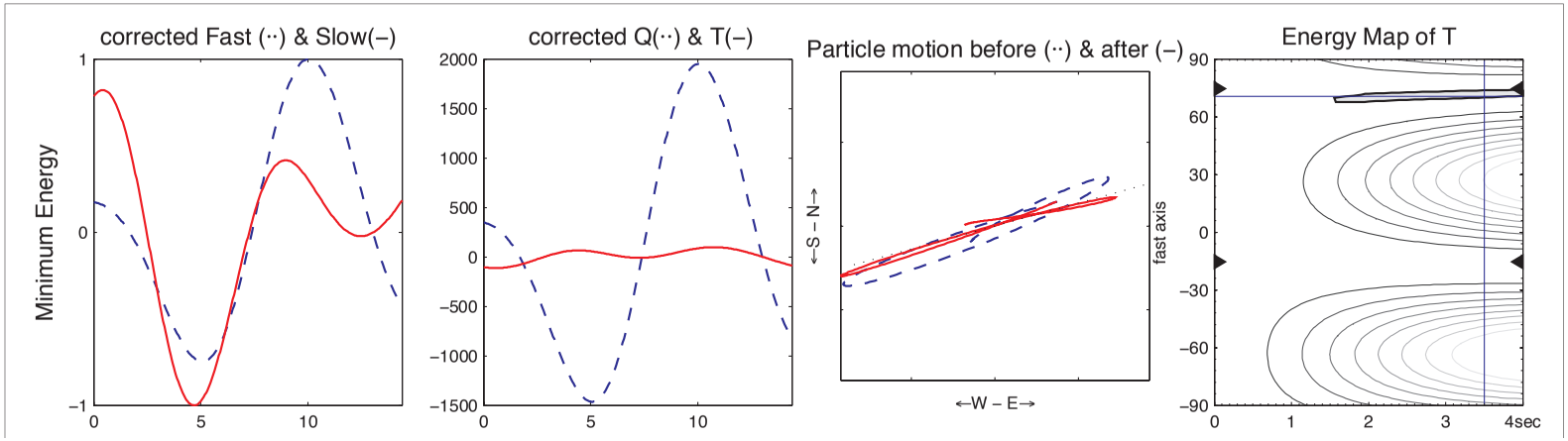

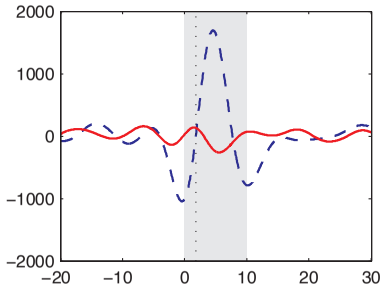

Event: **27-Jul-2003 (208) 02:04 -21.08N -176.59E 213km Mw=6.6**
Station: **BBLV** Backazimuth: **255.6º** Distance: **107.06º**
init.Pol.: **83.3º** Filter: **0.020Hz - 0.12Hz** SNR_{SC}:**19.3**

Rotation Correlation:	-Inf<	39° <	Inf	0.0<0.1s<Inf
Minimum Energy:	-15<	-8° <	3	0.6<2.9s<4.0
Eigenvalue:	23<	72° <	78	0.3<0.8s<1.6

Quality: **fair** IsNull: **Yes** Phase: **SKS**

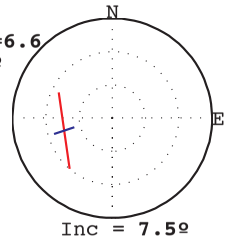

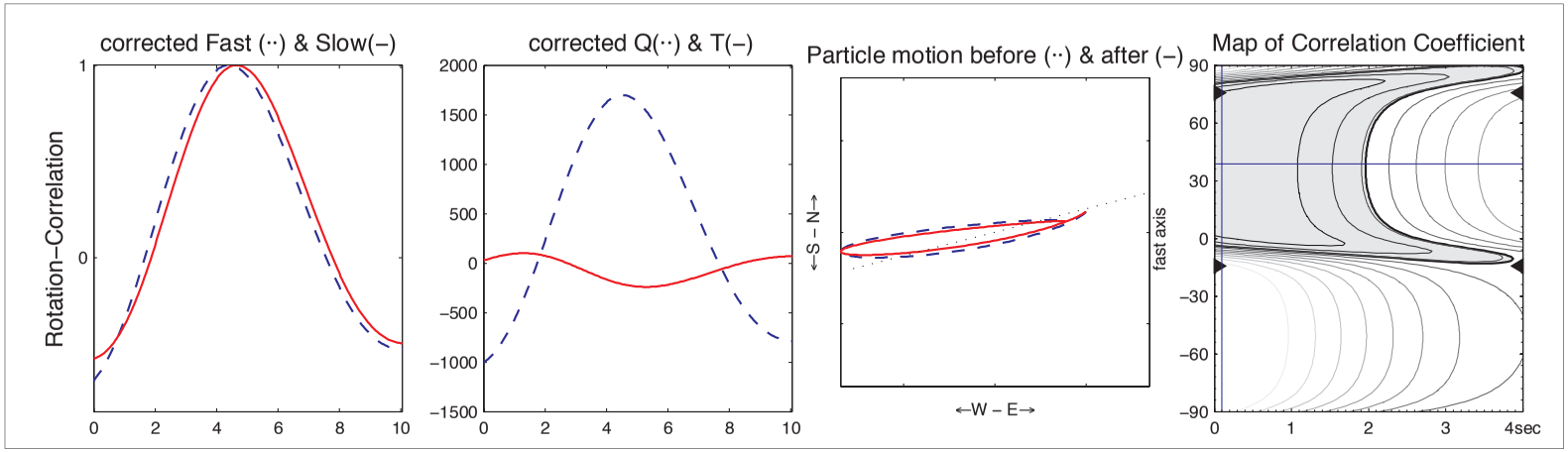

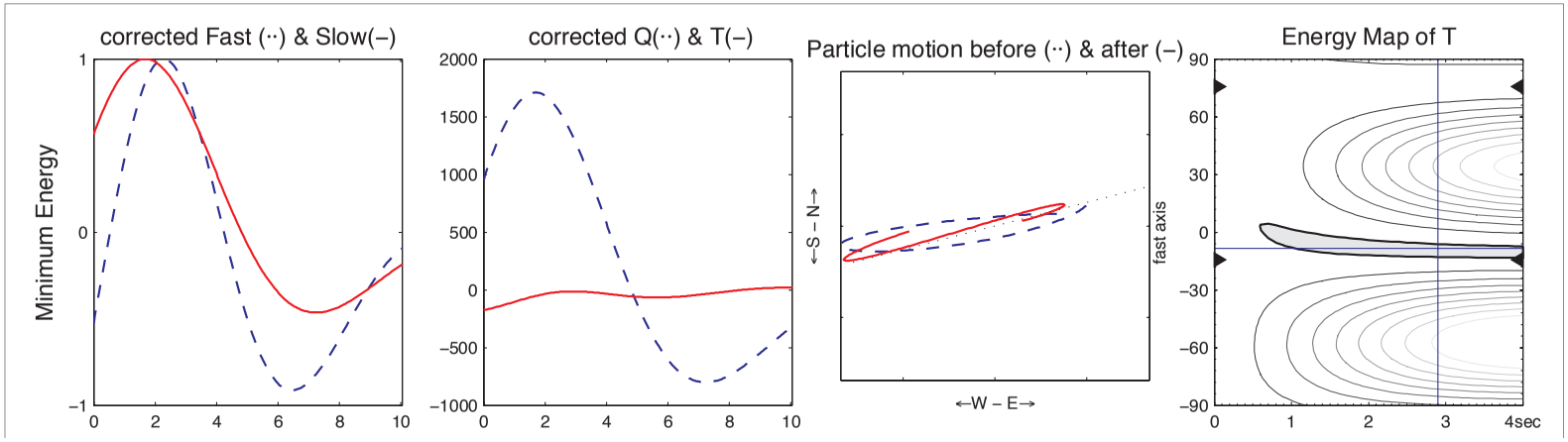

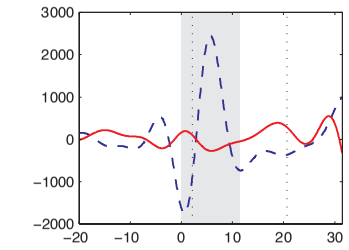

Event: **27-Jul-2003 (208) 06:25 47.15N 139.25E 470km Mw=6.7**
Station: **BBLV** Backazimuth: **334.7º** Distance: **92.17º**
init.Pol.: **155.5º** Filter: **0.020Hz – 0.12Hz** SNR_{SC}:**49.8**

Rotation Correlation:	78<	−64° < −25	0.0<0.0s<0.8
Minimum Energy:	68<	69° < 72	1.4<4.0s<4.0
Eigenvalue:	70<	69° < 72	3.6<4.0s<4.0

Quality: **good** IsNull: **Yes** Phase: **SKS**

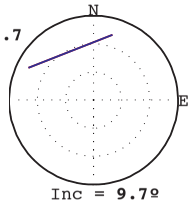

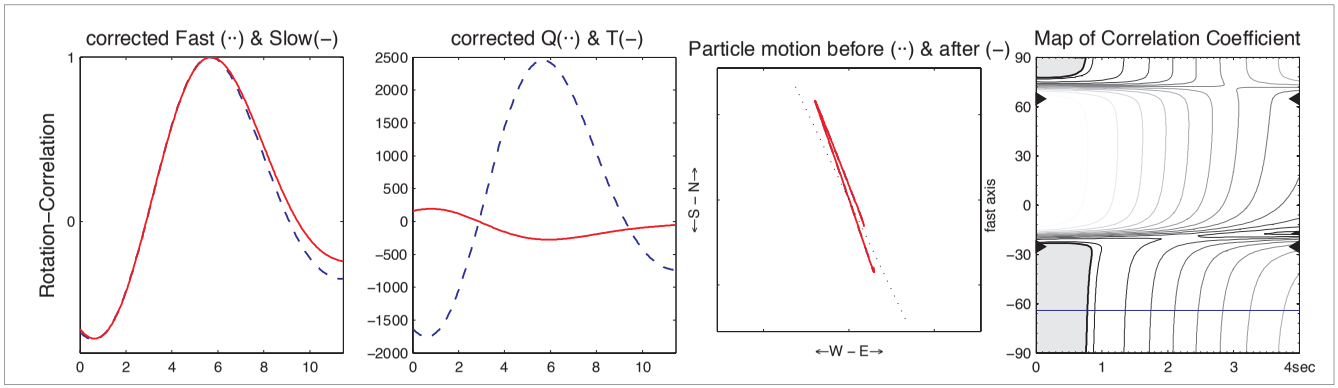

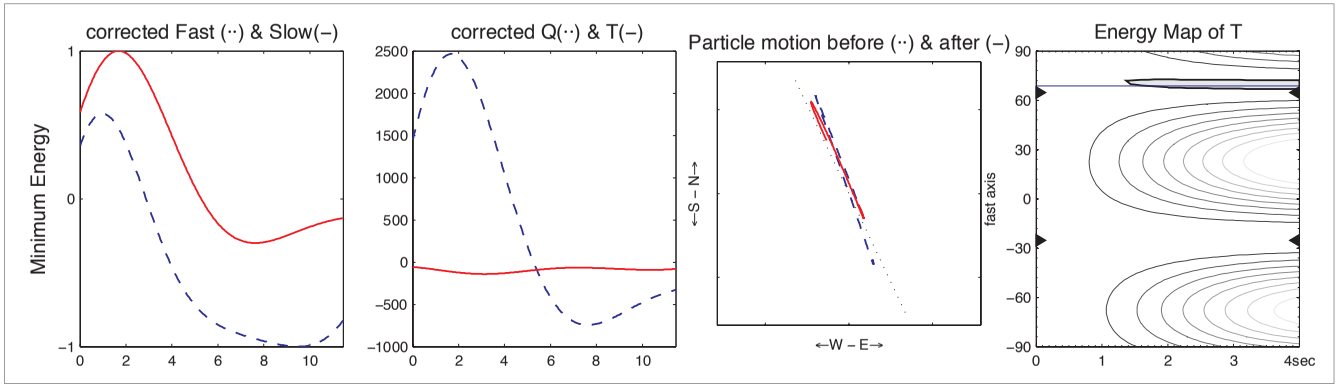

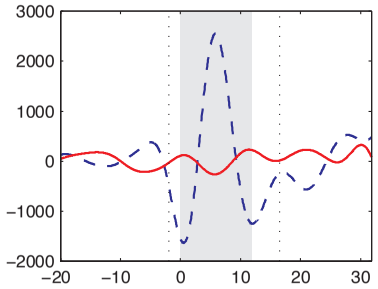

Event: **27-Jul-2003 (208) 06:25 47.15N 139.25E 470km** Mw=**6.7**
Station: **BLACK** Backazimuth: **334.7º** Distance: **92.17º**
init.Pol.: **159.1º** Filter: **0.020Hz – 0.12Hz** SNR_{SC}:**20.2**

Rotation Correlation:	74< −64° < −22	0.0<0.0s<1.4
Minimum Energy:	−25< −21° < −21	3.0<4.0s<4.0
Eigenvalue:	−21< −19° < −21	3.1<4.0s<4.0

Quality: **good** IsNull: **Yes** Phase: **SKS**

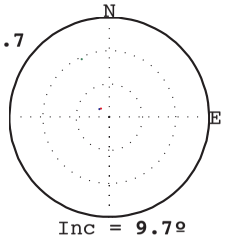

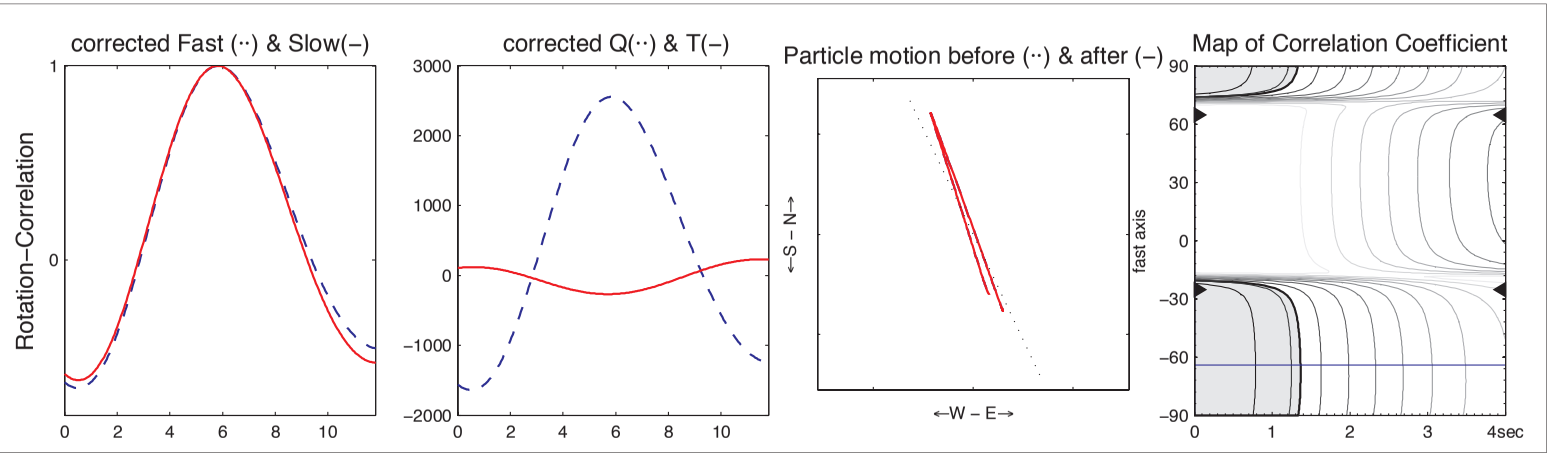

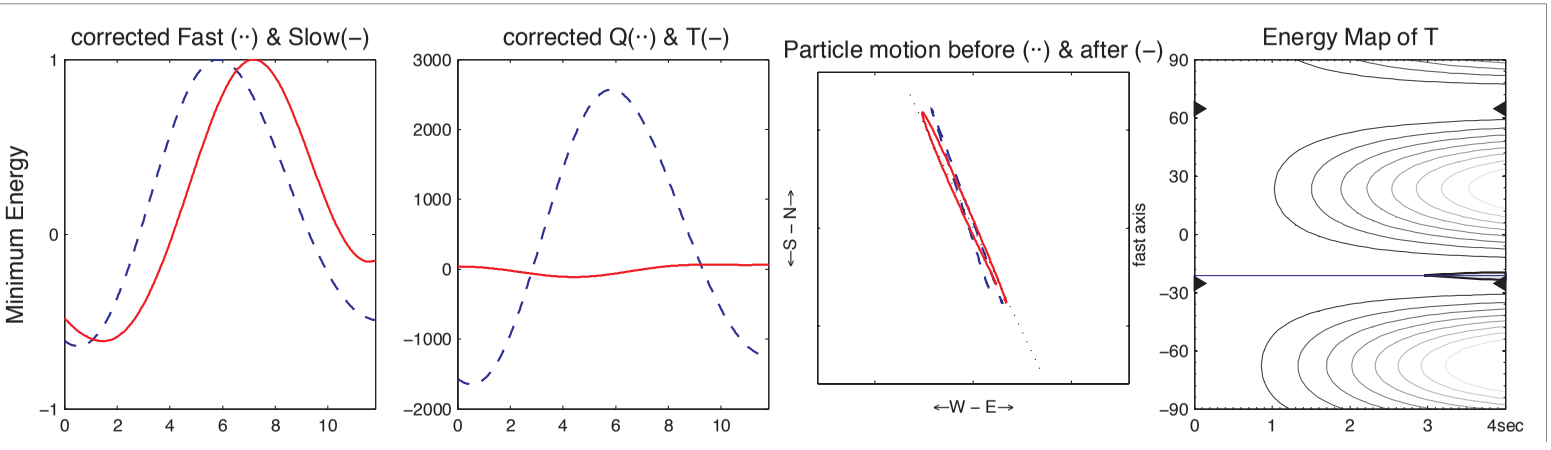

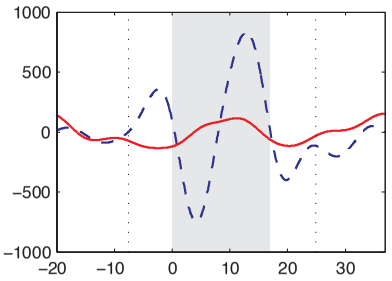

Event: **02-Sep-2003 (245) 18:28 -15.23N -173.22E 10km** Mw=6.4
Station: **ACFLR** Backazimuth: **258.5º** Distance: **100.27º**
init.Pol.: **76.1º** Filter: **0.010Hz - 0.10Hz** SNR_{sc}:**11.9**

Rotation Correlation: -Inf< 25° < Inf 0.0<0.6s<Inf
Minimum Energy: -7< 72° < 78 0.1<4.0s<4.0
Eigenvalue: -15< 62° < 74 0.3<1.2s<4.0
Quality: **fair** IsNull: **Yes** Phase: **SKS**

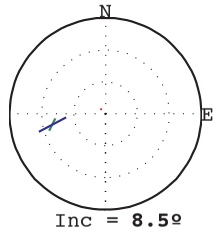

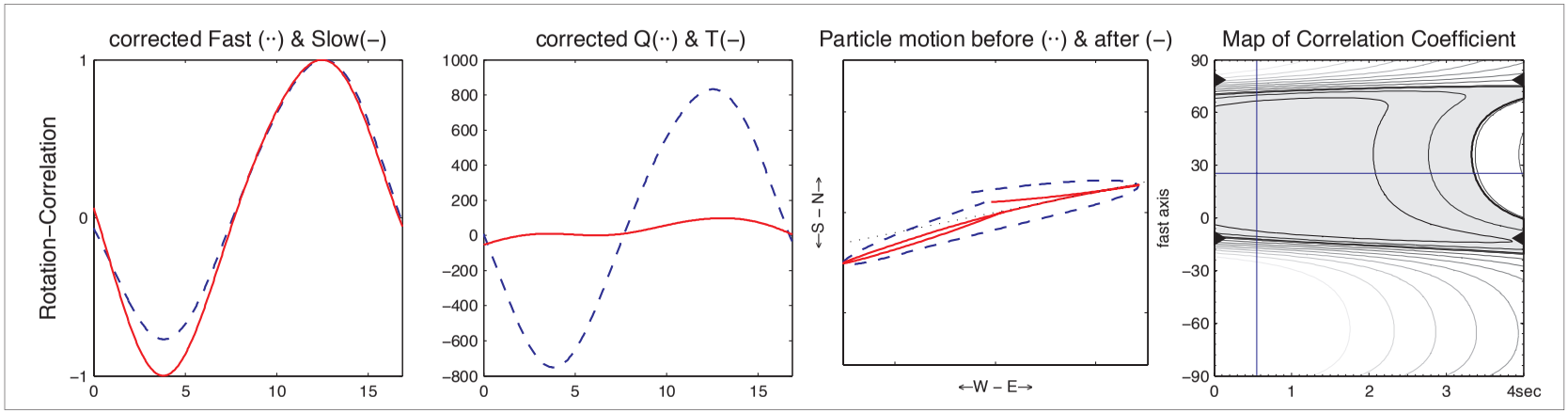

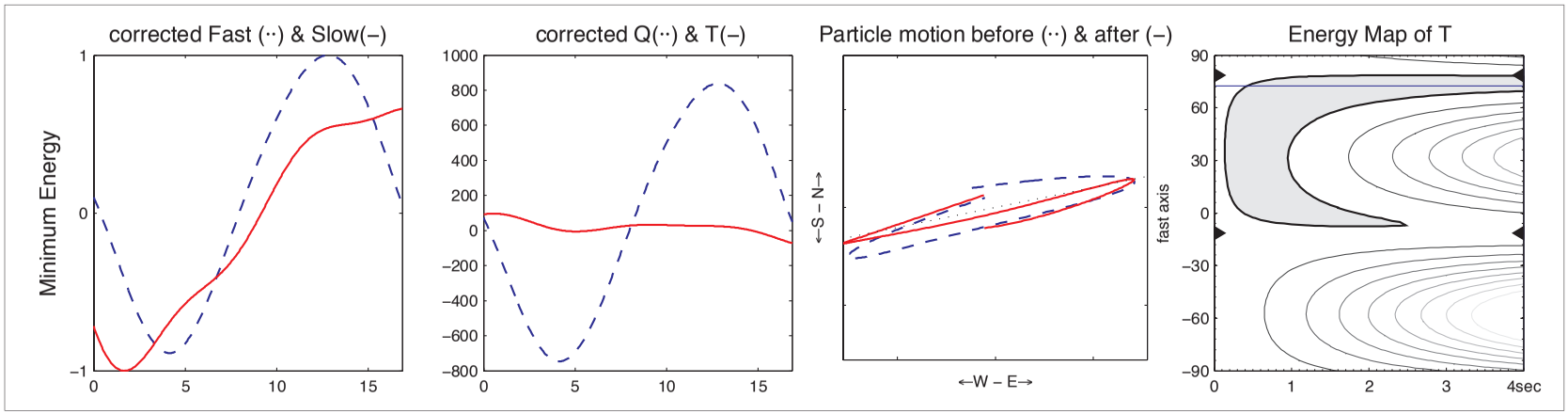

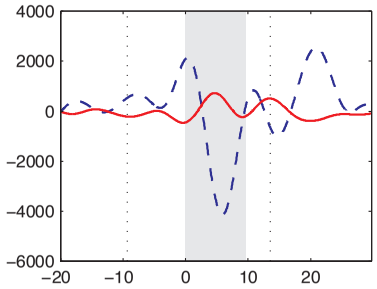

Event: **27-Sep-2003 (270) 11:33 50.04N 87.81E 16km Mw=7.3**
Station: **BRNCH** Backazimuth: **8.1º** Distance: **95.75º**
init.Pol.: **198.6º** Filter: **0.020Hz - 0.12Hz** SNR_{SC}:**21.3**

Rotation Correlation:	-Inf<	57° < Inf	0.0<0.2s<Inf
Minimum Energy:	9<	16° < -88	0.1<2.0s<4.0
Eigenvalue:	50<	-86° < -78	0.4<0.9s<1.9

Quality: **fair** IsNull: **Yes** Phase: **SKS**

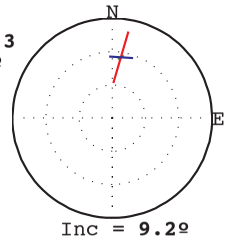

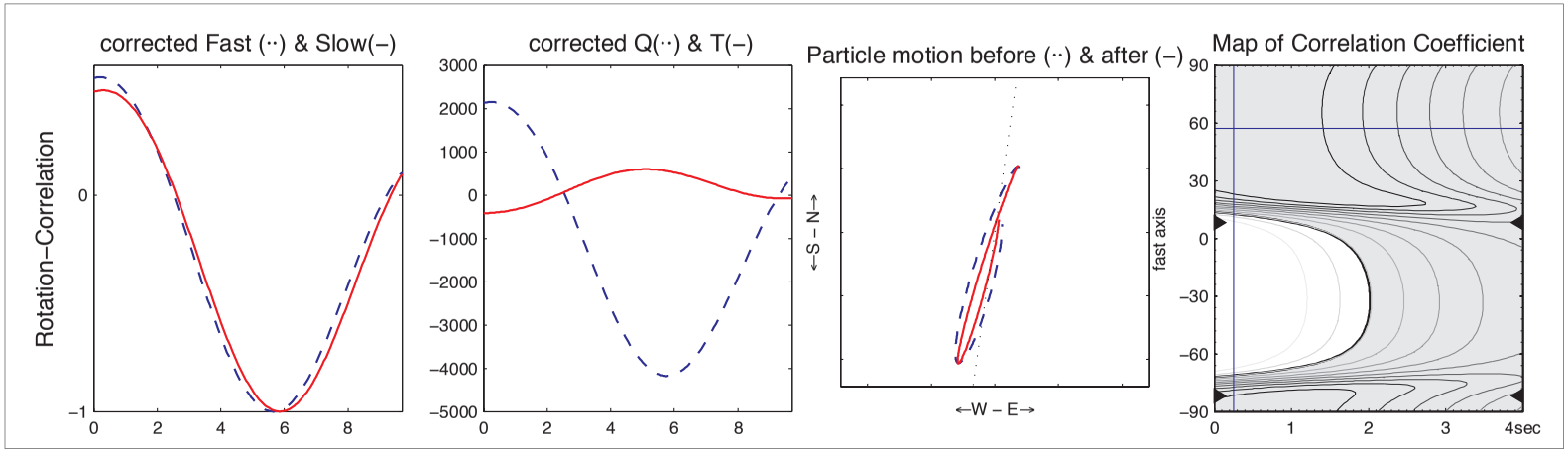

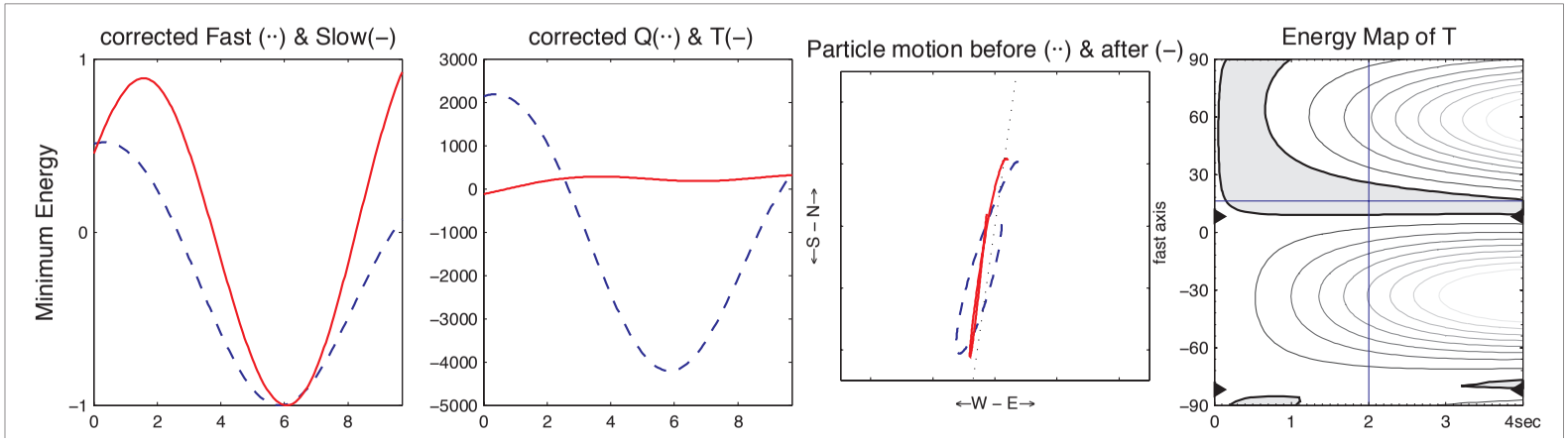

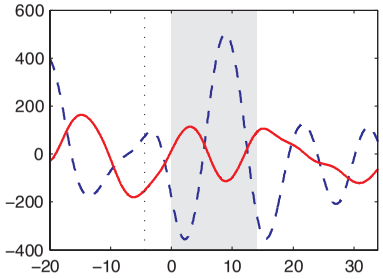

Event: **30-Sep-2003 (273) 14:08 -30.44N -177.40E 10km** Mw=6.4
Station: **ACFLR** Backazimuth: **246.9º** Distance: **111.31º**
init.Pol.: **82.3º** Filter: **0.020Hz - 0.12Hz** SNR_{SC}: **6.4**

Rotation Correlation: -Inf< 35° < Inf 0.0<0.0s<Inf
Minimum Energy: -23< -15° < -11 1.9<4.0s<4.0
Eigenvalue: 66< 81° < 84 0.2<2.1s<4.0
Quality: **fair** IsNull: **Yes** Phase: **SKS**

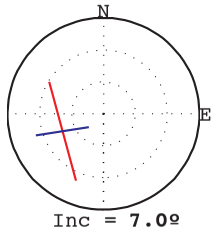

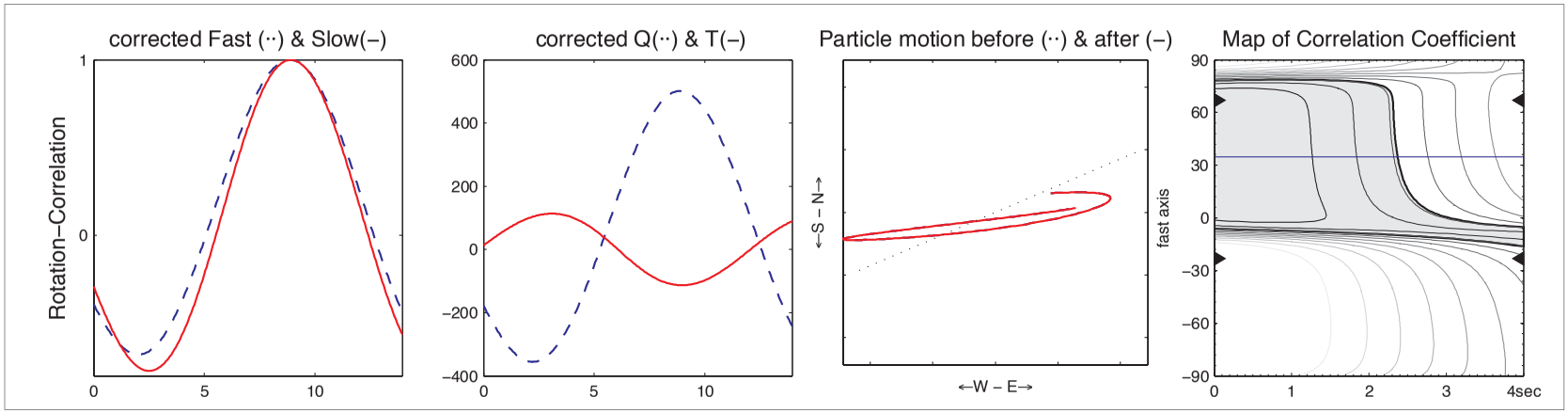

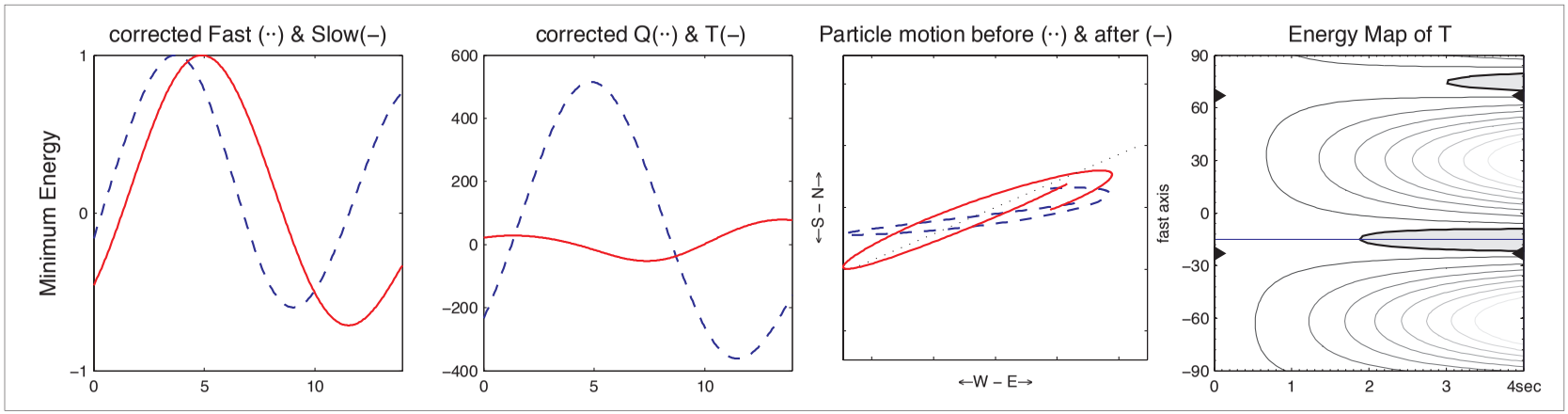

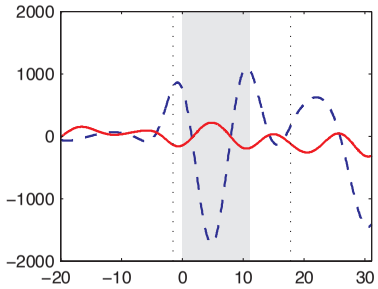

Event: **08-Oct-2003 (281) 09:06 42.65N 144.57E 32km Mw=6.7**
Station: **BLACK** Backazimuth: **329.1º** Distance: **93.83º**
init.Pol.: **157.5º** Filter: **0.020Hz - 0.12Hz** SNR_{SC}:**11.5**

Rotation Correlation:	69< −68° < −26	0.0<0.0s<1.6
Minimum Energy:	−33< −27° < −25	2.2<4.0s<4.0
Eigenvalue:	−90< −25° < 88	0.0<0.2s<1.9

Quality: **fair** IsNull: **Yes** Phase: **SKS**

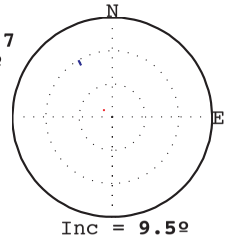

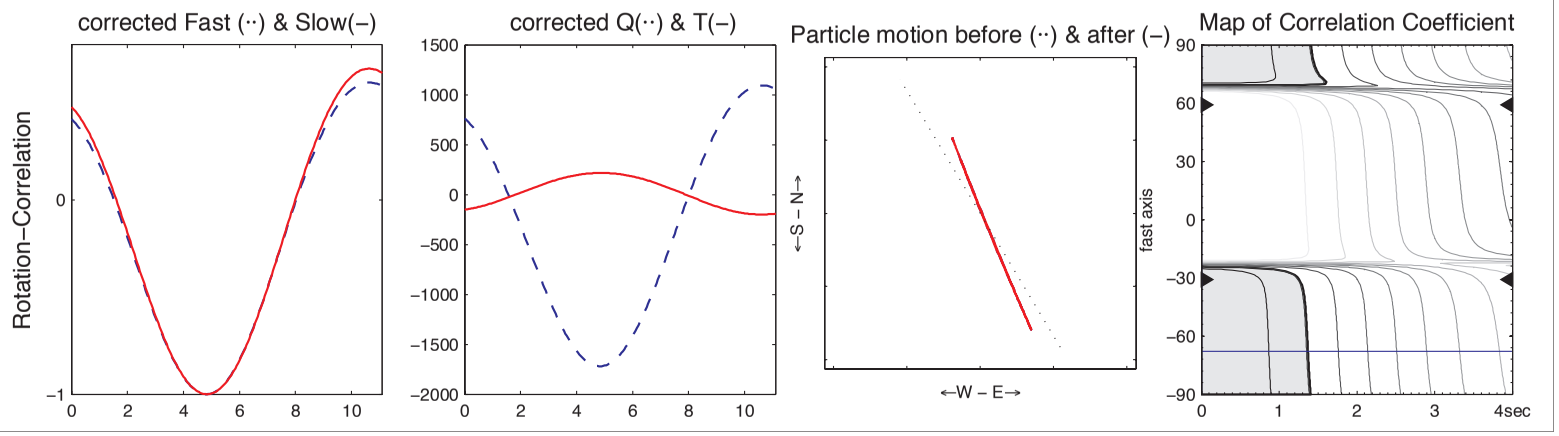

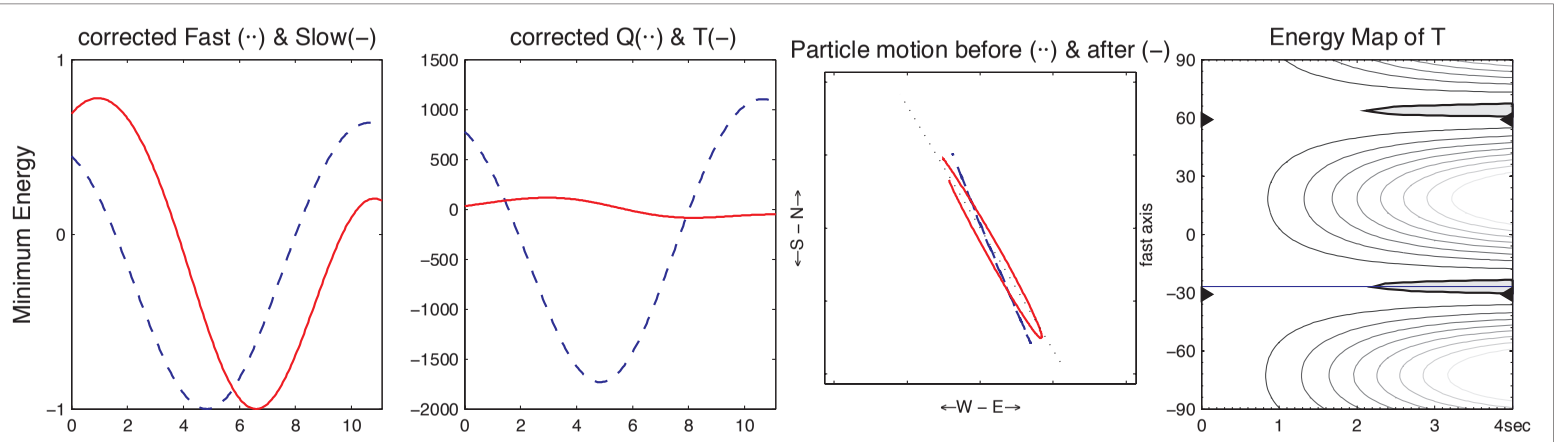

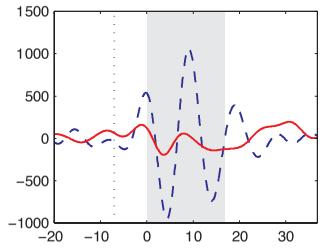

Event: **25-Dec-2003 (359) 20:42 -22.25N 169.49E 10km Mw=6.5**
Station: **AGBLF** Backazimuth: **260.1º** Distance: **117.18º**
init.Pol.: **74.1º** Filter: **0.020Hz - 0.12Hz** SNR_{SC}: **9.6**

Rotation Correlation:	8<	28° < 49	0.0<0.1s<0.4
Minimum Energy:	-17<	-14° < -11	2.7<4.0s<4.0
Eigenvalue:	-17<	70° < 78	0.0<0.7s<4.0

Quality: **good** IsNull: **Yes** Phase: **SKS**

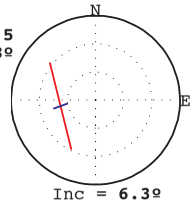

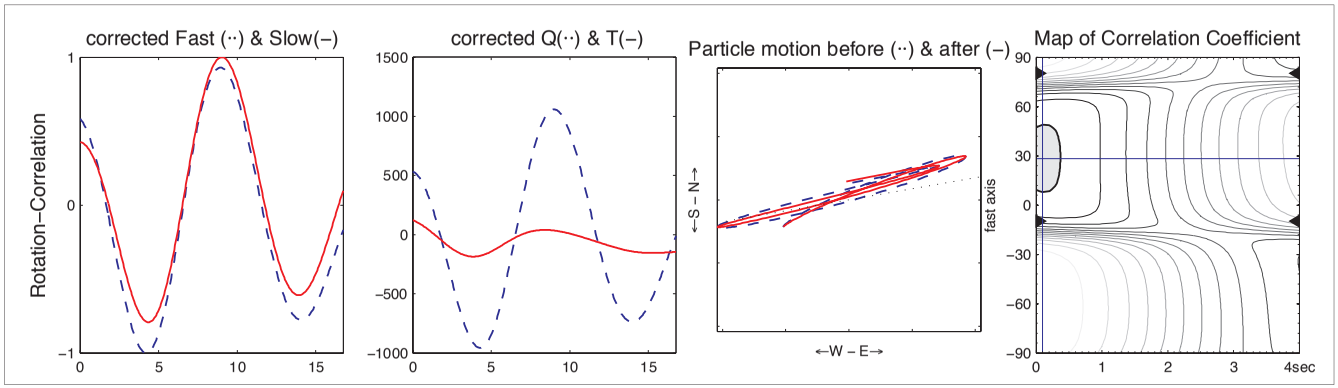

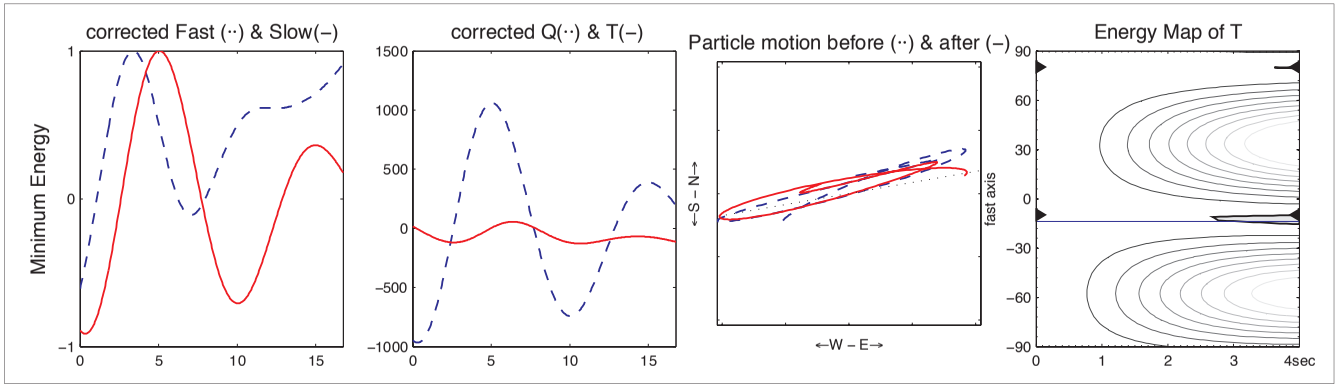

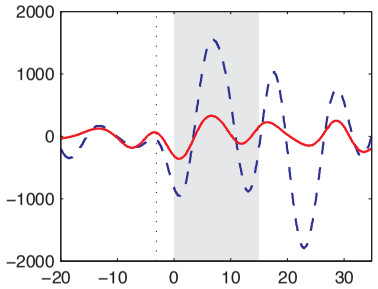

Event: **03-Jan-2004 (003) 16:23 -22.25N 169.68E 22km** Mw=7.1
Station: **AGBLF** Backazimuth: **260.0º** Distance: **117.03º**
init.Pol.: **77.8º** Filter: **0.020Hz - 0.12Hz** SNR_{SC}:**12.5**

Rotation Correlation:	−1<	23° <	49	0.0<0.0s<0.5
Minimum Energy:	74<	74° <	80	2.4<4.0s<4.0
Eigenvalue:	72<	74° <	80	3.0<4.0s<4.0

Quality: **fair** IsNull: **Yes** Phase: **SKS**

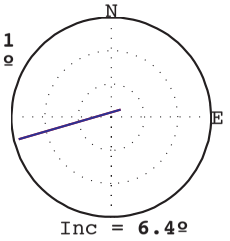

Inc = **6.4º**

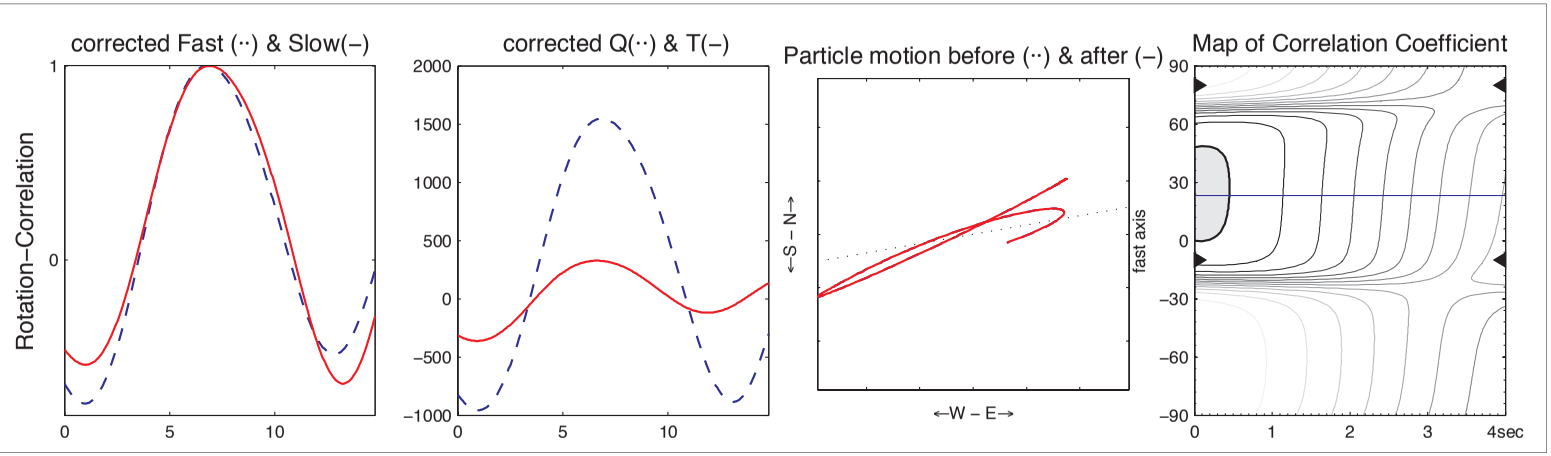

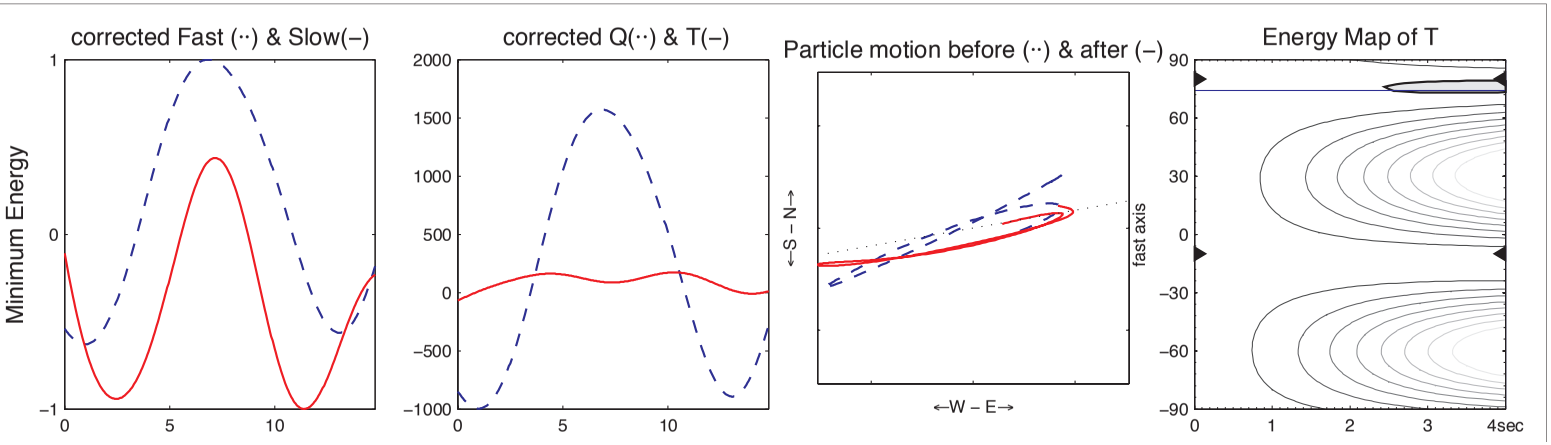

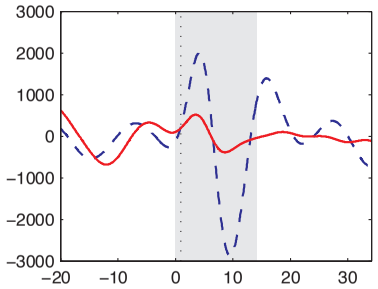

Event: **25-Jan-2004 (025) 11:43 -16.83N -174.20E 130km Mw=6.6**
Station: **AGBLF** Backazimuth: **257.1º** Distance: **101.15º**
init.Pol.: **68.0º** Filter: **0.020Hz - 0.12Hz** SNR_{SC}: **8.9**

Rotation Correlation:	−21<	22° < 66	0.0<0.1s<2.5
Minimum Energy:	48<	73° < 80	0.2<4.0s<4.0
Eigenvalue:	-Inf<	69° < Inf	0.0<4.0s<Inf

Quality: **fair** IsNull: **Yes** Phase: **SKS**

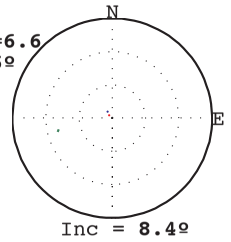

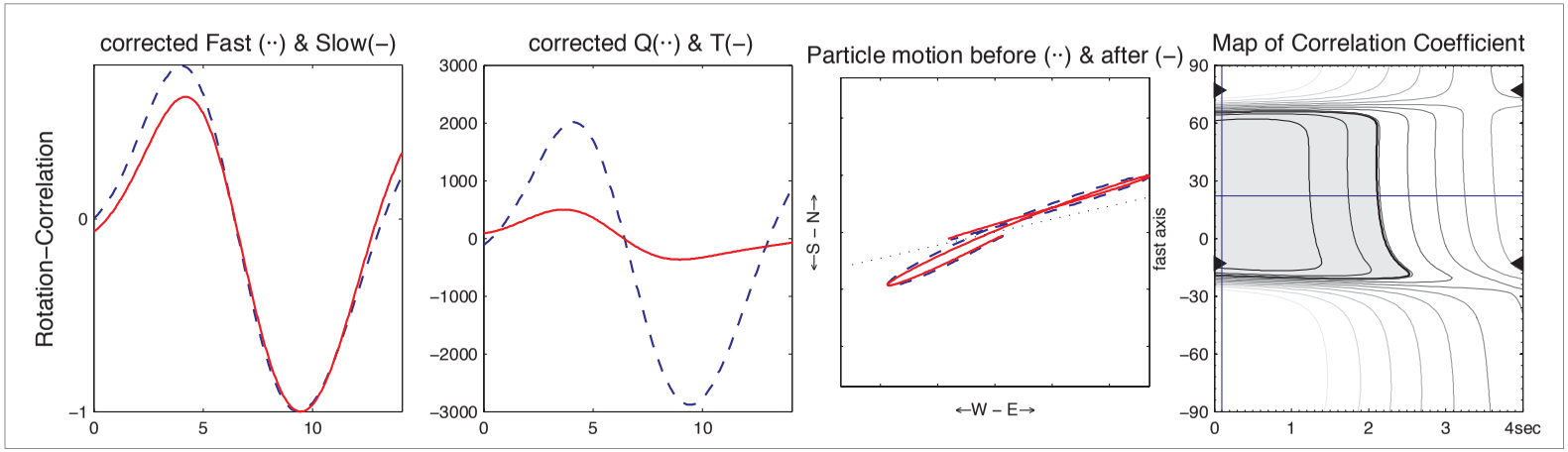

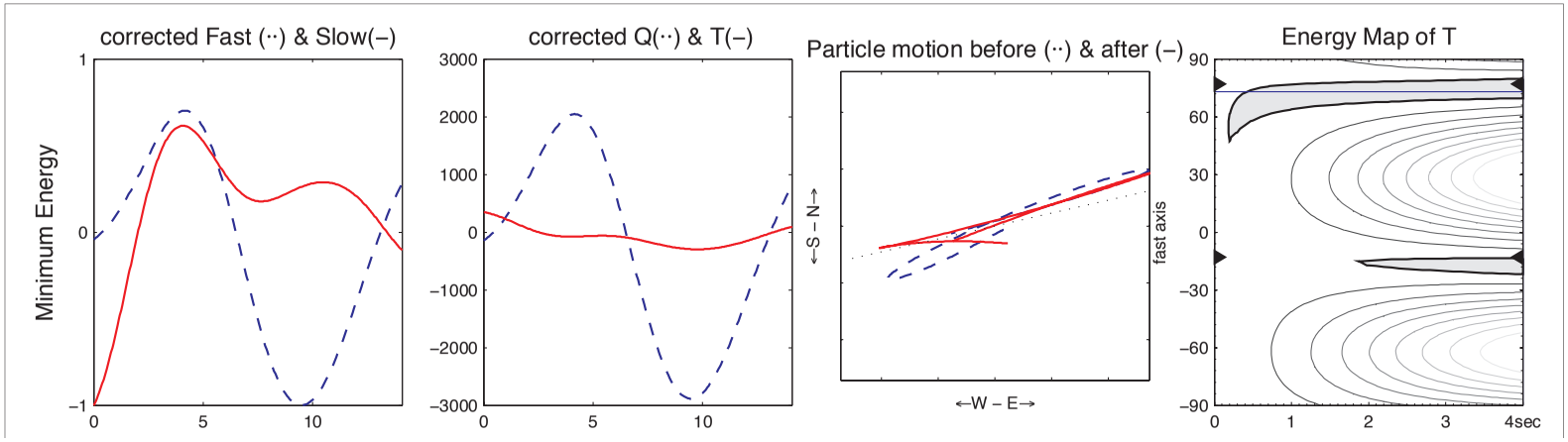

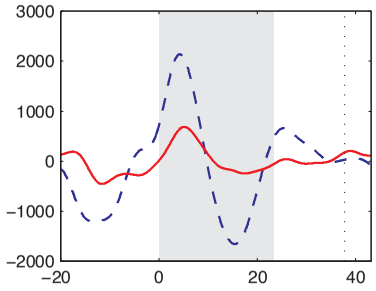

Event: **09-Mar-2004 (069) 22:07 -32.56N -177.97E 10km** Mw=**5.8**
Station: **RUFIN** Backazimuth: **245.8º** Distance: **114.00º**
init.Pol.: **54.3º** Filter: **0.020Hz - 0.12Hz** SNR_{SC}: **5.7**

Rotation Correlation: 58< −84° < −43 0.0<0.5s<3.6
Minimum Energy: −70< −36° < −29 0.6<4.0s<4.0
Eigenvalue: 54< −46° < −39 0.2<1.8s<4.0
Quality: **fair** IsNull: **Yes** Phase: **SKS**

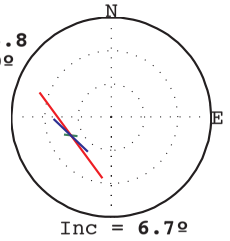

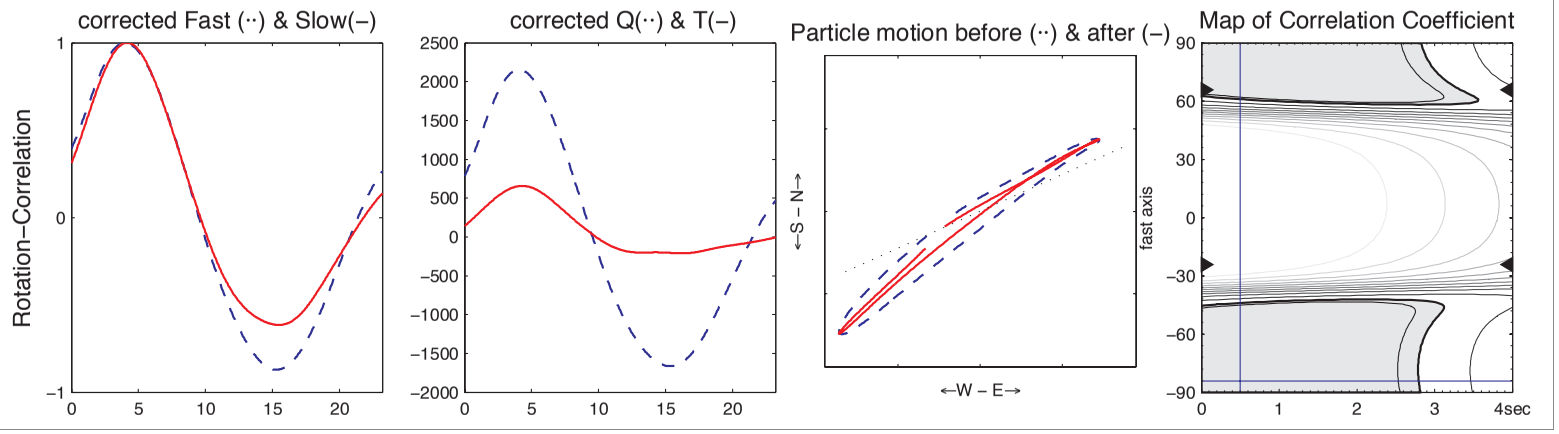

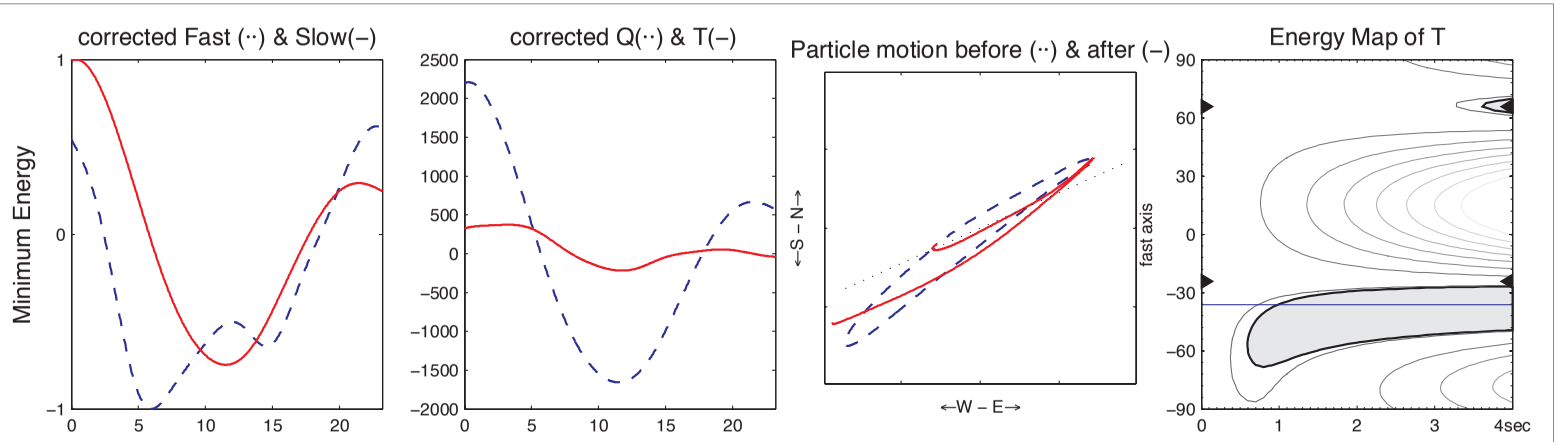

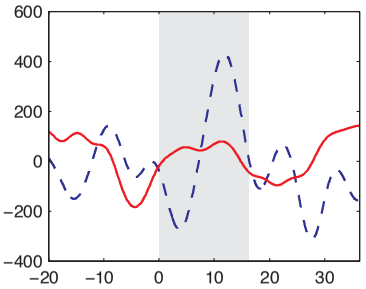

Event: **09-Mar-2004 (069) 22:56 -32.26N -178.36E 18km** Mw=**6.2**
Station: **WOAK** Backazimuth: **246.3º** Distance: **114.16º**
init.Pol.: **63.5º** Filter: **0.020Hz - 0.12Hz** SNR_{SC}: **6.7**

Rotation Correlation: -Inf< 16° < Inf 0.0<0.5s<Inf
Minimum Energy: -Inf< 58° < Inf 0.0<4.0s<Inf
Eigenvalue: -Inf< -6° < Inf 0.0<0.6s<Inf
Quality: **fair** IsNull: **Yes** Phase: **SKS**

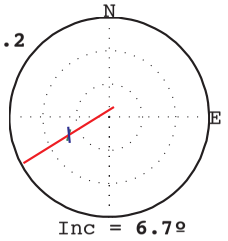

Inc = **6.7º**

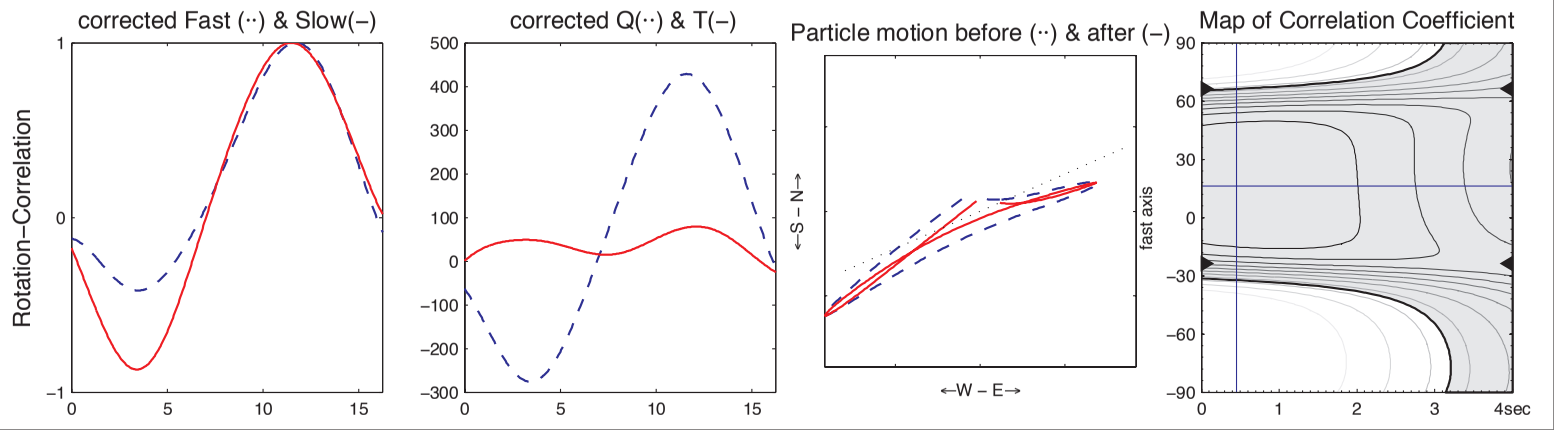

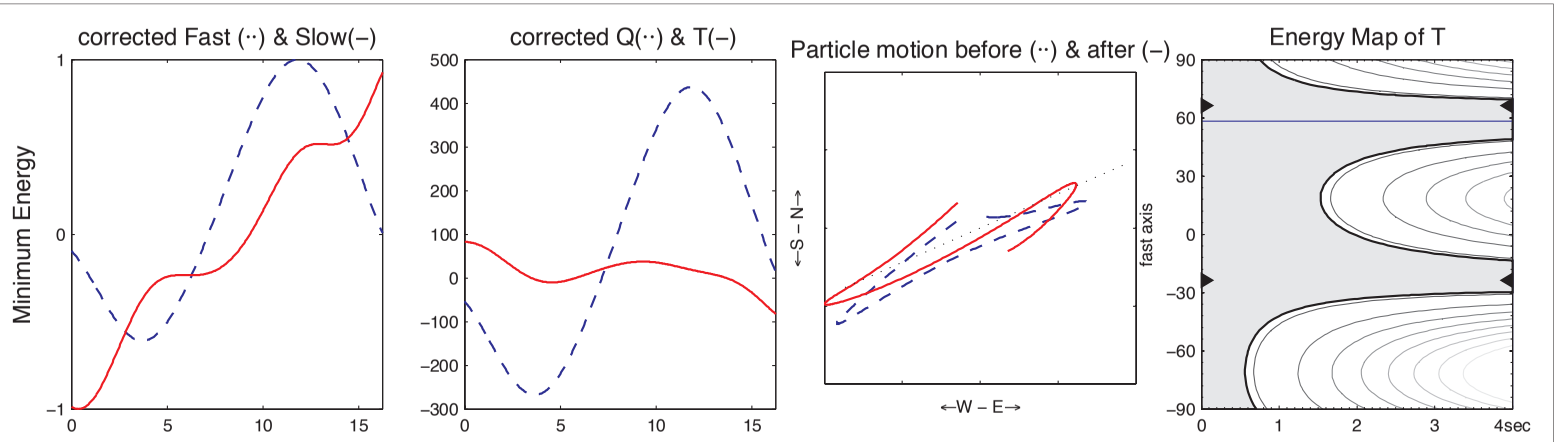

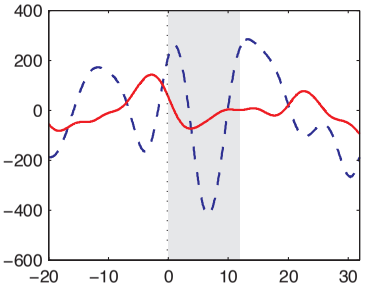

Event: **14-Mar-2004 (074) 16:30 -17.27N -172.32E 12km** Mw=**5.9**
Station: **DFORK** Backazimuth: **257.1º** Distance: **101.99º**
init.Pol.: **76.3º** Filter: **0.020Hz - 0.12Hz** SNR_{SC}:**13.9**

Rotation Correlation: -Inf< 28° < Inf 0.0<0.2s<Inf
Minimum Energy: -Inf< 75° < Inf 0.0<4.0s<Inf
Eigenvalue: -17< 63° < 76 0.3<0.9s<4.0
Quality: **fair** IsNull: **Yes** Phase: **SKS**

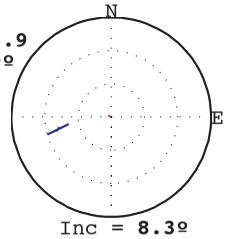

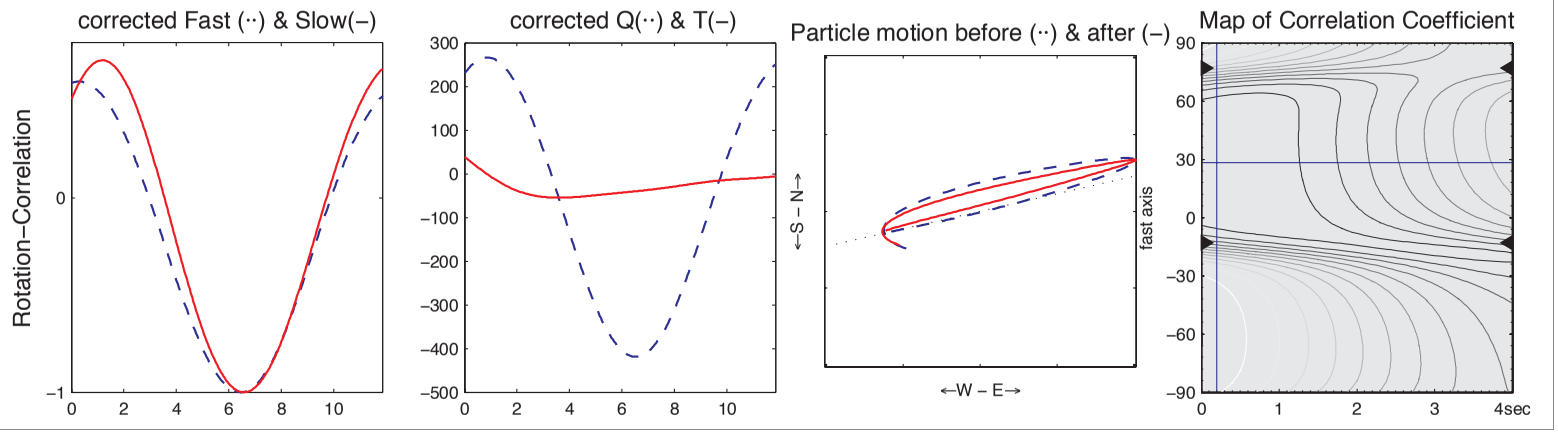

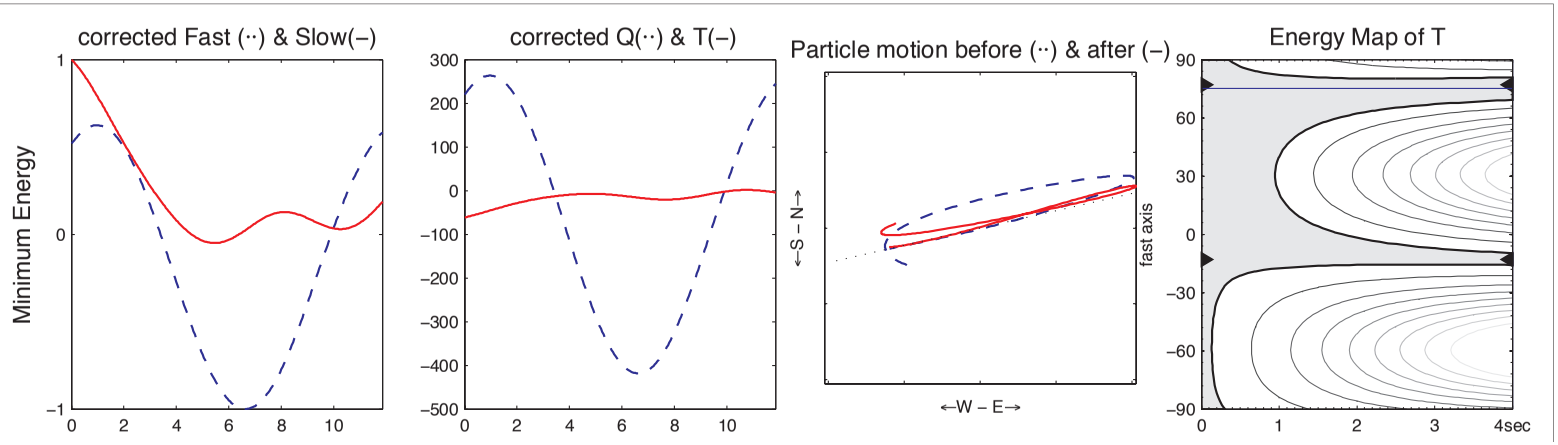

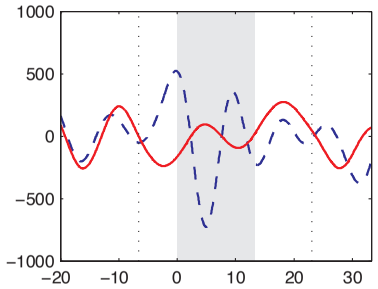

Event: **05-Apr-2004 (096) 21:24 36.51N 71.03E 187km Mw=6.5**
Station: **GREEN** Backazimuth: **24.2º** Distance: **104.15º**
init.Pol.: **214.2º** Filter: **0.020Hz - 0.12Hz** SNR_{SC}:**12.1**

Rotation Correlation:	−42<	−11° < 18	0.0<0.0s<0.3
Minimum Energy:	−64<	−60° < −60	2.8<4.0s<4.0
Eigenvalue:	-Inf<	30° < Inf	0.0<0.4s<Inf

Quality: **fair** IsNull: **Yes** Phase: **SKS**

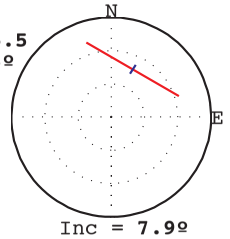

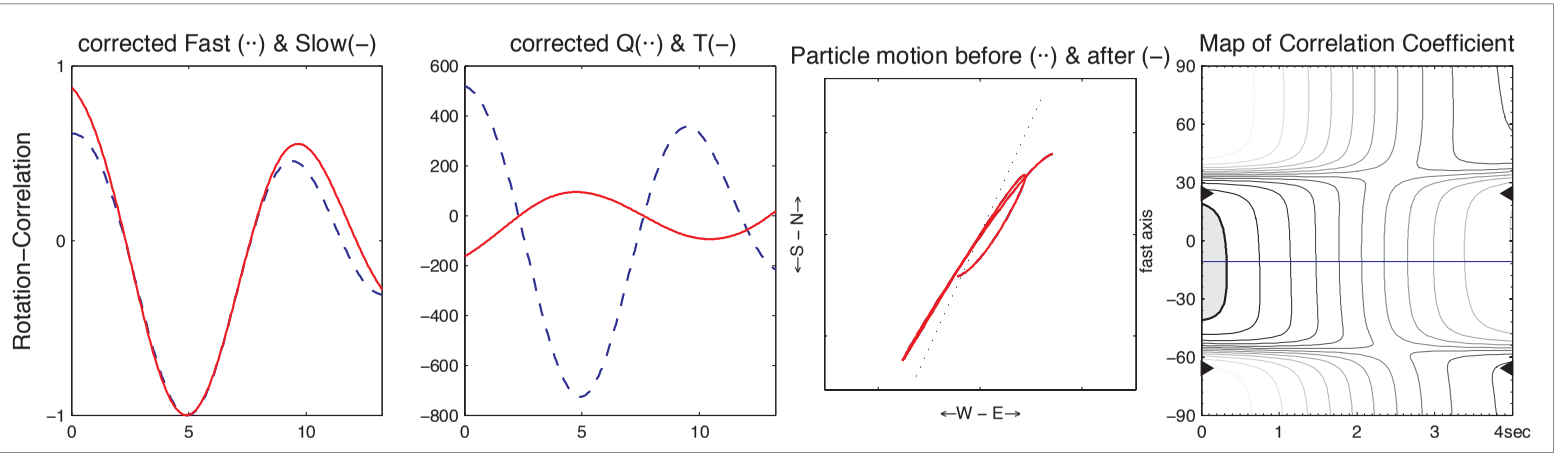

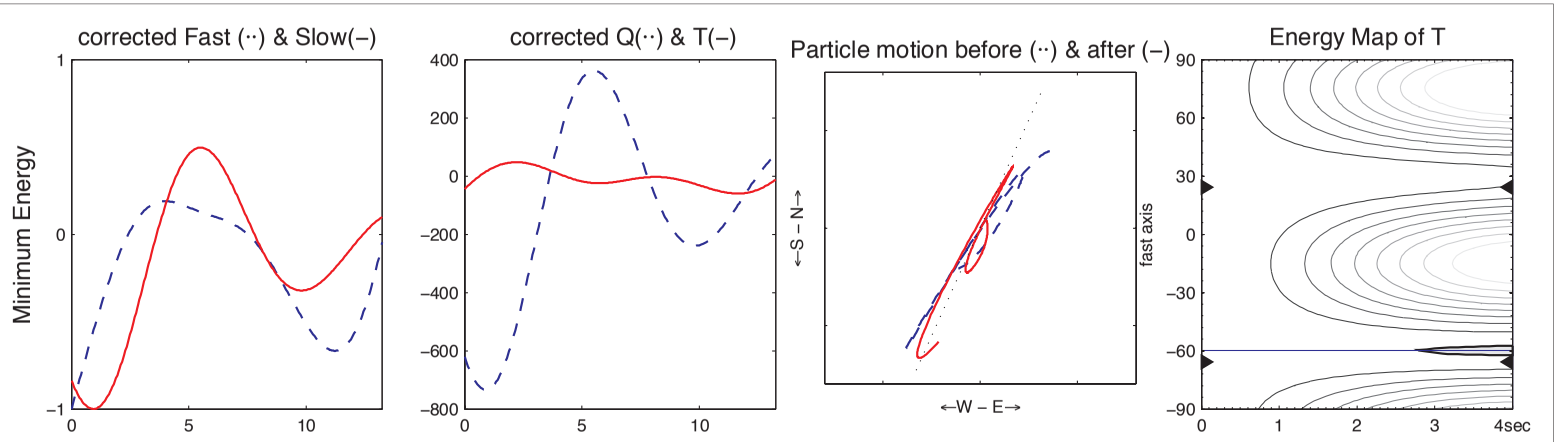

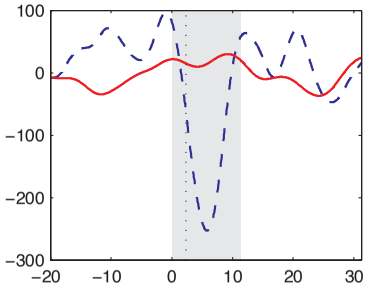

Event: **09-Apr-2004 (100) 15:23 -13.17N 167.20E 228km** Mw=6.4
Station: **TIMBR** Backazimuth: **271.9º** Distance: **116.67º**
init.Pol.: **89.8º** Filter: **0.020Hz - 0.12Hz** SNR_{SC}:**13.2**

Rotation Correlation: -Inf< 52° < Inf 0.0<0.1s<Inf
Minimum Energy: -Inf< 90° < Inf 0.0<3.3s<Inf
Eigenvalue: -Inf< 18° < Inf 0.0<0.3s<Inf
Quality: **good** IsNull: **Yes** Phase: **SKS**

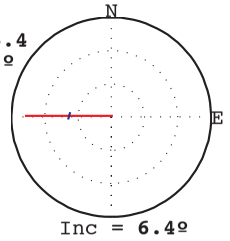

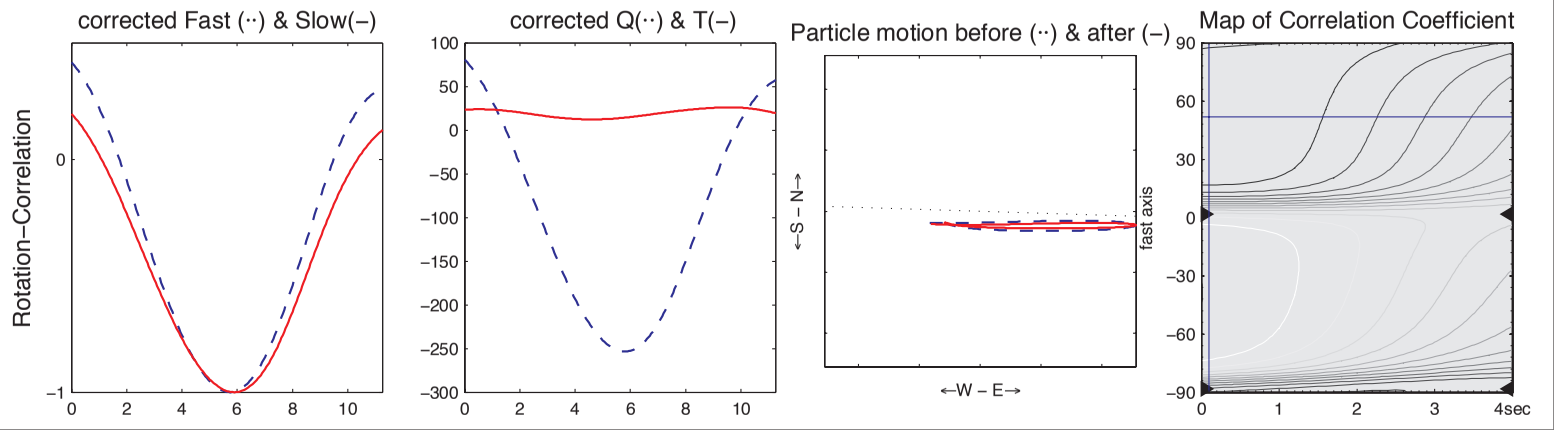

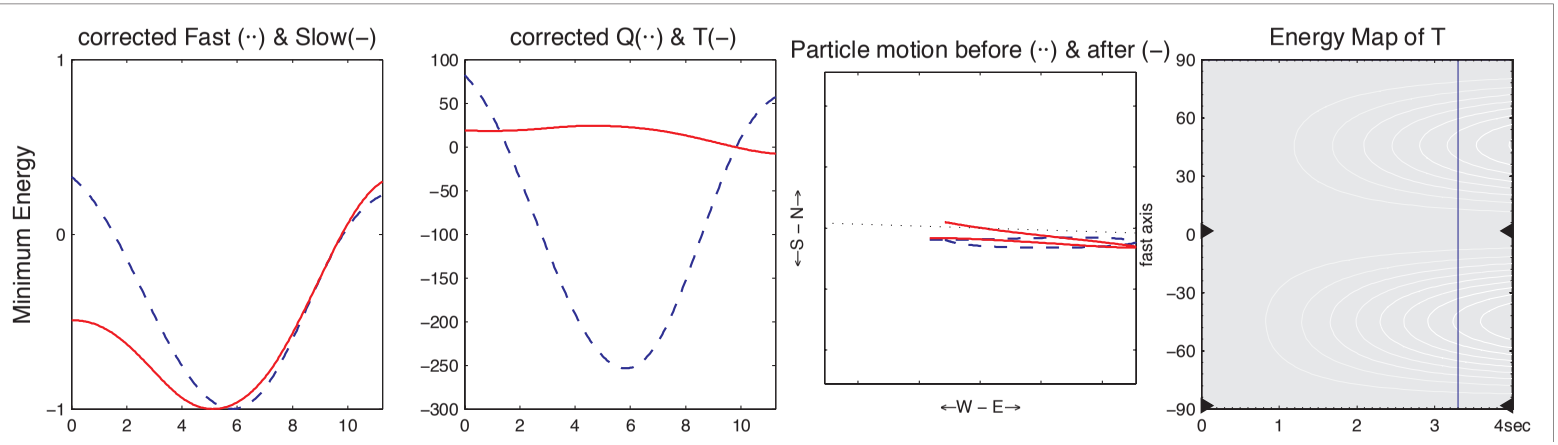

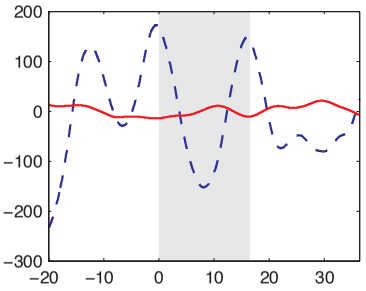

Event: **27-Apr-2004 (118) 23:28 -17.76N 167.76E 10km** Mw=**6.0**
Station: **TIMBR** Backazimuth: **267.1º** Distance: **118.56º**
init.Pol.: **87.6º** Filter: **0.020Hz - 0.12Hz** SNR_{SC}:**39.4**

Rotation Correlation:	5<	45° <	85	0.0<0.0s<1.6
Minimum Energy:	-1<	1° <	5	1.1<3.0s<4.0
Eigenvalue:	-1<	1° <	82	0.3<3.0s<4.0

Quality: **good** IsNull: **Yes** Phase: **SKS**

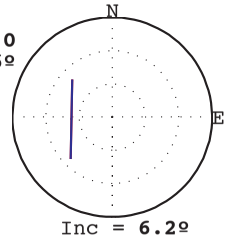

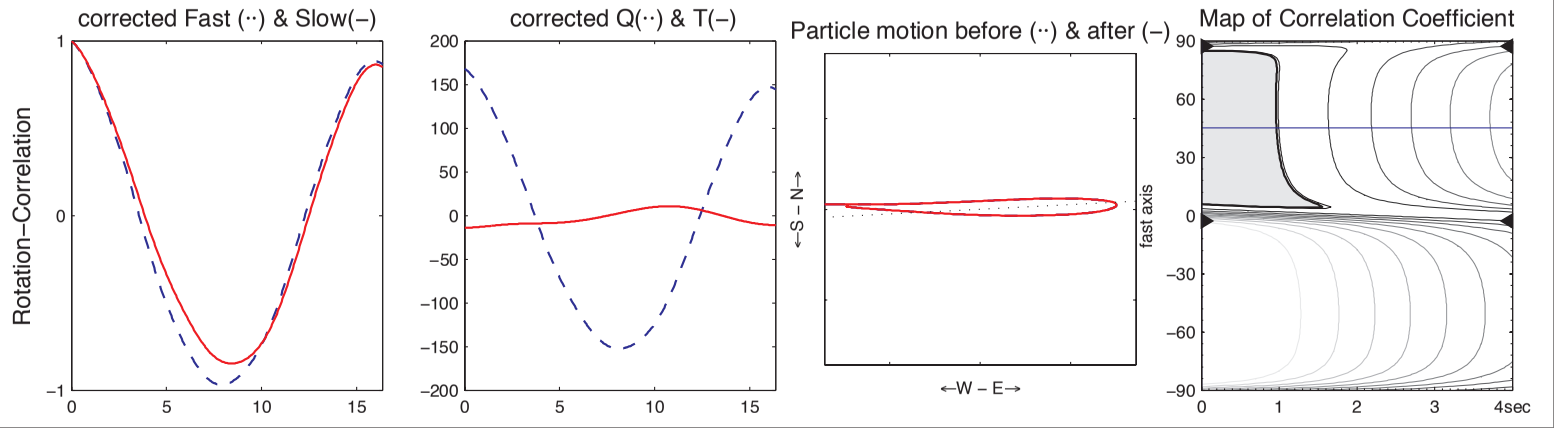

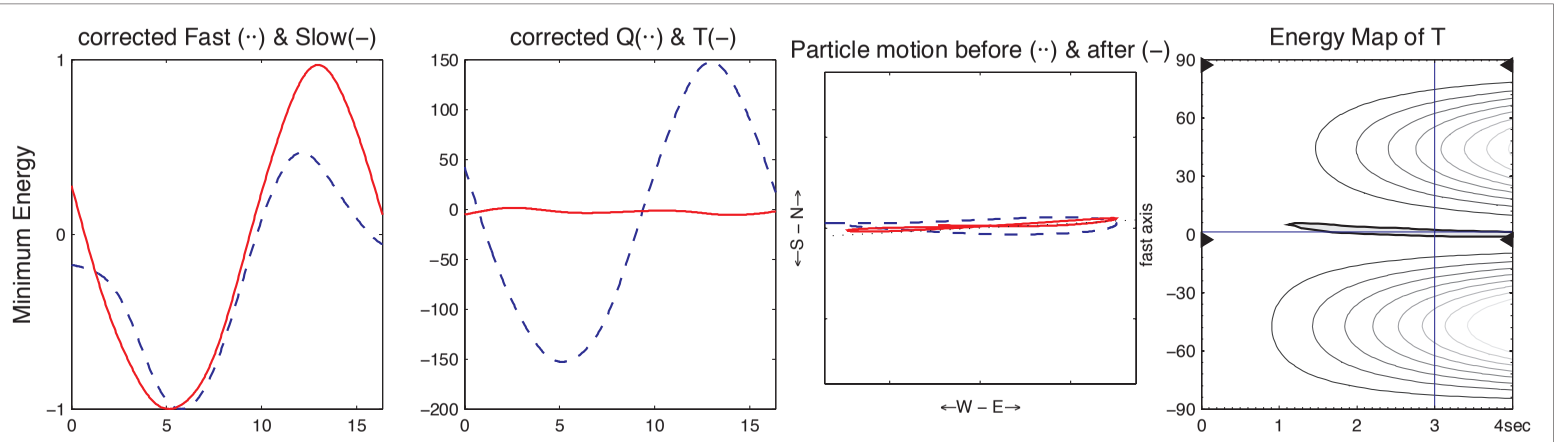

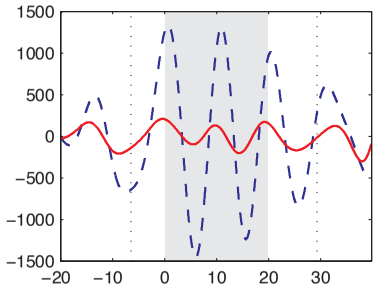

Event: **29-May-2004 (150) 20:56 34.25N 141.41E 16km Mw=6.3**
Station: **DWDAN** Backazimuth: **326.6º** Distance: **101.69º**
init.Pol.: **156.3º** Filter: **0.020Hz - 0.12Hz** SNR_{SC}:**16.0**

Rotation Correlation:	66<	−83° <	−50	0.0<0.1s<0.6
Minimum Energy:	−41<	−37° <	−37	1.7<2.8s<3.7
Eigenvalue:	54<	−31° <	−29	0.2<3.9s<4.0

Quality: **fair** IsNull: **Yes** Phase: **SKS**

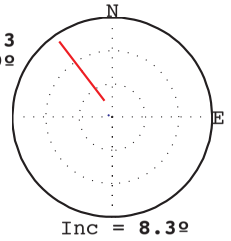

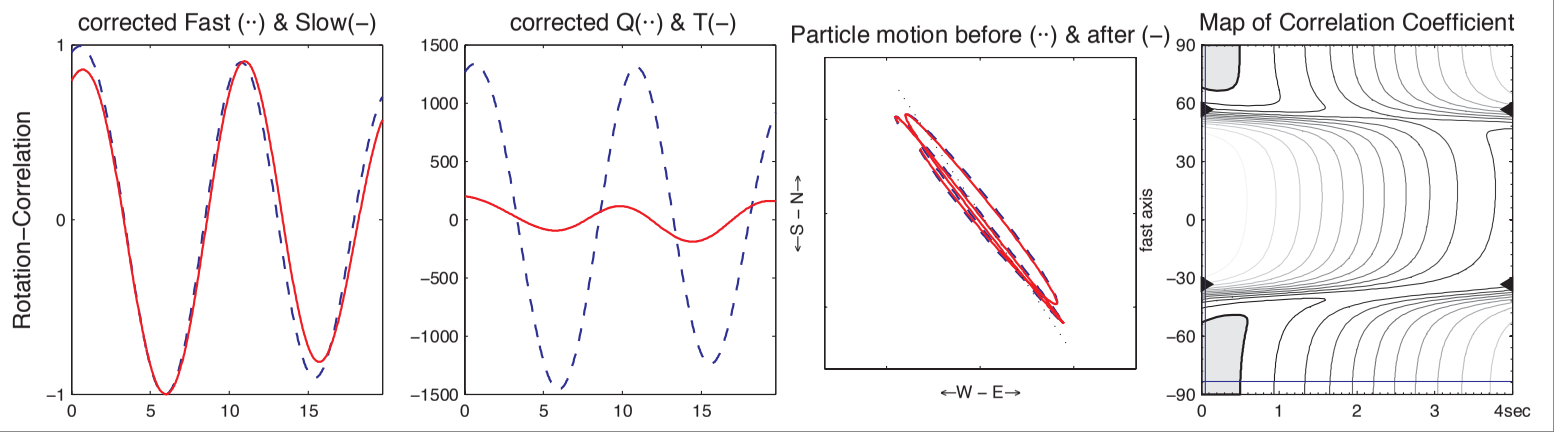

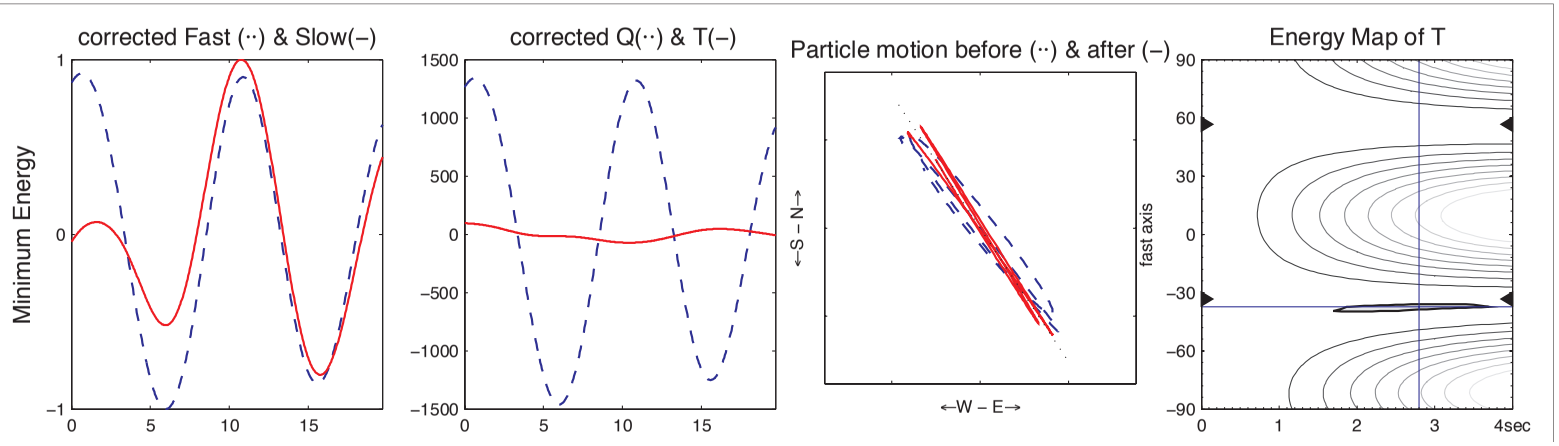

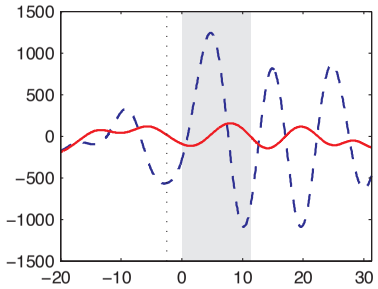

Event: **29-May-2004 (150) 20:56 34.25N 141.41E 16km Mw=6.3**
Station: **WOAK** Backazimuth: **326.6º** Distance: **101.69º**
init.Pol.: **136.2º** Filter: **0.020Hz - 0.12Hz** SNR_{SC}:**24.9**

Rotation Correlation: -Inf< **15°** < Inf 0.0<0.2s<Inf
Minimum Energy: -31< **-21°** < 46 0.3<1.1s<3.2
Eigenvalue: -37< **-35°** < -37 3.8<4.0s<4.0
Quality: **good** IsNull: **Yes** Phase: **SKS**

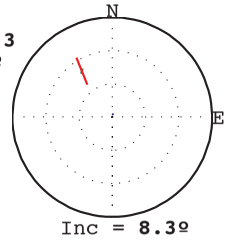

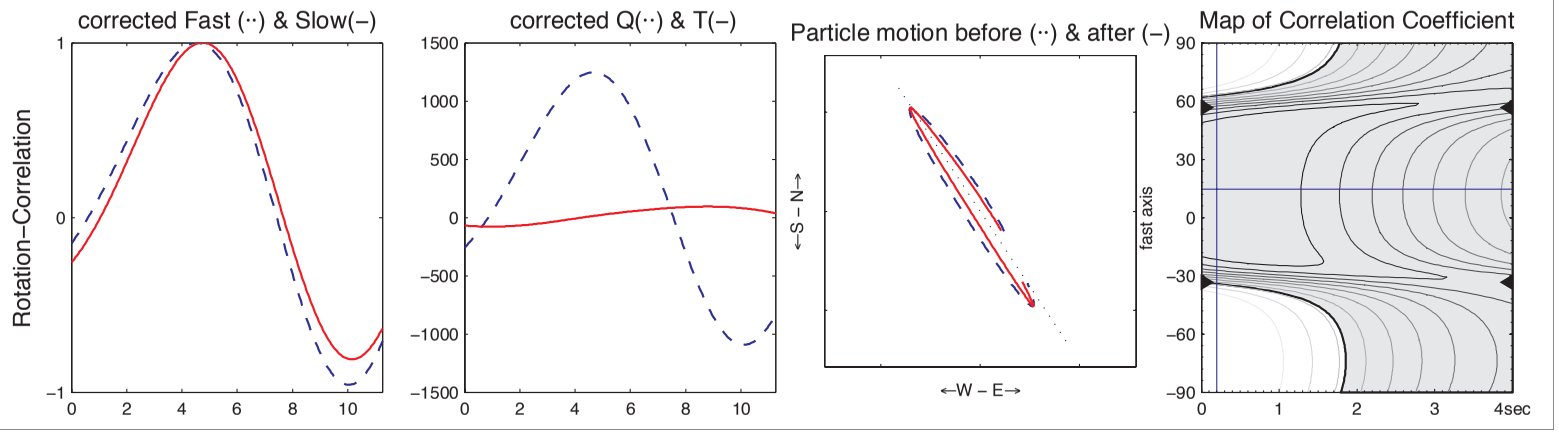

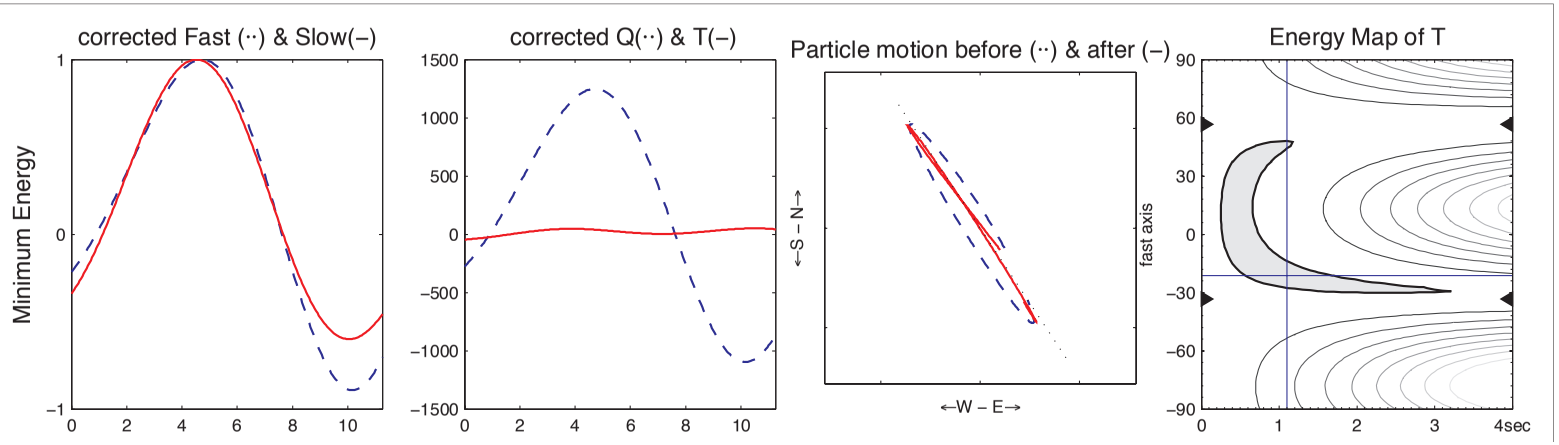

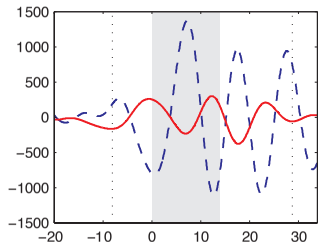

Event: **29-May-2004 (150) 20:56 34.25N 141.41E 16km Mw=6.3**
Station: **BLACK** Backazimuth: **326.3º** Distance: **102.14º**
init.Pol.: **160.6º** Filter: **0.020Hz - 0.12Hz** SNR_{SC}:**13.6**

Rotation Correlation:	78<	−67° < −32	0.0<0.0s<0.5
Minimum Energy:	−29<	−26° < −25	3.3<4.0s<4.0
Eigenvalue:	70<	68° < 70	2.5<2.9s<3.4

Quality: **good** IsNull: **Yes** Phase: **SKS**

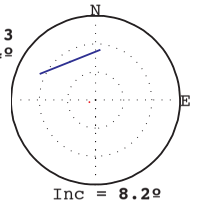

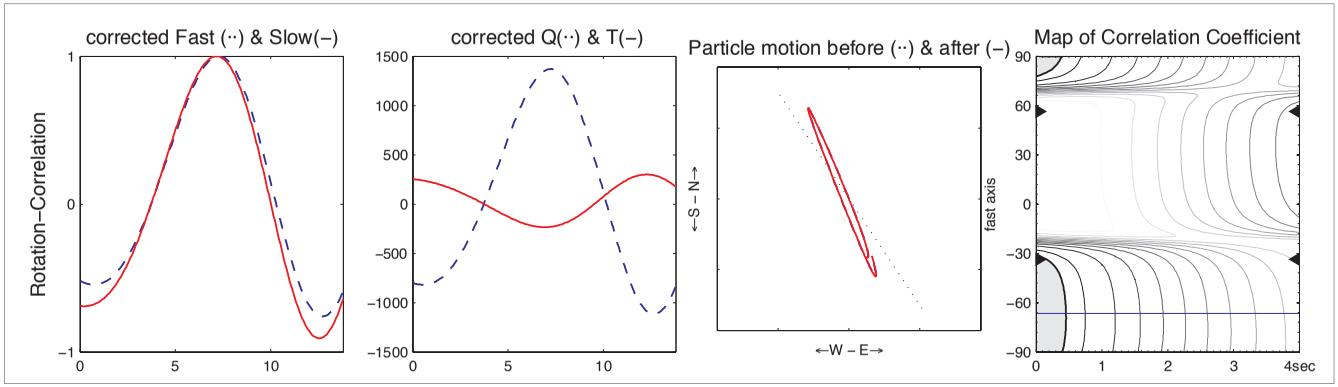

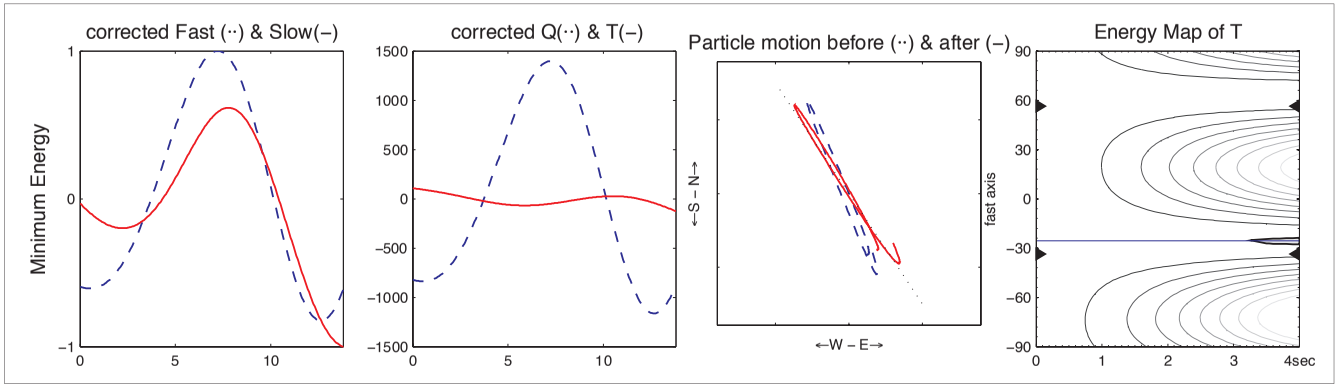

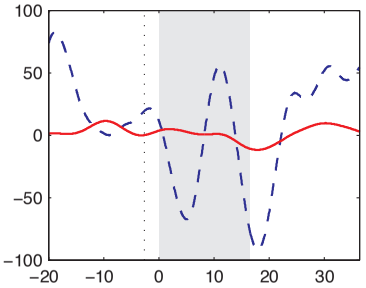

Event: **22-Jun-2004 (174) 09:04 -10.90N 166.26E 153km** Mw=**5.8**
Station: **TIMBR** Backazimuth: **274.6º** Distance: **116.23º**
init.Pol.: **92.9º** Filter: **0.020Hz - 0.12Hz** SNR_{SC}:**10.2**

Rotation Correlation: 37< 50° < 65 0.0<0.0s<0.1
Minimum Energy: -Inf< 15° < Inf 0.0<0.3s<Inf
Eigenvalue: -Inf< 5° < Inf 0.0<4.0s<Inf
Quality: **fair** IsNull: **Yes** Phase: **SKS**

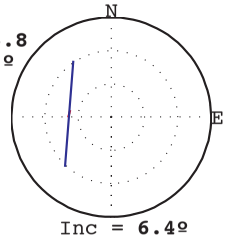

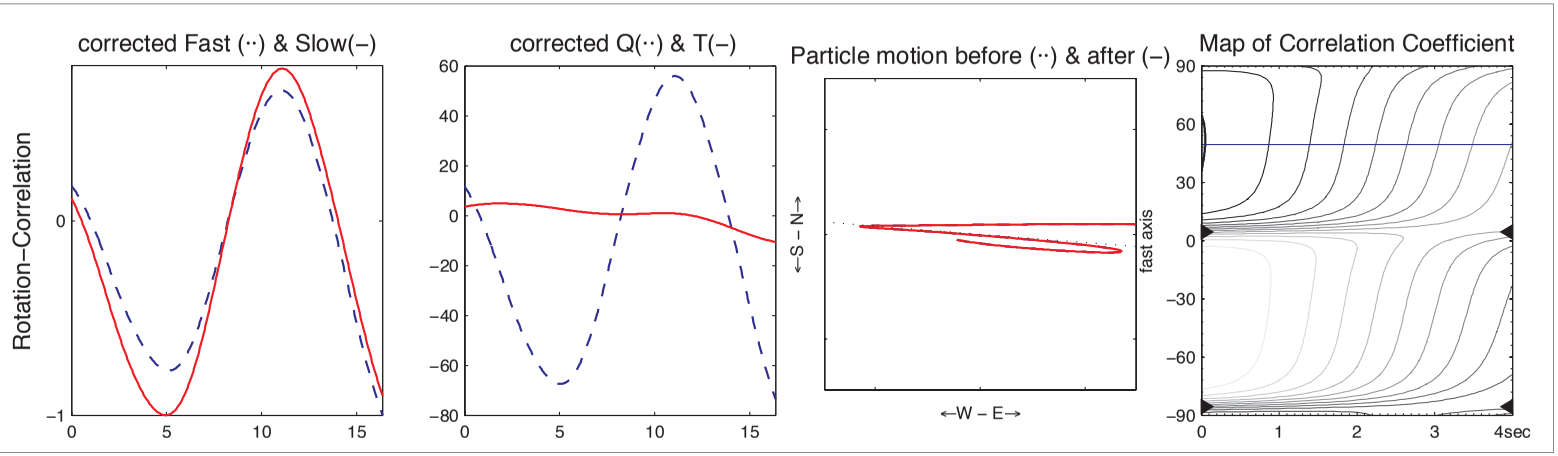

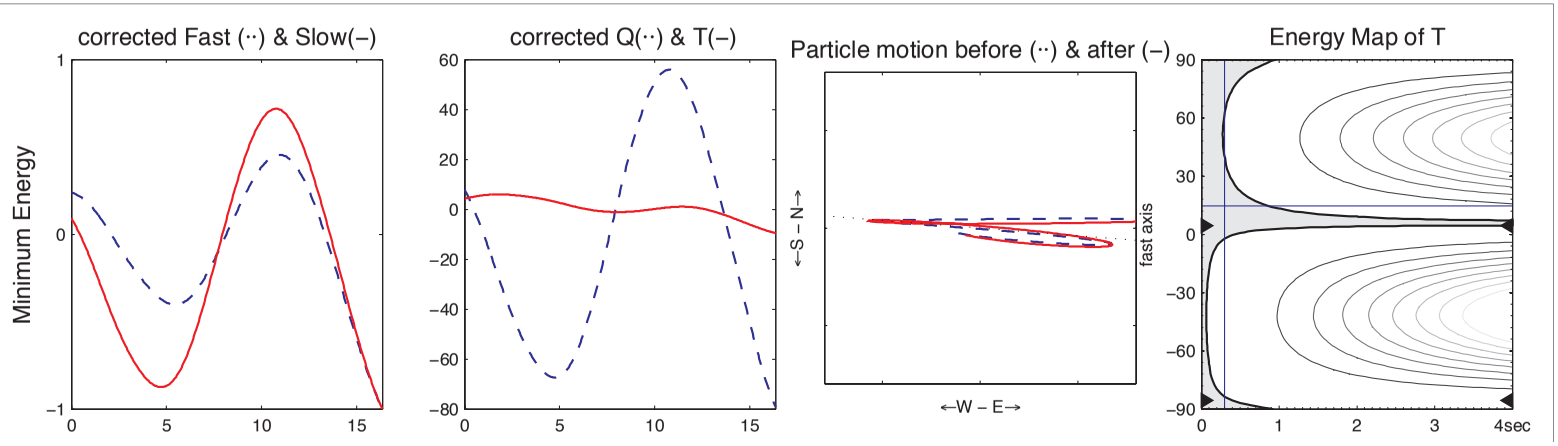

10. BIBLIOGRAPHY

Barruol, G., Silver, P.G., and A. Vauchez. 1997. Seismic Anisotropy in the Eastern United States: Deep Structure of a Complex Continental Plate. *Journal of Geophysical Research* 102(B4): 8329-8348.

Bowman, J.R., and M. Ando. 1987. Shear wave splitting in the upper-mantle wedge above the Tonga subduction zone. *Geophysical Journal of the Royal Astronomical Society* 88: 25-41.

Chevrot, S. 2000. Multichannel analysis of shear wave splitting. Journal of Geophysical Research. 105(B9): 21579-21590.

Christensen, N.I. 1984. The magnitude, symmetry, and origin of upper mantle anisotropy based on fabric analyses of ultramafic tectonites. *Geophysical Journal of the Royal Astronomical Society* 76: 89-111.

Fouch, M.J., Fischer, K.M., Parmentier, E.M., Wysession, M.E., and T.J. Clarke. 2000. Shear Wave Splitting, Continental Keels, and Patterns of Mantle Flow. *Journal of Geophysical Research* 105(B3): 6255-6275.

Fukao, Y. 1984. Evidence from core-reflected shear waves for anisotropy in the earth's mantle. *Nature* 309: 695-698.

Grand, S.P. 1994. Mantle shear structure beneath the Americas and surrounding oceans. *Journal of Geophysical Research* 99(B6): 11591-11621.

Heintz, M., and B.L.N. Kennett. 2005. Continental Scale Shear Wave Splitting Analysis; Investigation of Seismic Anisotropy Underneath the Australian Continent. *Earth and Planetary Science Letters* 236(1-2): 106-119.

Heintz, M., Vauchez, A., Assumpção, M., Barruol, G., and M. Egydio-Silva. 2003. Shear Wave Splitting in SE Brazil; an Effect of Active Or Fossil Upper Mantle Flow, Or both? *Earth and Planetary Science Letters* 211(1-2): 79-95.

Horton, J.W. 2006. Geologic Map of the Kings Mountain and Grover Quadrangles, Cleveland and Gaston Counties, North Carolina, and Cherokee and York Counties, South Carolina. United States Geological Survey, United

States Department of the Interior. http://pubs.usgs.gov (accessed 21 March 2010).

IRIS SeismiQuery. 2009. Database Query Tool. Incorporated Research Institutions for Seismology. http://www.iris.edu/SeismiQuery/ (Accessed 8 October 2009).

Long, M.D. 2009. [Shear Wave Splitting in the Southeastern United States]. Unpublished data.

Long, M.D., and P.G. Silver. 2009. Shear Wave Splitting and Mantle Anisotropy: Measurements, Interpretations, and New Directions. *Surveys in Geophysics* 30: 407-461.

Nicolas, A., and N.I. Christensen. 1987. Formation of anisotropy in upper mantle peridotites – a review. In *Composition, structure, and dynamics of the lithosphere-asthenosphere system*, ed. K. Fuchs and C. Froideveaux, 111-123. Washington, D.C.: American Geophysical Union.

Shearer, P.M. 1999. *Introduction to Seismology*. Cambridge: Cambridge University Press.

Silver, P.G. 1996. Seismic Anisotropy Beneath the Continents: Probing the Depths of Geology. *Annual Review of Earth and Planetary Sciences* 24: 385-432.

Silver, P.G., and W.W. Chan. 1991. Shear wave splitting and subcontinental mantle deformation. *Journal of Geophysical Research* 96(B10): 16429-16454.

Silver, P.G., and W.E. Holt. 2002. The mantle flow field beneath western North America. *Science* 295: 1054-1057.

Silver, P.G., and M.K. Savage. 1994. The interpretation of shear-wave splitting parameters in the presence of two anisotropic layers. *Geophysical Journal International* 119: 949-963.

Taylor, S.R. 1989. Geophysical framework of the Appalachians and adjacent Grenville Province. In *Geophysical Framework of the Continental United States*, ed. L.C. Pakiser and W.D. Mooney, 317-348. Boulder, Colorado: Geological Society of America.

Van der Lee, S., and G. Nolet. 1997. Upper mantle *S* velocity structure of North America." *Journal of Geophysical Research* 102(B10): 22815-22838.

Willoughby, R.H., Howard, C.S., and P.G. Nystrom. 2005. Generalized Geologic Map of South Carolina. South Carolina Geological Survey, South Carolina Department of Natural Resources. http://www.dnr.sc.gov/geology/ (accessed 21 March 2010).

Wuestefeld, A., Bokelmann, G., Zaroli, C., and G. Barruol. 2008. SplitLab; a Shear-Wave Splitting Environment in Matlab. *Computers & Geosciences* 34(5): 515-528.

Zhang, S., and S. Karato. 1995. Lattice preferred orientation of olivine aggregates deformed in simple shear. *Nature* 415: 777-780.